(11)

NOLTR 72-80

CALCULATION OF MAGNUS FORCES ON AXISYMMETRIC BODIES AT SMALL ANGLES OF ATTACK WITH INCOMPRESSIBLE TURBULENT BOUNDARY LAYERS

By
Neal Tetervin

21 MARCH 1972

NOL

NAVAL ORDNANCE LABORATORY, WHITE OAK, SILVER SPRING, MARYLAND

NOLTR 72-80

157

UNCLASSIFIED
Security Classification

DOCUMENT CONTROL DATA - R & D

(Security classification of title, body of abstract and indexing annotation must be entered when the overall report is classified)

1 ORIGINATING ACTIVITY (Corporate author) Naval Ordnance Laboratory Silver Spring, Maryland 20910	2a. REPORT SECURITY CLASSIFICATION Unclassified 2b. GROUP

3 REPORT TITLE
Calculation of Magnus Forces on Axisymmetric Bodies at Small Angles of Attack with Incompressible Turbulent Boundary Layers

4 DESCRIPTIVE NOTES (Type of report and inclusive dates)

5. AUTHOR(S) (First name, middle initial, last name)
Neal Tetervin

6 REPORT DATE 21 March 1972	7a. TOTAL NO. OF PAGES 161	7b. NO OF REFS 20
8a. CONTRACT OR GRANT NO b. PROJECT NO. ORD Task 35A-001-100-31 c. d.	9a. ORIGINATOR'S REPORT NUMBER(S) NOLTR 72-80 9b. OTHER REPORT NO(S) (Any other numbers that may be assigned this report)	

10. DISTRIBUTION STATEMENT
Approved for public release; distribution unlimited

11. SUPPLEMENTARY NOTES	12 SPONSORING MILITARY ACTIVITY Naval Ordnance Systems Command Washington, D.C. 20360

13 ABSTRACT

The Magnus force is found by adding the boundary layer displacement surface to the body and then calculating the force on the resulting non-axisymmetric body. The displacement surface is calculated by the simultaneous integration of a differential equation for a streamline, two partial-differential boundary layer integral-momentum equations with the boundary layer thickness and the tangent of the angle between the local direction of the surface friction and potential flow streamline as dependent variables, and a partial differential equation for the displacement surface thickness. The method is applied to a half-ellipsoid of fineness ratio 5 at 4 degrees angle of attack. Slender-body theory is used to calculate the force.

DD FORM 1 NOV 65 1473 (PAGE 1)
S/N 0101-807-6801

UNCLASSIFIED
Security Classification

14 KEY WORDS	LINK A		LINK B		LINK C	
	ROLE	WT	ROLE	WT	ROLE	WT
Magnus forces and moments						
Spinning bodies of revolution						
Turbulent boundary layer						
Slender-body theory						
Three-dimensional boundary layers						

NOLTR 72-80 21 March 1972

CALCULATION OF MAGNUS FORCES ON AXISYMMETRIC BODIES AT SMALL ANGLES OF ATTACK WITH INCOMPRESSIBLE TURBULENT BOUNDARY LAYERS

This report presents the derivation of a method for calculating the Magnus force and moment on a spinning body of revolution. For an example the force and moment on a fineness ratio 5 half-ellipsoid at an angle of attack of 4 degrees with a non-dimensional spin speed of .25 are calculated.

Appreciation is expressed to Mrs. Carolyn Piper and to Mrs. Rita Bell who programmed the metnod on an electronic computer and conducted the calculations. This work was supported by the Naval Ordnance Systems Command, under ORD Task 35A-001-100-31.

ROBERT WILLIAMSON II
Captain, USN

L. H. Schindel

L. H. SCHINDEL
By direction

CONTENTS

ILLUSTRATIONS

ILLUSTRATIONS (Con't)

TABLE

NOMENCLATURE

$\hat{a}$	unit vector parallel to body surface in plane θ = constant, positive in direction of increasing x
a	angle from meridian θ = constant to tangent to potential flow streamline, positive in direction of increasing θ
a_o	constant, Equation (40)
A	$q_e - \omega r_o \sin a$
dA	element of area on resultant body, body plus displacement surface
$\hat{b}$	$\hat{c} \times \hat{a}$, unit vector parallel to body surface in plane x = constant
b_o	constant, Equation (40)
B	$\omega r_o \sin a$
$\hat{c}$	unit vector normal to body surface, outward from surface
c_1	constant, Equation (79)
c_2	constant, Equation (80)
c_3	c_2/c_1
c_4	constant, Equation (83)
C	$\omega r_o \cos a$
C_D	drag coefficient based on area $\pi \bar{r}_M^2$
C_n	Magnus yawing moment coefficient (Equation (154))
C_N	normal force coefficient (Equation (152))
C_p	pressure coefficient $\dfrac{\bar{P}-\bar{p}_\infty}{\frac{\rho_\infty}{2} \bar{V}_\infty^2}$
C_Y	Magnus side force coefficient (Equation (153))
d	displacement of origin of x, r, θ system from origin of ξ, h, β system (Figure 8)

D_1	$\sqrt{\Delta s_x^2 + \left(\frac{\partial \delta^*}{\partial s_x} \Delta s_x\right)^2}$
D_2	$\sqrt{r_o^2 \Delta\theta^2 + \left(\frac{\partial \delta^*}{\partial \theta} \Delta\theta\right)^2}$
$\hat{e}_1$	unit vector in direction of free stream velocity (Figure 8)
$\hat{e}_2$	unit vector normal to $\hat{e}_1$ and in ξ, x plane (Figure 8)
$\hat{e}_3$	$\hat{e}_1 \times \hat{e}_2$ (Figure 8)
$\bar{F}$	$\bar{F}_Y + i\,\bar{F}_Z$, complex Magnus force on portion of body between cross section $\xi = C$ and body nose
$\bar{F}_Y$	component of Magnus force $\bar{F}$ along Y axis (Figure 6)
$\bar{F}_Z$	component of Magnus force $\bar{F}$ along Z axis (Figure 6)
G_i	function (See Table I)
h	radial distance in plane ξ = constant (Figure 8)
h_o	radial distance to point on body in plane ξ = constant (Figure 6)
$\hat{h}$	unit radial vector in plane ξ = constant (Figure 8)
$\hat{i}$	unit vector along body axis (Figure 8)
i	$\sqrt{-1}$
I	radius of starting circle, (Equation (100))
$\hat{j}$	unit vector normal to $\hat{i}$ and in x, ξ plane (Figure 8)
J_i	parameter (See Table III)
k	constant in friction formula (Equation (95))
K_1, K_2	parameters for ellipsoid (Equations (150) and (151))
ℓ	exponent (Equation (40))
$\bar{L}$	reference length
m	exponent in friction formula (Equation (95))
M	Mach number
$\bar{M}_Y$	Magnus moment about nose of body acting on portion of body between cross section $\xi = C$ and the body nose, positive as shown in Figure 1

n	exponent in velocity profile formula (Equation (52))
$\hat{n}$	unit vector normal to body plus displacement surface, outward from surface
N	number of base radii behind base beyond which wake thickness is constant and equal to R_W^*
$\vec{N}$	vector normal to body plus displacement surface, outward from surface
p	spin rate parameter $\frac{\bar{\omega}\bar{r}_M}{\bar{V}_\infty}$
P	static pressure
q_e	velocity at outer edge of boundary layer
Q	right hand side of Equation (24)
$\vec{Q}$	velocity vector (Equation (105))
r	radial distance in plane x = C (Figure 8)
r_o	radius of body of revolution
r_M	maximum radius of body of revolution
r'	radial coordinate of section of resultant body in Z' plane (Figure 7)
$\hat{r}$	unit vector along radial direction in x = constant plane (Figure 8)
R	radial coordinate of resultant body, $r_o + \delta^*$
Re_L	reference Reynolds number $\frac{\bar{V}_\infty \bar{L}}{\bar{\nu}}$
R_W	displacement radius of wake (Equation (C-1))
R_W^*	constant displacement radius of wake far behind body (Equation (C-1))
s	distance on body surface along potential flow streamline
s_x	distance along body surface in plane θ = constant
s_θ	distance along body surface in plane x = constant
s_ξ	distance along section of body plus displacement surface in plane ξ = constant (Figure 7)

$\vec{S}$	vector from origin of ξ, h, β system of coordinates (Figure 8)
t	thickness ratio, minor axis divided by major axis for ellipsoid
T	temperature
u	velocity parallel to surface and in plane θ = constant
$u_{e;\,s}$	value of $\frac{du_e}{ds_x}$ at stagnation point
u_q	velocity parallel to surface and in direction of q_e
v	velocity parallel to surface and in plane x = constant
v_q	velocity parallel to surface and normal to direction of q_e
V_s	velocity along circle in Z plane (Figure 7)
V_s'	velocity along cross section in Z' and z_o planes (Figure 7)
V_n	velocity normal to circle in Z plane (Figure 7)
V_n'	velocity normal to cross section in Z' and z_o planes (Figure 7)
$\bar{V}_\infty$	magnitude of free stream velocity
$\vec{V}_e$	velocity vector along displacement surface (Equation (10))
w	velocity normal to body surface
x	distance along axis of revolution
x_o	value of x at intersection of axis of revolution and plane ξ = C
y	distance from body surface in direction normal to surface
y_q	value of y slightly larger than δ
Y	coordinate in z_o plane (Figure 6)
z_o	complex plane coinciding with plane ξ = constant and having origin of coordinates on ξ axis, z_o = Y + i Z (Figure 6, 7)
Z'	complex plane coinciding with plane ξ = constant and having origin of coordinates on x axis (Figure 7)

Z	complex plane in which section of body plus displacement surface is a circle as a result of a transformation (Figure 7)
α	angle of attack of body
β_o	$\tan^{-1} \psi$
β	angular coordinate in ξ = constant plane (Figures 6, 7, 8)
$\hat{\beta}$	unit vector in direction of increasing β (Figures 6, 8)
γ	angular coordinate in Z' plane (Figure 7)
Δ	integration interval 2π divided into equal steps of length Δ (Equation (144))
δ	boundary layer thickness
δ^*	boundary layer displacement thickness defined by Equation (23)
∇	gradient symbol
ε	$(\sigma - \gamma)$ see Equation (128)
ζ	y/δ
η	starting angle (Equation (100))
$\hat{\theta}$	unit vector normal to $\hat{r}$ and in direction of increasing θ (Figure 8) ($\hat{\theta} = \hat{r} \times \hat{i}$)
θ	angular coordinate (Figure 2)
κ	ratio of specific heat at constant pressure to specific heat at constant volume
λ	radial coordinate in circle plane (Figure 7)
$\overline{\mu}$	viscosity
$\overline{\nu}$	kinematic viscosity $\overline{\mu}/\overline{\rho}$
$\hat{\nu}$	unit vector normal to section of body ξ = constant (Figures 6, 7)
ξ	distance in direction of free stream velocity (Figures 6, 8)
$\overline{\rho}$	density
σ	angle in Z plane (Figure 7)

τ_w wall shear stress

τ_{w_x} wall shear stress along θ = constant direction

τ_{w_θ} wall shear stress along x = constant direction

ϕ angle between surface of body and x axis in plane θ = constant (Figure 2)

Φ three-dimensional perturbation velocity potential (Equation (105))

Φ_o two-dimensional perturbation velocity potential in plane $\xi = c$

χ_1 angle defined by Equations (12) and (13)

χ_2 angle defined by Equations (14) and (15)

ψ tangent of angle measured from direction of potential flow streamline to direction of surface shear stress, positive in direction of increasing θ

ω angular spin velocity of body $\frac{\bar{\omega}\ \bar{L}}{\bar{V}_\infty}$, positive as shown in (Figure 1)

Ω defined by $r' = r_o e^{\Omega}$ (Equation (124))

Ω_o defined by $\lambda = r_o e^{\Omega_o}$ (Equation (125))

Subscripts

b at base of body

e at outer edge of boundary layer

M maximum value

s at stagnation point

w at surface

W wake

δ^* on displacement thickness surface

∞ very far ahead of body

Superscripts

"	fluctuating quantity
< >	mean value
*	value very far behind base
___	dimensional quantity

INTRODUCTION

When a spinning body of revolution is flying at an angle of attack, a force normal to the angle of attack plane acts on the body. Associated with this side force is a moment. The force and moment are known as the Magnus force and moment. Although the Magnus force is usually only a small fraction of the normal force it, and its moment about the body center of gravity, can have an important effect on the body trajectory. In order to predict the Magnus force and moment and in order to better understand experimental results a theory is needed.

The problem is to calculate the Magnus force and moment given only the shape of a body of revolution, its speed along the flight path, its spin rate, its angle of attack, and the properties of the atmosphere. If the flow were symmetric about the plane formed by the axis of the body and the free-stream velocity vector there would be no side force, a force perpendicular to the plane of symmetry. There would also be no yawing moment. Because, however, the fluid through which the body is moving is viscous, a boundary layer is present on the body. The spin of the body combined with the angle of attack causes the boundary layer to be unsymmetric with respect to the plane of symmetry, the plane formed by the axis of revolution and the free-stream velocity vector. The resultant configuration is shown in Figure 1. Because the symmetry of the flow about the angle of attack plane is destroyed by the unsymmetric boundary layer a side force and moment exist. For the symmetry to be destroyed, both spin and angle of attack must be present.

In the present investigation the Magnus force and moment are calculated for a body with no separation of the boundary layer. The boundary layer is therefore thin over the entire body and there are no regions of vorticity shed into the flow ahead of the body base. To calculate the Magnus force and moment for such a flow the inviscid flow around the body is found first. Then the boundary layer displacement thickness surface surrounding the body is calculated by use of boundary layer theory. The displacement thickness surface is added to the body and the force and moment calculated for the resultant body in an inviscid flow.

This method for the calculation of the Magnus force and moment is that of Martin (Reference 1) who presents a theory for the Magnus force and moment on a cylinder at a small angle of attack. The

boundary layer is laminar and incompressible. Quantities of higher order than the second in angle of attack, spin velocity, and distance from the leading edge and their products with one another are neglected. Martin finds that the Magnus force is directly proportional to the product of the angle of attack, spin velocity ratio, body length, and the displacement thickness at the body base at zero angle of attack. For turbulent flow Martin replaces a calculated constant of proportionality by an unknown coefficient.

Platou (Reference 2) presents experimental data for supersonic flow and concludes that Martin's incompressible flow theory predicts the correct order of magnitude for 3 to 5 caliber bodies with laminar boundary layers. To apply Martin's theory to a bullet shaped body an arbitrary allowance must be made for the nose portion of non-constant diameter. The extrapolation of Martin's theory to turbulent flow correctly predicts the Magnus force to be directly proportional to the product of angle of attack and spin rate. Platou also finds that the theory of Kelly and Thacker (Reference 3), which includes a radial pressure gradient and skin friction effect, does not agree with Martin's prediction nor does it agree with the experimental result that the Magnus force depends on the spin to the first power.

Sedney (Reference 4) calculates the Magnus force and moment on a slender spinning cone at a small angle of attack in supersonic flow. The boundary layer flow is laminar. Terms of higher order than the first in angle of attack, spin velocity, and in the product of spin velocity and angle of attack are neglected. The method follows Martin and also, like Martin, Sedney uses slender-body theory to calculate the force and moment on the body that results when the boundary layer displacement surface is added to the body of revolution. No experimental test of the predictions seems to be available.

In the present investigation a method is developed to calculate the Magnus force and moment for a body of revolution of general shape with an unseparated turbulent boundary layer. Although the boundary layer calculation is for incompressible flow, the calculation method can be used for Mach numbers up to the transonic range because Mach number effects on boundary layer flow are usually small for local Mach numbers less than unity. The boundary layer calculation is based on the momentum integral method. The force on the body is calculated by slender-body theory (References 5 and 6). A discussion is given of the calculation of the force by a more exact method than slender-body theory, namely, the method of Hess and Smith (References 7 and 8).

ANAYLSIS

In order to calculate the force and moment on a spinning body the effective shape of the body in an inviscid flow is needed. The effective shape is found by calculating the boundary layer displacement surface and adding it to the body of revolution. The displacement surface δ^* is the surface, which, added to a body in an inviscid flow, results in a body with the same streamlines as those outside

the boundary layer in the real viscous flow (Reference 9). Therefore, because according to boundary layer theory the pressure difference across the boundary layer is negligible, the pressure on the real body in the viscous flow is the same as on the body plus δ^* in the inviscid flow.

Displacement Surface

To find the displacement surface, δ^*, use is made of the fact that the streamlines outside the boundary layer are not changed by replacing the body with the boundary layer over it in the viscous flow by the body with δ^* added to it in an inviscid flow. Consequently the velocity component w on these streamlines is also unchanged. To find w on a streamline near the outer edge of the boundary layer the continuity equation is used; for a steady flow with the coordinate system shown in Figure 2 it is

$$\cos\phi \frac{\partial}{\partial x}(\rho u r) + \frac{\partial}{\partial \theta}(\rho v) + \frac{\partial}{\partial y}(\rho w r) = 0 \qquad (1)$$

where ρ, u, and v are time mean values and ρw is $(\rho w + \langle \rho" w" \rangle)$. Equation (1) is the same as Equation (19) page 414 Reference 10 when r is put equal to r_o. The coordinate system is fixed in the fluid and the body rotates around its axis of symmetry. All quantities are non-dimensional; the velocities are non-dimensionalized by $\bar{V}_\infty$, the lengths by $\bar{L}$, the densities by $\bar{\rho}_\infty$, and the pressures and shear stresses by $\bar{\rho}_\infty \bar{V}_\infty^2$.

An integration of (1) with respect to y up to y_q, where y_q is slightly greater than the boundary layer thickness, results in

$$(\rho w)_{y_q} = -\frac{\cos\phi}{r} \int_o^{y_q} \frac{\partial}{\partial x}(\rho u r)\, dy - \frac{1}{r} \int_o^{y_q} \frac{\partial}{\partial \theta}(\rho v)\, dy \qquad (2)$$

For an inviscid flow over the body with δ^* added to it the result for $(\rho w)_{y_q}$ is

$$(\rho w)_{y_q} = -\frac{\cos\phi}{r}\int_{\delta^*}^{y_q}\frac{\partial}{\partial x}(\rho_e u_e r)dy - \frac{1}{r}\int_{\delta^*}^{y_q}\frac{\partial}{\partial\theta}(\rho_e v_e)dy + (\rho w)_{\delta^*} \qquad (3)$$

The term $(\rho w)_{\delta^*}$ appears because the δ^* surface has a slope with respect to the body and w is normal to the surface without δ^*. In Equation (3) ρ, u, and v have the subscript "e" because the flow is inviscid and the velocity varies negligibly slowly with y.

Then, because the streamline at y_q is the same for both the viscous and the inviscid flow ρw is also the same. Therefore, equating (2) and (3) the result is

$$-\frac{\cos\phi}{r}\int_{o}^{y_q}\frac{\partial}{\partial x}[r(\rho_e u_e - \rho u)]dy - \frac{1}{r}\int_{o}^{y_q}\frac{\partial}{\partial\theta}(\rho_e v_e - \rho v)dy$$

$$+\frac{\cos\phi}{r}\int_{o}^{\delta^*}\frac{\partial}{\partial x}(\rho_e u_e r)dy + \frac{1}{r}\int_{o}^{\delta^*}\frac{\partial}{\partial\theta}(\rho_e v_e)dy + (\rho w)_{\delta^*} = 0 \qquad (4)$$

The relations

$$\frac{\partial}{\partial x}\int_0^{\delta^*}\rho_e u_e r\,dy = \int_0^{\delta^*}\frac{\partial}{\partial x}(\rho_e u_e r)\,dy + \frac{\partial \delta^*}{\partial x}\, r\rho_e u_e \tag{5}$$

$$\frac{\partial}{\partial \theta}\int_0^{\delta^*}\rho_e v_e\,dy = \int_0^{\delta^*}\frac{\partial}{\partial \theta}(\rho_e v_e)\,dy + \frac{\partial \delta^*}{\partial \theta}\rho_e v_e \tag{6}$$

$$\frac{\partial}{\partial x}\int_0^{y_q} r(\rho_e u_e - \rho u)\,dy = \int_0^{y_q}\frac{\partial}{\partial x}\,[r(\rho_e u_e - \rho u)]\,dy \tag{7}$$

$$\frac{\partial}{\partial \theta}\int_0^{y_q}(\rho_e v_e - \rho v)\,dy = \int_0^{y_q}\frac{\partial}{\partial \theta}(\rho_e v_e - \rho v)\,dy \tag{8}$$

are now used in Equation (4). The distance r is taken as the body radius r_o, consistent with the thin boundary layer assumption. In the integrals in Equations (5), (6), (7), and (8), $\rho_e u_e$ and $\rho_e v_e$ are equal to their values at y_q. This causes an error of $0(\delta^2)$ in the integrals, which is negligible with respect to the integrals themselves which are of $0(\delta)$. Then Equation (4) becomes

$$- \frac{\cos\phi}{r_o} \frac{\partial}{\partial x} r_o \int_o^{y_q} (\rho_e u_e - \rho u)\,dy - \frac{1}{r_o} \frac{\partial}{\partial \theta} \int_o^{y_q} (\rho_e v_e - \rho v)\,dy + \frac{\delta^*}{r_o} \cos\phi \frac{\partial}{\partial x}(r_o \rho_e u_e)$$

$$+ \frac{\delta^*}{r_o} \frac{\partial}{\partial \theta}(\rho_e v_e) + (\rho w)_{\delta^*} = 0 \qquad (9)$$

To find $(\rho w)_{\delta^*}$ use is made of the fact that in the inviscid flow over the body with δ^* added to it the velocity component normal to the displacement surface δ^* is zero. The velocity vector $\vec{V}_e$ along the δ^* surface is

$$\vec{V}_e = \hat{a}\, u_e + \hat{b}\, v_e + \hat{c}\, w_e \qquad (10)$$

where $\hat{a}$ is a unit vector along the body surface and in the x direction, $\hat{b}$ is a unit vector along the body surface in a plane x = constant, and $\hat{c}$ is a unit vector normal to the body surface and outward. The condition for no velocity normal to the displacement surface is

$$\vec{V}_e \cdot \vec{N} = 0 \qquad (11)$$

where $\vec{N}$ is a vector normal to the body plus δ^* and outward from the surface. To find $\vec{N}$ note that $\vec{N}$ is normal to each of the two vectors $(\hat{a} \cos \chi_1 + \hat{c} \sin \chi_1)$ and $(\hat{b} \cos \chi_2 + \hat{c} \sin \chi_2)$ which lie in the displacement surface along θ = c and x = c, respectively. The angles χ_1 and χ_2 are given by

$$\cos\chi_1 = \frac{\Delta s_x}{D_1} \qquad (12)$$

$$\sin\chi_1 = \frac{\frac{\partial \delta^*}{\partial s_x} \Delta s_x}{D_1} \tag{13}$$

$$\cos\chi_2 = \frac{r_o \Delta\theta}{D_2} \tag{14}$$

$$\sin\chi_2 = \frac{\frac{\partial \delta^*}{\partial \theta} \Delta\theta}{D_2} \tag{15}$$

where

$$D_1 = \sqrt{\Delta s_x^2 + \left(\frac{\partial \delta^*}{\partial s_x} \Delta s_x\right)^2} \tag{16}$$

and

$$D_2 = \sqrt{r_o^2 \Delta\theta^2 + \left(\frac{\partial \delta^*}{\partial \theta} \Delta\theta\right)^2} \tag{17}$$

Then

$$\vec{N} = (\hat{a} \cos\chi_1 + \hat{c} \sin\chi_1) \times (\hat{b} \cos\chi_2 + \hat{c} \sin\chi_2) \tag{18}$$

or

$$\vec{N} = \hat{c}\cos\chi_1\cos\chi_2 - \hat{b}\cos\chi_1\sin\chi_2 - \hat{a}\sin\chi_1\cos\chi_2 \tag{19}$$

Then (11) becomes

$$\vec{V}_e \cdot \vec{N} = w_e\cos\chi_1\cos\chi_2 - v_e\cos\chi_1\sin\chi_2 - u_e\sin\chi_1\cos\chi_2 = 0 \tag{20}$$

or with (12) through (17),

$$w_e = u_e \frac{\partial\delta^*}{\partial s_x} + \frac{v_e}{r_o} \frac{\partial\delta^*}{\partial\theta} \tag{21}$$

or

$$(\rho w)_{\delta^*} = \rho_e u_e \cos\phi \frac{\partial\delta^*}{\partial x} + \frac{\rho_e v_e}{r_o} \frac{\partial\delta^*}{\partial\theta} \tag{22}$$

When (22) is substituted into (9) the result, after rearranging terms, is

$$\cos\phi\frac{\partial}{\partial x}\{r_o[\rho_e u_e\delta^* - \int_o^{y_q}(\rho_e u_e - \rho u)dy]\} + \frac{\partial}{\partial\theta}[\rho_e v_e\delta^* - \int_o^{y_q}(\rho_e v_e - \rho v)dy] = 0 \tag{23}$$

Equation (23) is the equation for the displacement surface δ^* (see Reference 9). The Equation (23) is a partial differential equation for δ^*. When Equation (23) is expanded the result is

$$r_o\cos\phi\rho_e u_e\frac{\partial\delta^*}{\partial x} + \rho_e v_e\frac{\partial\delta^*}{\partial\theta} = -\delta^*\left[r_o\cos\phi\frac{\partial\rho_e u_e}{\partial x} + \cos\phi\frac{\partial r_o}{\partial x}\rho_e u_e + \frac{\partial\rho_e v_e}{\partial\theta}\right]$$

$$+ \cos\phi\frac{\partial r_o}{\partial x}\int_o^\delta(\rho_e u_e-\rho u)dy + r_o\cos\phi\frac{\partial}{\partial x}\int_o^\delta(\rho_e u_e-\rho u)dy$$

$$+ \frac{\partial}{\partial\theta}\int_o^\delta(\rho_e v_e-\rho v)dy \qquad (24)$$

where the upper limit y_q in (23) has been replaced by δ in (24); δ is the smallest value of y for which simultaneously $\rho u = \rho_e u_e$ and $\rho v = \rho_e v_e$.

Equation (24) is a Lagrange linear partial differential equation. To obtain a solution the two subsidiary equations

$$\frac{dx}{r_o\cos\phi\rho_e u_e} = \frac{d\theta}{\rho_e v_e} \qquad (25)$$

and

$$\frac{dx}{r_o\cos\phi\rho_e u_e} = \frac{d\delta^*}{Q} \qquad (26)$$

are to be integrated; the quantity Q is the right hand side of Equation (24). Equation (25) is

$$\frac{d\theta}{dx} = \frac{v_e}{r_o u_e \cos\phi} \tag{27}$$

and is the equation of an inviscid flow streamline over the body. To integrate (26) requires that the integrals in (24) be known. That is, the boundary layer velocity distribution and thickness must be known. When the boundary layer properties are known, Equations (25) and (26) are integrated together thereby giving δ^* along a streamline. By integrating (25) and (26) along a sufficient number of streamlines the displacement surface δ^* on the body is calculated.

Momentum Integral Equations

For thin boundary layers the equations of motion are (Reference 10 page 14)

$$\rho u \cos\phi \frac{\partial u}{\partial x} + \frac{\rho v}{r_o}\frac{\partial u}{\partial \theta} + \rho w \frac{\partial u}{\partial y} - \frac{\cos\phi}{r_o}\frac{\partial r_o}{\partial x}\rho v^2 = -\cos\phi\frac{\partial P}{\partial x} + \frac{\partial \tau_x}{\partial y} \tag{28}$$

and

$$\rho u \cos\phi \frac{\partial v}{\partial x} + \frac{\rho v}{r_o}\frac{\partial v}{\partial \theta} + \rho w \frac{\partial v}{\partial y} + \frac{\cos\phi}{r_o}\frac{\partial r_o}{\partial x}\rho uv = -\frac{1}{r}\frac{\partial P}{\partial \theta} + \frac{\partial \tau_\theta}{\partial y} \tag{29}$$

and the continuity equation is

$$\frac{\cos\phi}{r_o}\frac{\partial}{\partial x}(\rho u r_o) + \frac{1}{r_o}\frac{\partial}{\partial \theta}(\rho v) + \frac{\partial}{\partial y}(\rho w) = 0 \tag{1a}$$

To obtain the momentum integral equations the x equation of motion (28) and the θ equation of motion (29) are integrated with respect to y in the usual way with the help of the equation of continuity. The result for the x equation is

$$r_o\cos\phi\frac{\partial}{\partial x}\int_o^\delta \rho u(u_e-u)dy + \sin\phi\int_o^\delta \rho u(u_e-u)dy + r_o\cos\phi\frac{\partial u_e}{\partial x}\int_o^\delta (\rho_e u_e-\rho u)dy \tag{30}$$

$$+\frac{\partial}{\partial\theta}\int_o^\delta \rho v(u_e-u)dy + \frac{\partial u_e}{\partial\theta}\int_o^\delta (\rho_e v_e-\rho v)dy - \sin\phi\int_o^\delta (\rho_e v_e^2-\rho v^2)dy = \tau_{w_x} r_o$$

For the θ equation the result is

$$\frac{\partial}{\partial\theta}\int_o^\delta \rho v(v_e-v)dy + \frac{\partial v_e}{\partial\theta}\int_o^\delta (\rho_e v_e-\rho v)dy + r_o\cos\phi\frac{\partial}{\partial x}\int_o^\delta \rho u(v_e-v)dy$$

$$+\sin\phi\int_o^\delta \rho u(v_e-v)dy + r_o\cos\phi\,\frac{\partial v_e}{\partial x}\int_o^\delta (\rho_e u_e-\rho u)dy + \sin\phi\int_o^\delta (\rho_e u_e v_e-\rho uv)dy$$

$$= \tau_{w_\theta} r_o \tag{31}$$

These equations are the same as on page 416 of Reference 10 in different notation. In order to use the momentum Equations (30) and (31) to calculate the terms $\int_o^\delta (\rho_e u_e-\rho u)dy$ and $\int_o^\delta (\rho_e v_e-\rho v)dy$ in Equation (24) for the displacement surface δ^* an expression for the velocity profile through the boundary layer is needed.

Velocity Profile

The velocity profile of the velocity component in the direction of the outer streamline is assumed to be

$$\frac{u_q - u_{q,w}}{q_e - u_{q,w}} = f(\zeta) \tag{32}$$

where $\zeta=y/\delta$, and the velocity profile for the velocity component perpendicular to the outer streamline is assumed to be

$$\frac{v_q - v_{q,w}}{q_e - u_{q,w}} = \psi g(\zeta) f(\zeta) \tag{33}$$

In (32) and (33) q_e is the speed along the streamline at the outer edge of the boundary layer; u_q is the speed in the direction of the outer streamline and v_q is the speed in the direction perpendicular to the outer streamline. The quantity ψ is an as yet undetermined parameter. At the surface (see Figure 3)

$$u_{q,w} = \omega r_o \sin a, \tag{34}$$

and

$$v_{q,w} = \omega r_o \cos a, \tag{35}$$

where a is the angle between the outer streamline and a line $\theta=c$. Also, from (32) $f(o)=0$ and $f(1)=1$. At $\zeta=1$, $v_q=0$ by definition. Therefore from (33) and $f(1)=1$ it follows that

$$g(1) = \frac{-v_{q,w}}{\psi(q_e - u_{q,w})} \tag{36}$$

Also, division of (33) by (32) results in

$$\frac{v_q - v_{q,w}}{u_q - u_{q,w}} = \psi_q \tag{37}$$

As $y \to o$ (37) becomes

$$\mathop{\mathcal{L}}_{y\to o} \frac{v_q - v_{q,w}}{u_q - u_{q,w}} = \psi\, g(o) \tag{38}$$

The quantity $g(o)$ is put equal to unity. Then (38) becomes

$$\mathop{\mathcal{L}}_{y\to o} \frac{\partial v_q}{\partial u_q} = \mathop{\mathcal{L}}_{y\to o} \frac{\frac{\partial v_q}{\partial y}}{\frac{\partial u_q}{\partial y}} = \psi \tag{39}$$

The quantity $\bar{\mu}_w \left(\frac{\partial \bar{v}_q}{\partial \bar{y}}\right)_w$ equals the shear on the surface in a direction normal to the outer streamline; a positive value means the shear acts in the direction of increasing θ. The quantity $\bar{\mu}_w \left(\frac{\partial \pi_q}{\partial \bar{y}}\right)_w$ is equal to the shear acting on the surface in the direction of the outer streamline flow. Consequently ψ is the tangent of the angle measured from the direction of the outer streamline to the direction of the surface shear stress; ψ is positive in the direction of increasing θ.

The function $g(\zeta)$ is taken to be

$$g(\zeta) = (1-\zeta)^{\ell} + a_o + b_o\, \zeta \tag{40}$$

The condition g(o)=1, previously imposed, gives $a_o=0$. From the expression (36) for g(1) and from (40), the result is

$$b_o = - \frac{v_{q,w}}{\psi[q_e - u_{q,w}]}$$

Therefore (40) becomes

$$g(\zeta) = (1-\zeta)^{\ell} - \frac{v_{q,w}}{\psi[q_e - u_{q,w}]} \zeta \qquad (41)$$

The exponent ℓ is found by considering conditions at the stagnation point of a rotating body at an angle of attack; thus the stagnation point is not on the axis of rotation. At the stagnation point the outer stream velocity is zero and the surface has a rotational velocity ωr_o. Let

$$v = \omega r_o F(\zeta) \qquad (42)$$

where F(o)=1 and F(1)=0, that is, the fluid has velocity ωr_o at the surface and zero velocity outside the boundary layer. Also, u, the velocity in the direction of s_x is zero at the stagnation point. The relations between the velocity components u_q and v_q and the velocity components u and v are

$$u_q = u\cos a + v\sin a \qquad (43)$$

and

$$v_q = - u\sin a + v\cos a \qquad (44)$$

At the stagnation point (43) and (44) becomes, with (42),

$$u_q = \omega r_o F \sin a \tag{45}$$

and

$$v_q = \omega r_o F \cos a \tag{46}$$

Equations (45), (34), (32) and $q_e=0$ result in

$$F = 1-f \tag{47}$$

From (34), (35), $q_e=0$, (46) and (47) are used in (33) the result is

$$\cot a = \psi g \tag{48}$$

From (39), (45) and (46) it follows that

$$\cot a = \psi \tag{49}$$

Therefore from (48) it follows that $g=1$ for all ζ at the stagnation point. Now consider Equation (41). At the stagnation point $q_e=0$, $\psi=\cot a$, and relations (45) and (46) with $F(o)=1$ hold.

Equation (41) then becomes

$$g(\zeta) = (1-\zeta)^{\ell} + \zeta \tag{50}$$

Therefore to have $g(\zeta)=1$ at the stagnation point, put $\ell=1$. Then (41) becomes

$$g(\zeta) = 1 - \zeta \left\{ 1 + \frac{v_{q,w}}{[q_e - u_{q,w}]} \right\} \tag{51}$$

The velocity profile (32) is taken to be a power profile by putting

$$f(\zeta) = \zeta^n \tag{52}$$

Because the velocities that appear in the two momentum integral Equations (30) and (31) contain u and v it is necessary to express u and v in terms of the velocities u_q and v_q that appear in (32) and (33). The relations are

$$u = u_q \cos a - v_q \sin a \tag{53}$$

and

$$v = u_q \sin a + v_q \cos a \tag{54}$$

When u_q and v_q are found from (32) and (33) and (34), (35), (51), and (52) are used, Equations (53) and (54) become

$$u = (A\zeta^n + B)\cos a - [A\psi(\zeta^n - \zeta^{n+1}) + C(1-\zeta^{n+1})] \sin a \tag{55}$$

and

$$v = (A\zeta^n+B)\sin a + [A\psi(\zeta^n-\zeta^{n+1}) + C(1-\zeta^{n+1})]\cos a \tag{56}$$

where

$$A = q_e - u_{q,w} = q_e - \omega r_o \sin a \tag{57}$$

$$B = u_{q,w} = \omega r_o \sin a \tag{58}$$

$$C = v_{q,w} = \omega r_o \cos a \tag{59}$$

Differential Equations for δ and ψ

Expressions (55) and (56) are put into the integral momentum Equations (30) and (31) and the integrals evaluated. The density is taken constant from here on in the boundary layer analysis. A sample term is $\int_o^\delta (u_e-u)dy$ which is written as $\delta\int_o^1 (u_e-u)d\zeta$

The result is

$$\int_o^1 (u_e-u)d\zeta = A\frac{n}{n+1}\cos a - A\psi\frac{n}{n+1}\sin a + (A\psi+C)\frac{n+1}{n+2}\sin a$$

or

$$\int_o^1 (u_e-v)d\zeta = AG_7\cos a + \psi AG_2\sin a + CG_4\sin a$$

where

$$G_2 = \frac{1}{(n+1)\ (n+2)}$$

$$G_4 = \frac{n+1}{n+2}$$

$$G_7 = \frac{n}{n+1}$$

There are fourteen G's; they are listed in Table 1.

In Table II are listed the integrals that occur in Equations (30) and (31). The procedure results in two partial differential equations with δ and ψ as dependent variables and x and θ as independent variables. The x equation, the result of (30) and (55) and (56) is

$$r_o\cos\phi\frac{\partial\delta}{\partial x}[\psi^2 J_1+\psi J_2+J_3] + r_o\cos\phi\frac{\partial\psi}{\partial x}\,\delta[2\psi J_1+J_2]$$

$$+ \frac{\partial\delta}{\partial\theta}[\psi^2 J_6+\psi J_7+J_8] + \frac{\partial\psi}{\partial\theta}\,\delta[2\psi J_6+J_7]$$

$$= r_o\,\tau_{w_x} - \delta\{[\psi^2\frac{\partial J_1}{\partial x} + \psi\frac{\partial J_2}{\partial x} + \frac{\partial J_3}{\partial x}]r_o\cos\phi \qquad (60)$$

$$+[\psi^2 J_1+\psi J_2+J_3]\frac{\partial r_o}{\partial x}\cos\phi + r_o\cos\phi\frac{\partial u_e}{\partial x}[\psi J_4+J_5]$$

$$+[\psi^2\frac{\partial J_6}{\partial\theta}+ \psi\frac{\partial J_7}{\partial\theta}+ \frac{\partial J_8}{\partial\theta}] + \frac{\partial u_e}{\partial\theta}[\psi J_{18}+J_{19}]$$

$$-[\psi^2 J_9+\psi J_{10}+J_{11}]\frac{\partial r_o}{\partial x}\cos\phi\}$$

The θ equation, the result of (31) and (55) and (56) is

$$r_o\cos\phi\frac{\partial\delta}{\partial x}[\psi^2 J_6+\psi J_{14}+J_{15}] + r_o\cos\phi\frac{\partial\psi}{\partial x}\delta\ [2\psi J_6+J_{14}]$$

$$+ \frac{\partial\delta}{\partial\theta}[\psi^2 J_9+\psi J_{12}+J_{13}] + \frac{\partial\psi}{\partial\theta}\,\delta[2\psi J_9+J_{12}] \qquad (61)$$

$$= r_o\tau_{w_0} - \delta\{[\psi^2\frac{\partial J_6}{\partial x}+\psi\frac{\partial J_{14}}{\partial x} + \frac{\partial J_{15}}{\partial x}]r_o\cos\phi + [\psi^2 J_6+\psi J_{14}+J_{15}]\frac{\partial r_o}{\partial x}\cos\phi$$

$$+ \frac{\partial v_e}{\partial x}\,[\psi J_4+J_5]r_o\cos\phi + [\psi^2\frac{\partial J_9}{\partial\theta} + \psi\frac{\partial J_{12}}{\partial\theta} + \frac{\partial J_{13}}{\partial\theta}]$$

$$+ \frac{\partial v_e}{\partial\theta}\,[\psi J_{18}+J_{19}] + [\psi^2 J_6+\psi J_{16}+J_{17}]\frac{\partial r_o}{\partial x}\cos\phi\}$$

The J's are listed in Table III. They are independent of δ and ψ and are calculated from the inviscid flow velocity distribution over the body, spin rate, and the distribution $r_o(x)$.

The simultaneous solution of (60) and (61) gives $\frac{\partial\delta}{\partial x}$, $\frac{\partial\delta}{\partial\theta}$, $\frac{\partial\psi}{\partial x}$ and $\frac{\partial\psi}{\partial\theta}$ at a point x,θ. An iteration process is used. First (60) and (61) are solved for $(\frac{\partial\delta}{\partial x})_1$ and $(\frac{\partial\psi}{\partial x})_1$ with $\frac{\partial\delta}{\partial\theta} = 0$ and $\frac{\partial\psi}{\partial\theta} = 0$. Then the values of $(\frac{\partial\delta}{\partial x})_1$ and $(\frac{\partial\psi}{\partial x})_1$ are substituted into (60) and (61), and (60) and (61) are solved for $(\frac{\partial\delta}{\partial\theta})_1$ and $(\frac{\partial\psi}{\partial\theta})_1$. Then $(\frac{\partial\delta}{\partial\theta})_1$ and $(\frac{\partial\psi}{\partial\theta})_1$ are substituted into (60) and (61), and (60) and (61) are solved for $(\frac{\partial\delta}{\partial x})_2$ and $(\frac{\partial\psi}{\partial x})_2$. These values of $(\frac{\partial\delta}{\partial x})_2$ and $(\frac{\partial\psi}{\partial x})_2$ are substituted into (60) and (61), and (60) and (61) solved for $(\frac{\partial\delta}{\partial\theta})_2$ and $(\frac{\partial\psi}{\partial\theta})_2$. These values are then used to find $(\frac{\partial\delta}{\partial x})_3$ and $(\frac{\partial\psi}{\partial x})_3$ which are used to find $(\frac{\partial\delta}{\partial\theta})_3$ and $(\frac{\partial\psi}{\partial\theta})_3$ and so on until further iteration produces a negligible change in $(\frac{\partial\delta}{\partial x})$, $(\frac{\partial\delta}{\partial\theta})$, $(\frac{\partial\psi}{\partial x})$ and $(\frac{\partial\psi}{\partial\theta})$. In the calculations the

iteration is stopped either after 25 iterations or when $\left(\frac{\delta_i}{\delta_{i-1}} - 1\right)_{x+\Delta x}$ and $\left(\frac{\psi_i}{\psi_{i-1}} - 1\right)_{x+\Delta x}$ are both less than .001. The subscript i is the iteration number; $\delta_{x+\Delta x}$ and $\psi_{x+\Delta x}$ are the values of δ and ψ at the next point along a streamline. They are found from

$$\Delta\delta = \left[\left(\frac{\partial\delta}{\partial x}\right)_\theta + \left(\frac{\partial\delta}{\partial\theta}\right)_x \frac{d\theta}{dx}\right] \Delta x \tag{62}$$

and

$$\Delta\psi = \left[\left(\frac{\partial\psi}{\partial x}\right)_\theta + \left(\frac{\partial\psi}{\partial\theta}\right)_x \frac{d\theta}{dx}\right] \Delta x \tag{63}$$

where $\frac{d\theta}{dx}$ is obtained from Equation (27), the equation for a streamline.

Initial Conditions for δ and ψ

In order to begin the integration of (60) and (61), the values of δ and ψ at the stagnation point are needed. Up to now a method for calculating δ at the stagnation point of a spinning body when the stagnation point is not on the axis of rotation has not been found. Consequently, the needed value of δ is obtained by extrapolation from the value of δ at the stagnation point on a spinning body at zero angle of attack and the value of δ at the stagnation point of a non-spinning body at an angle of attack. Thus, it is assumed that δ at the stagnation point when spin and angle of attack are both present can be written as

$$\delta_{\alpha,p} = \delta_{o,o} + \left(\frac{\partial\delta}{\partial p}\right)_{o,o} p + \left(\frac{\partial\delta}{\partial\alpha}\right)_{o,o} \alpha \tag{64}$$

or with

$$\left(\frac{\partial \delta}{\partial p}\right)_{o,o} = \left(\frac{\delta_{o,p} - \delta_{o,o}}{p}\right)$$

and

$$\left(\frac{\partial \delta}{\partial \alpha}\right)_{o,o} = \left(\frac{\delta_{\alpha,o} - \delta_{o,o}}{\alpha}\right)$$

Equation (64) becomes

$$\delta_{\alpha,p} = \delta_{o,p} + \delta_{\alpha,o} - \delta_{o,o} \tag{65}$$

For $\alpha = 0$ the inviscid flow streamlines lie along θ = constant and the entire flow is independent of θ. Therefore to find $\delta_{o,p}$ and $\delta_{o,o}$ there is used, $a = 0$, $v_e = 0$, and $\frac{\partial}{\partial \theta} = 0$, in (60) and (61). As the stagnation point is approached $A \to q_e \to u_e$, $B \to o$, and $c \to \omega r_o$. There is obtained, not putting $u_e = o$, $r_o = o$ yet,

$$\begin{aligned} J_1 &= 0 & J_5 &= u_e G_7 \\ J_2 &= 0 & J_6 &= 0 \\ J_3 &= u_e^2 G_7 G_8 & J_7 &= u_e^2 G_{14} \\ J_4 &= 0 & J_8 &= -u_e \omega r_o G_{10} \\ J_9 &= u_e^2 G_{11} & J_{15} &= -u_e \omega r_o G_9 \\ J_{10} &= -2u_e \omega r_o G_5 & J_{16} &= -u_e^2 G_{13} \end{aligned} \tag{66}$$

$$J_{11} = \omega^2 r_o^2 G_6 \qquad J_{17} = -u_e \omega r_o G_9$$

$$J_{12} = -2u_e \omega r_o G_5 \qquad J_{18} = -u_e G_2 \qquad (66)$$

$$J_{13} = \omega^2 r_o^2 G_6 \qquad J_{19} = -\omega r_o G_4$$

$$J_{14} = -u_e^2 G_{13}$$

Because a = 0 for all x it can be shown that

$$\frac{\partial J_1}{\partial x} = 0 \qquad \frac{\partial J_6}{\partial x} = 0$$

$$\frac{\partial J_2}{\partial x} = 0 \qquad \frac{\partial J_{14}}{\partial x} = -2u_e \frac{\partial u_e}{\partial x} G_{13} \qquad (67)$$

$$\frac{\partial J_3}{\partial x} = 2u_e \frac{\partial u_e}{\partial x} G_8 G_7 \qquad \frac{\partial J_{15}}{\partial x} = 0$$

When these values are substituted into (60) and the resulting equation is divided through by $r_o u_e^2$ the result is

$$\frac{\partial \delta G_7 G_8}{\partial x} \cos\phi = \frac{\tau_{wx}}{u_e^2} - \delta \left\{ \frac{1}{u_e} \frac{\partial u_e}{\partial x} \cos\phi \ (2G_7 G_8 + G_7) \right.$$

$$+ \frac{G_7 G_8}{r_o} \frac{\partial r_o}{\partial x} \cos\phi - \frac{\psi^2 G_{11}}{r_o} \frac{\partial r_o}{\partial x} \cos\phi + \frac{2\psi\omega}{u_e} G_5 \frac{\partial r_o}{\partial x} \cos\phi \qquad (68)$$

$$\left. - \frac{\omega^2 r_o}{u_e^2} G_6 \frac{\partial r_o}{\partial x} \cos\phi \right\}$$

At $\alpha = 0$ the relations $u_e = u'_{e,s} r_o$, and $r_o = s_x$ hold. Also $\frac{\partial(\ )}{\partial x} \cos\phi = \frac{\partial(\ )}{\partial s_x}$. The friction coefficient is written as

$$\frac{\tau_{w_x}}{\bar{u}_e^2} = \frac{\bar{\mu}\left(\frac{\partial \bar{u}}{\partial y}\right)_w}{\bar{\rho}\,\bar{u}_e^2} = \frac{\bar{\nu}\left(\frac{\partial u/u_e}{\partial \zeta}\right)_w}{\bar{V}_\infty u_e \delta \bar{L}} = \frac{\left(\frac{\partial u/u_e}{\partial \zeta}\right)_w}{u'_{e,s} r_o\, \delta\, Re_L} \tag{69}$$

When these relations are substituted into (68), the result is

$$\frac{\partial \delta G_7 G_8}{\partial s} = \frac{1}{u'_{e,s} r_o \delta}\left\{ \frac{\left(\frac{\partial u/u_e}{\partial \zeta}\right)_w}{Re_L} - u'_{e,s}\delta^2 [3G_7G_8 + G_7 - \psi^2 G_{11} \right.$$

$$\left. + \frac{2\psi\omega}{u'_{e,s}} G_5 - \frac{\omega^2}{u'^2_{e,s}} G_6] \right\} \tag{70}$$

The quantity $\delta G_7 G_8$ is equal to the ratio of the momentum thickness to the boundary layer thickness δ, $\int_0^1 \zeta^n(1-\zeta^n)d\zeta$. At the stagnation point $r_o = 0$. Consequently to avoid an infinite value of $\frac{\partial \delta G_7 G_8}{\partial s}$,

which is physically unrealistic, it is necessary that the term inside the braces on the right hand side of (70) be zero; that is,

$$\frac{\left(\frac{\partial u/u_e}{\partial \zeta}\right)_w}{\delta^2 u'_{e,s} Re_L} - (3G_7G_8+G_7) + \psi^2 G_{11} - 2\psi \frac{\omega}{u'_{e,s}} G_5 + \frac{\omega^2}{u'^2_{e,s}} G_6 = 0 \qquad (71)$$

When the relations (66) and (67) are used in (61) and the same procedure used that was used to obtain (71) the result is

$$\frac{\left(\frac{\partial v/u_e}{\partial \zeta}\right)_w}{\delta^2 u'_{e,s} Re_L} + 4\psi G_{13} + 4 \frac{\omega}{u'_{e,s}} G_9 = 0 \qquad (72)$$

The ratio $\left(\frac{\partial v/u_e}{\partial \zeta}\right)_w$ can be replaced by an expression involving $\left(\frac{\partial u/u_e}{\partial \zeta}\right)_w$ by using (56) with "a" = 0. That is

$$v = u_e\psi(\zeta^n-\zeta^{n+1}) + \omega r_o(1-\zeta^{n+1}) \qquad (73)$$

Then

$$\frac{\partial v/u_e}{\partial \zeta} = \psi[n\zeta^{n-1}-(n+1)\zeta^n] - \omega r_o(n+1)\zeta^n \qquad (74)$$

Also, from (55)

$$\frac{\partial u/u_e}{\partial \zeta} = n\zeta^{n-1} \tag{75}$$

Therefore from (74) and (75)

$$\left(\frac{\partial v/u_e}{\partial \zeta}\right)_w = \psi \left(\frac{\partial u/u_e}{\partial \zeta}\right)_w \tag{76}$$

Then, with (76), Equation (72) becomes

$$\frac{\psi\left(\frac{\partial u/u_e}{\partial \zeta}\right)_w}{\delta^2 u'_{e,s} Re_L} + 4\psi G_{13} + \frac{4\omega}{u'_{e,s}} G_9 = 0$$

$$\psi_s = \frac{\frac{-4\omega}{u'_{e,s}} G_9}{\left(\frac{\partial u/u_e}{\partial \zeta}\right)_w \frac{1}{\delta^2 u'_{e,s} Re_L} + 4G_{13}} \tag{77}$$

when ψ from (77) is substituted into (71) the result can be written as

$$\frac{1}{\delta^2 u'_{e,s} Re_L}\left(\frac{\partial u/u_e}{\partial \zeta}\right)_w - (3G_7G_8+G_7) + \left(\frac{\omega}{u'_{e,s}}\right)^2 \left\{ \frac{16G_{11}G_9{}^2}{\left[\left(\frac{\partial u/u_e}{\partial \zeta}\right)_w \left(\frac{1}{\delta^2 u'_{e,s} Re_L}\right)+4G_{13}\right]^2} + \frac{8G_9G_5}{\left(\frac{\partial u/u_e}{\partial \zeta}\right)_w \frac{1}{(\delta^2 u'_{e,s} Re_L)} +4\ G_{13}} + G_6 \right\} = 0 \qquad (78)$$

Equation (78) is solved for $\left(\frac{\partial u/u_e}{\partial \zeta}\right)_w \quad \frac{1}{\delta^2 u'_{e,s} Re_L}$ by iteration. When a value is taken for $\left(\frac{\partial u/u_e}{\partial \zeta}\right)_w$, δ is known. In the present investigation $\left(\frac{\partial u/u_e}{\partial \zeta}\right)_w$ is taken as unity which is consistent with laminar flow at the stagnation point and a "power" profile. When $\left(\frac{\partial u/u_e}{\partial \zeta}\right)_w \quad \frac{1}{\delta^2 u'_{e,s} Re_L}$ is known, a substitution into (77) gives ψ.

Thus δ_s and ψ_s can be found for $\alpha = 0$, both for spin and no spin.

The value of δ_s for $\alpha \neq 0$, $\omega = 0$ is found by similar procedure. For $\omega = 0$, the parameters B and C are zero and A = q_e. Near the stagnation point the flow outside the boundary layer can be expressed as (p. 462 Reference 10)

$$u_e = c_1 s_x \qquad (79)$$

$$v_e = c_2 s_\theta \qquad (80)$$

where s_x and s_θ are distances measured from the stagnation point along θ = constant and x = constant, respectively. The equation for a streamline is

$$\frac{ds_\theta}{ds_x} = \frac{v_e}{u_e} \tag{81}$$

or with (79) and (80),

$$\frac{ds_\theta}{ds_x} = c_3 \frac{s_\theta}{s_x} \tag{82}$$

where $c_3 = c_2/c_1$. Equation (82) results in

$$s_\theta = c_4 s_x^{c_3} \tag{83}$$

or

$$\frac{ds_\theta}{ds_x} = c_4 c_3 s_x^{c_3-1} \tag{84}$$

At a stagnation point that is off the axis of revolution of an elongated body of revolution, the radius of curvature of the surface in a plane θ = constant is greater than the radius of curvature in a plane x = c. Consequently $c_2 > c_1$ and so $c_3 > 1$. Therefore all the streamlines except the one for $c_4 = \infty$ have $\frac{ds_\theta}{ds_x} = 0$ at the stagnation point (see Figure 4). Thus for all the streamlines except the one for $c_4 = \infty$, the angle a is zero at the stagnation point. The stagnation point is a nodal point of attachment (p 76 Reference 10).

The values for the J's at the stagnation point are obtained by putting $\omega = 0$ in (66). Moreover, going to the stagnation point but not putting $u_e = 0$ yet, it can be shown that

$$\frac{\partial J_1}{\partial x} = 0 \qquad \frac{\partial J_6}{\partial \theta} = - u_e{}^2 G_{11} \frac{\partial a}{\partial \theta}$$

$$\frac{\partial J_2}{\partial x} = -u_e{}^2 G_1 \frac{\partial a}{\partial x} \qquad \frac{\partial J_7}{\partial \theta} = 2u_e \frac{\partial u_e}{\partial \theta} G_{14}$$

$$\frac{\partial J_3}{\partial x} = 2u_e \frac{\partial u_e}{\partial x} G_8 G_7 \qquad \frac{\partial J_8}{\partial \theta} = u_e{}^2 G_{12} \frac{\partial a}{\partial \theta}$$

$$\frac{\partial J_6}{\partial x} = -u_e{}^2 G_{11} \frac{\partial a}{\partial x} \qquad \frac{\partial J_9}{\partial \theta} = 2u_e \frac{\partial u_e}{\partial \theta} G_{11} \tag{85}$$

$$\frac{\partial J_{14}}{\partial x} = -2u_e \frac{\partial u_e}{\partial x} G_{13} \qquad \frac{\partial J_{12}}{\partial \theta} = -u_e{}^2 (2G_{13} - G_2) \frac{\partial a}{\partial \theta}$$

$$\frac{\partial J_{15}}{\partial x} = u_e{}^2 (2G_9 - G_8) \frac{\partial a}{\partial x} \qquad \frac{\partial J_{13}}{\partial \theta} = 0$$

These relations together with

$$\tau_{w_\theta} = \psi \tau_{w_x}$$

are used (61) and the resulting equation divided through by $u_e{}^2$. The result is

$$-r_o\cos\phi\frac{\partial\delta}{\partial x}G_{13}\,\psi - r_o\cos\phi\frac{\partial\psi}{\partial x}\delta G_{13} + \frac{\partial\delta}{\partial\theta}\psi^2 G_{11} + 2\psi\frac{\partial\psi}{\partial\theta}\delta G_{11}$$

$$= r_o\frac{\tau_{w_x}}{u_e^2}\psi + \delta\left[\frac{2}{u_e}\frac{\partial u_e}{\partial x}G_{13}\psi r_o\cos\phi + 2\psi G_{13}\frac{\partial r_o}{\partial x}\cos\phi + \psi^2 G_{11}\frac{\partial a}{\partial x}r_o\cos\phi\right. \qquad (86)$$

$$+ (2G_9 - G_8)\frac{\partial a}{\partial x}r_o\cos\phi + \frac{\partial v_e}{\partial x}\frac{1}{u_e}G_7 r_o\cos\phi - \psi^2\frac{2}{u_e}\frac{\partial u_e}{\partial\theta}G_{11} + \psi(2G_{13} - G_2)\frac{\partial a}{\partial\theta}$$

$$\left. + \psi\frac{G_2}{u_e}\frac{\partial v_e}{\partial\theta}\right]$$

Now use

$$\frac{\tau_{w_x}}{u_e^2} = \frac{\left(\frac{\partial u/u_e}{\partial\zeta}\right)_w}{Re_L\,\delta\,u_e} \qquad \text{(See Equation (69))} \qquad (87)$$

Also, on the line $\theta = \pi$

$$\frac{\partial a}{\partial x} = 0 \qquad \text{(Appendix A)} \qquad (88)$$

and at the stagnation point

$$\left(\frac{\partial a}{\partial \theta}\right)_s = -\frac{1}{2} \frac{\left(\frac{\partial^2 u_e}{\partial \theta^2}\right)_s}{\left(\frac{\partial v_e}{\partial \theta}\right)_s} \qquad \text{(Appendix A)} \tag{89}$$

Because neither $\left(\frac{\partial^2 u_e}{\partial \theta^2}\right)_s$ nor $\left(\frac{\partial v_e}{\partial \theta}\right)_s$ is zero (Appendix A) the term $\left(\frac{\partial a}{\partial \theta}\right)_s$ is neither zero nor infinite. When (87), (88), (89), and $\frac{1}{u_e}\frac{\partial v_e}{\partial x} = 0$ (Appendix A) are used, the right hand side of (86) becomes

$$\psi\left\{ r_o \frac{\left(\frac{\partial u/u_e}{\partial \zeta}\right)_w}{Re_L\, \delta\, u_e} + \delta\left[\frac{2}{u_e}\frac{\partial u_e}{\partial x} G_{13} r_o \cos\phi + 2G_{13}\frac{\partial r_o}{\partial x}\cos\phi - \frac{2\psi}{u_e}\frac{\partial u_e}{\partial \theta} G_{11}\right.\right.$$

$$\left.\left. + (2G_{13}-G_2)\frac{\partial a}{\partial \theta} + \frac{G_2}{u_e}\frac{\partial v_e}{\partial \theta}\right]\right\} \tag{90}$$

To prevent (90) from becoming infinite as u_e approaches zero at the stagnation point it is necessary that $\psi = 0$ at the stagnation point. Therefore the value of ψ at a stagnation point for $\alpha \neq 0$, $\omega = 0$ is zero.

When $\psi = 0$ and (66) with $\omega = 0$ and (85) are used in (60) the result is

$$r_o \cos\phi \frac{\partial \delta}{\partial x} u_e^2 G_7 G_8 + \frac{\partial \psi}{\partial \theta}\delta u_e^2 G_{14} = r_o \tau_{w_x} \delta \left(2u_e \frac{\partial u_e}{\partial x} r_o \cos\phi\, G_7 G_8\right.$$

$$\left. + u_e^2 G_7 G_8 \cos\phi \frac{\partial r_o}{\partial x} + r_o \cos\phi\, u_e \frac{\partial u_e}{\partial x} G_7 + u_e^2 G_{12}\frac{\partial a}{\partial \theta}\right) \tag{91}$$

Equation (91) is divided through by u_e^2. The term τ_{w_x} becomes $\frac{\tau_{w_x}}{u_e^2}$ which is written as $\frac{1}{u_e \delta Re_L} \left(\frac{\partial u/u_e}{\partial \zeta}\right)_w$. The relation $u_e = u'_{e,s} s_x$ where s_x is measured from the stagnation point is also used, as is the relation $G_{12} = G_7 G_8$. Then (91) becomes

$$r_o \frac{\partial \delta}{\partial s_x} G_{12} + \frac{\partial \psi}{\partial \theta} \delta G_{14} = \frac{r_o}{u'_{e,s} s_x \delta Re_L} \left(\frac{\partial u/u_e}{\partial \zeta}\right)_w - \delta \left[\frac{r_o}{s_x}(2G_7 G_8 + G_7) + G_7 G_8 \left(\frac{\partial r_o}{\partial s_x} + \frac{\partial a}{\partial \theta}\right)\right] \tag{92}$$

In order to prevent the right hand side of (92) from becoming infinite as s_x becomes zero it is necessary that

$$\frac{1}{u'_{e,s} \delta Re_L} \left(\frac{\partial u/u_e}{\partial \zeta}\right)_w - \delta (2G_7 G_8 + G_7) = 0 \tag{93}$$

or

$$\delta_s = \left[\frac{\left(\frac{\partial u/u_e}{\partial \zeta}\right)_w}{u'_{e,s} Re_L \quad (2G_7 G_8 + G_7)}\right]^{\frac{1}{2}} \tag{94}$$

Thus, for $\alpha \neq 0$, $\omega = 0$ the value of δ at the stagnation point is given by (94). The starting value of δ can now be obtained from (65), (78), and (94).

For $\alpha = 0$ the starting value of ψ is gotten from (77). For $\alpha \neq 0$, $\omega = 0$ the starting value of $\dot{\psi}$ is zero. For $\alpha \neq 0$, $\omega \neq 0$ the value of ψ at the stagnation point is obtained by use of (39). Thus

for all streamlines except the one for $c_4 = \infty$ (See (83) and Figure 4) v_q lies in the plane x = constant through the stagnation point because a = 0 there. Therefore at the surface $v_q = \omega r_o$ and $(\frac{\partial v_q}{\partial y}) < 0$ (see (46), (47)). Also $u_q = 0$ for all y at the stagnation point; therefore $\frac{\partial u_q}{\partial y} = 0$ for all y. Thus it follows from (39) that $\psi = -\infty$ for all streamlines at the stagnation point except the one for $c_4 = \infty$. For $c_4 = \infty$, $a = \pi/2$ and similar reasoning results in $\psi = 0$. Thus ψ is double valued at the stagnation point. The integrations are made for $c_4 = \infty$ so that $\psi = -\infty$ is the starting value.

Friction Coefficient

The component of the friction coefficient in the direction of q_e, the velocity at the outer edge of the boundary layer, is approximated by a formula based on δ and on the magnitude of the component in the direction of q_e of the relative velocity of q_e with respect to the surface. The formula is

$$\frac{\bar{\tau}_{w_{q_e}}}{\bar{\rho}[\bar{q}_e - \bar{u}_{q,w}]^2} = \frac{k}{\left[\frac{\bar{\delta}|\bar{q}_e - \bar{u}_{q,w}|}{\bar{\nu}}\right]^m} \tag{95}$$

or

$$\frac{\bar{\tau}_{w_{q_e}}}{\bar{\rho}\bar{V}_\infty 2} = \tau_{w_{q_e}} = \frac{k}{Re_L^{\,m}} \frac{|A|^{2-m}}{\delta^m} \tag{96}$$

Equation (96) is consistent with the expression (32) for the velocity profile in the direction of q_e. The component τ_{w_x} along a meridian is given by (see Figure 5)

$$\tau_{w_x} = \tau_{w_{q_e}} (\cos a - \psi \sin a) \tag{97}$$

and the component in a plane x = constant by

$$\tau_{w_\theta} = \tau_{w_{q_e}} (\sin a + \psi \cos a) \tag{98}$$

Integration of Equation for Displacement Surface

The quantity, Q, in Equation (26) is the right hand side of Equation (24). The integrals $\int_0^\delta (u_e - u)dy$ and $\int_0^\delta (v_e - v)dy$ are given in Table II. The Equation (26) becomes

$$\frac{d\delta^*}{dx} = - \frac{Q}{r_o \cos\phi u_e}$$

or

$$\cos\phi \frac{d\delta^*}{dx} = -\delta^* \left(\frac{\cos\phi}{u_e} \frac{\partial u_e}{\partial x} + \frac{\cos\phi}{r_o} \frac{\partial r_o}{\partial x} + \frac{1}{r_o u_e} \frac{\partial v_e}{\partial \theta}\right)$$

$$+ \frac{\delta}{u_e} \cos\phi \left(\psi \frac{\partial J_4}{\partial x} + J_4 \frac{\partial \psi}{\partial x} + \frac{\partial J_5}{\partial x}\right) + \frac{\cos\phi}{u_e} \left(\frac{\partial \delta}{\partial x} + \frac{\delta}{r_o} \frac{\partial r_o}{\partial x}\right) (\psi J_4 + J_5)$$

$$+ \frac{\delta}{r_o u_e} \left(J_{18} \frac{\partial \psi}{\partial \theta} + \psi \frac{\partial J_{18}}{\partial \theta} + \frac{\partial J_{19}}{\partial \theta}\right) + \frac{1}{r_o u_e} \frac{\partial \delta}{\partial \theta} (J_{18} \psi + J_{19}) \tag{99}$$

The quantities δ, ψ, and their derivatives are obtained by use of (60), (61), (62) and (63). The derivatives of the J's are obtained by calculating the J's at $x+\Delta x$ and $\theta+\Delta^\theta$ and using $\frac{\partial J}{\partial x} \cong \frac{\Delta J}{\Delta x}$ and $\frac{\partial J}{\partial \theta} \cong \frac{\Delta J}{\Delta \theta}$. The velocity derivatives and $\frac{\partial r_o}{\partial x}$ are obtained from the velocity distribution and shape of the body. The initial value of δ^* is taken as $\frac{\delta_s}{2}$ which is valid for a power profile with n=1, the

approximation to a laminar profile at the stagnation point. In (99), the derivative $\frac{d\delta^*}{dx}$ is along a streamline. Thus (27), (60), (61), and (99) are integrated simultaneously step-by-step. The result is δ, ψ, δ^*, and the streamline path $\theta(x)$. Different streamlines are obtained by beginning the integrations at points on a circle of small radius in the tangent plane at the stagnation point. Through each point on the circle goes only one streamline; the entire streamline is thus fixed by choosing the point on the tangent circle. The relation for the initial value of θ in the integration is

$$\theta = \pi + \Delta\theta = \pi - \frac{I}{r} \sin \eta \qquad (100)$$

and the relation for the initial value of x is

$$x = x_s + \Delta x = x_s + I \cos\phi \cos \eta \qquad (101)$$

The angle η is zero along the meridian $\theta=\pi$ in the direction of positive x. The distance I is the radius of the starting circle.

Derivation of Equations for Magnus Force and Moment

After the displacement surface thickness δ^* has been computed it is added to the body. To calculate the force and moment on the resulting body, slender-body theory (References 5 and 6) can be used. In slender-body theory the force acting on the portion of the body between the nose and a section (C-C) perpendicular to the ξ axis (Figure 6) is given by

$$\frac{\bar{F}}{\bar{\rho}\frac{\bar{V}_\infty^2}{2}\bar{L}^2} = -2i \int_C \Phi_o \, dz_o \qquad \text{(page 50, Reference 6)} \qquad (102)$$

Here Φ_o is the perturbation potential in the z_o plane and is a solution of Laplace's equation.

Equation (102) can be placed in a form more convenient for use in the present analysis by integrating by parts. Then (102) becomes

$$\frac{\bar{F}}{\frac{\bar{\rho}\bar{V}_\infty^2}{2}\bar{L}^2} = -2i\left[z_{o_1}(\Delta\Phi_o) - \int_c z_o \frac{d\Phi_o}{ds_\xi}\, ds_\xi\right] \tag{103}$$

where $\Delta\Phi_o$ is the change in Φ_o in going around the section of the body, starting the ending at the point Z_1. Because $\Delta\Phi_o$ is zero, (See 9.3.15 of Reference 5), Equation (103) becomes

$$\frac{\bar{F}}{\frac{\bar{\rho}_\infty\bar{V}_\infty^2}{2}\bar{L}^2} = 2i \int_c z_o V_s'\, ds_\xi \tag{104}$$

In order to use (104), V_s' must be known along the contour c.

To find V_s' along c the velocity vector $\vec{Q}$ is written as

$$\vec{Q} = V_\infty\left(1+\frac{\partial\Phi}{\partial\xi}\right)\hat{e}_1 + V_\infty\frac{\partial\Phi}{\partial\nu}\hat{\nu} \tag{105}$$

where Φ is the perturbation potential, $\hat{e}_1$ is a unit vector along the ζ axis which is along $\vec{V}_\infty$, and the unit vector $\hat{\nu}$ is normal to the body cross section in a plane ξ=c (Figure 6). The unit normal $\hat{n}$ to the surface of the body is

$$\hat{n} = \frac{\nabla T}{|\nabla T|} \tag{106}$$

where T (ξ, h, β) = c is the equation of the body plus the displacement surface. Because there is no flow through the surface of the body

$$\vec{Q}\cdot\hat{n} = 0 \tag{107}$$

which, with (105) and (106), becomes

$$(1+\frac{\partial\Phi}{\partial\xi})\hat{e}_1\cdot\nabla T + \frac{\partial\Phi}{\partial\nu}\hat{\nu}\cdot\nabla T = 0 \tag{108}$$

To obtain an expression for $\hat{\nu}$ (Figure 6), the unit vector along s_ξ is written as

$$\hat{s} = \hat{h}\,\frac{dh_o}{ds_\xi} + \hat{\beta}h_o\frac{d\beta}{ds_\xi} \tag{109}$$

Then

$$\hat{\nu} = \hat{e}_1 x\hat{s} = -\hat{\beta}\frac{dh_o}{ds_\xi} + \hat{h}\,h_o\frac{d\beta}{ds_\xi} \tag{110}$$

The gradient ∇T is written as

$$\nabla T = \hat{e}_1 T_\xi + \hat{h}T_h + \frac{\hat{\beta}}{h}T_\beta \tag{111}$$

Then (108) becomes

$$(1+\frac{\partial\phi}{\partial\xi})T_\xi + \frac{\partial\phi}{\partial\nu}(T_h h_o \frac{d\beta}{ds_\xi} - \frac{T_\beta}{h_o}\frac{dh_o}{ds_\xi}) = 0 \qquad (112)$$

According to slender-body theory the body has a small slope in a plane $\beta=c$, therefore $T_\xi << 1$. Also the disturbance velocity $\frac{\partial\phi}{\partial\xi}$ is small. Therefore the product $\frac{\partial\phi}{\partial\xi} T_\xi$ in (112) is neglected with the result that

$$\frac{\partial\phi}{\partial\nu} = -\frac{T_\xi}{T_h h_o \frac{d\beta}{ds_\xi} - \frac{T_\beta}{h_o}\frac{dh_o}{ds_\xi}} \qquad (113)$$

But

$$ds_\xi = \sqrt{1+(\frac{1}{h_o}\frac{dh_o}{d\beta})^2}\, h_o d\beta \qquad (\xi=c) \qquad (114)$$

Also

$$T(\xi,h_o,\beta) = h_o - h_o(\xi,\beta) = c$$

Then

$$T_\xi = -\left(\frac{\partial h_o}{\partial \xi}\right)_\beta$$

and

$$T_\beta = -\left(\frac{\partial h_o}{\partial \beta}\right)_\xi$$

and

$$T_h = 1$$

Then (113) becomes

$$\frac{\partial \Phi_o}{\partial \nu} = \frac{\left(\frac{\partial h_o}{\partial \xi}\right)_\beta}{\sqrt{1+\frac{1}{h_o^2}\left(\frac{\partial h_o}{\partial \beta}\right)_\xi^2}} \qquad (115)$$

where Φ in (113) has been replaced by Φ_o. According to the approximations of slender-body theory, it is permissible to replace the three-dimensional disturbance potential Φ in (113) by Φ_o the two-dimensional disturbance potential that is a solution of Laplace's equation in a plane ξ=c.

When the displacement surface has been added to the body, Equation (115) is used to obtain $\frac{\partial \Phi_o}{\partial \nu}$, which equals V_n' the non-dimensional velocity normal to a section ξ=c. The expressions for

$(\frac{\partial h_o}{\partial \xi})_\beta$, h_o, and $(\frac{\partial h_o}{\partial \beta})_\xi$ are derived in Appendix B. Equation (115) gives the non-dimensional velocity normal to a body section $\xi=c$. In the calculation of $(\frac{\partial h_o}{\partial \xi})_\beta$ and $(\frac{\partial h_o}{\partial \beta})_\xi$ the quantity ξ occurs (see B-21 and B-22). The boundary layer calculations provide δ^* and other quantities as functions of x. Consequently ξ is found from a specified value of x. The value of ξ for a fixed value of x, however, depends on θ (See B-39). Consequently when x is fixed the value of ξ varies slightly with θ. The normal velocity $\frac{\partial \Phi_o}{\partial \nu}$ therefore is obtained on a curve that does not lie exactly in a plane $\xi=c$. By putting $R=r_o+\delta^*$ in (B-39) and noting that δ^*, $\sin\alpha$, and r_o are all small of $o(\alpha)$, it follows that the products $r_o \sin\alpha$ and $\delta^* \sin\alpha$ are of the $o(\alpha^2)$. Therefore, the departure from the plane

$$\xi_c = (d+x_o)\cos\alpha$$

of the curve on which $\frac{\partial \Phi_o}{\partial \nu}$ is calculated is of $o(\alpha^2)$, a small quantity when α is small.

If the value of ξ were fixed at the value given by

$$\xi_c = (d+x_o)\cos\alpha$$

the values of x such that $\xi=\xi_c$ could be found by putting $\xi=\xi_c=(d+x_o)\cos\alpha$ in (B-39) and solving for x to obtain

$$x = x_o - R(x,\theta)\cos\theta\tan\alpha \qquad (116)$$

The values of $\frac{\partial \delta^*}{\partial x}$ and $\frac{\partial \delta^*}{\partial \theta}$ for $x(\theta)$ would then be found by interpolation from the computed values of $\frac{\partial \delta^*}{\partial x}$ and $\frac{\partial \delta^*}{\partial \theta}$ at two values of x, one larger and one smaller than the largest and smallest value of x given by (116). This procedure was not carried out in the example calculation for the half-ellipsoid because the additional complication it would have introduced into the calculations was judged not to be justifiable. In the calculation of $(\frac{\partial h_o}{\partial \beta})$, $(\frac{\partial h_o}{\partial \xi})$ etc. (Appendix B),

the exact expressions involve hardly any more computation than expressions that would be obtained by neglecting terms of $o(\alpha^2)$. Consequently the exact expressions were used.

The next step in the process of finding V_s' for use in (104) is to move the origin of coordinates in a plane $\xi=c$ back to the axis of revolution , that is, to the x axis (see Figure 7). The equations for doing this are

$$r' = \sqrt{h_o^2 + 2h_o(1+x)\sin\alpha\cos\beta + (d+x)^2\sin^2\alpha} \qquad (117)$$

and

$$\cos\gamma = \frac{-h_o\sin\beta}{r'} \qquad (118)$$

At this stage in the calculation the vertical velocity V_n' along the distorted circle with its center on the x axis and lying in a ξ = constant plane is known. To find V_s' from V_n' conformal transformation theory as applied in Reference 11, 12 and 13 is used. The method of Reference 11 and 12 is used to transform the distorted circle in the r', γ plane into a circle in the λ, σ plane (Figure 7). Because

$$V_n' = \frac{\partial\Phi_o}{\partial\nu} \approx \frac{\Delta\Phi_o}{\Delta\nu} \qquad (119)$$

and

$$V_n = \frac{\partial\Phi_o}{\partial\lambda} \approx \frac{\Delta\Phi_o}{\Delta\lambda} \qquad (120)$$

and because the potential Φ_o at corresponding points in the Z' and Z planes (Figure 7) is unchanged by a conformal transformation of

the Z' plane into the Z plane (p 163 of Reference 14), it follows from (119) and (120) that

$$\frac{V_n}{V_n'} = \frac{\Delta\nu}{\Delta\lambda} \tag{121}$$

But $\Delta\nu = |dZ'|$ and $\Delta\lambda = |dZ|$; therefore (121) is

$$\frac{V_n}{V_n'} = \left|\frac{dZ'}{dZ}\right| \tag{122}$$

The ratio $\left|\frac{dZ'}{dZ}\right|$ for points on the cross sections in the Z and Z' planes is given by (Equation (37) of Reference 12), namely

$$\left|\frac{dZ'}{dZ}\right| = e^{\Omega-\Omega_o}\,\frac{\sqrt{1+\left(\frac{d\Omega}{d\gamma}\right)^2}}{1+\frac{d\varepsilon}{d\gamma}} \tag{123}$$

where for points on the cross sections in the Z' and Z planes,

$$Z' = r'e^{i\gamma} = r_o e^{\Omega+i\gamma} \tag{124}$$

and

$$Z = \lambda e^{i\sigma} = r_o e^{\Omega_o+i\sigma} \tag{125}$$

and

$$\varepsilon = \sigma - \gamma \tag{126}$$

The constant Ω_o is calculated by

(Page 8 of Reference 11 and Equation C of Reference 12)

$$\Omega_o = \frac{1}{2\pi} \int_0^{2\pi} \Omega(\gamma)\, d\gamma \tag{127}$$

The quantity ε is calculated from

(Equation 13 Reference 12)

$$\varepsilon(\sigma') = -\frac{1}{2\pi} \int_0^{2\pi} \Omega(\sigma) \cot \frac{\sigma - \sigma'}{2} d\sigma \tag{128}$$

Because δ^* is a small fraction of r_o, the cross section in the plane $\xi = c$ is almost a circle. Therefore the quantity σ in (128) can be replaced by γ (see Reference 11) so that the equation used to calculate ε is

$$\varepsilon(\gamma') = -\frac{1}{2\pi} \int_0^{2\pi} \Omega(\gamma) \cot \frac{\gamma - \gamma'}{2} d\gamma \tag{129}$$

For more distorted cross sections iteration is used (see Reference 12).

Once V_n is known on the circle in the λ, σ plane, the velocity V_s can be calculated from an equation given on page 5 of Reference 13; the equation is

$$V_s(\sigma') = -\frac{1}{2\pi}\int_0^{2\pi} V_n(\sigma)\cot\frac{\sigma-\sigma'}{2}d\sigma \tag{130}$$

When $V_s(\sigma)$ is known from (130), $V_s'(r',\gamma)$ is found from

$$V_s'(r',\gamma) = V_s(\sigma)\left|\frac{dZ}{dZ'}\right| \tag{131}$$

where $\left|\frac{dZ}{dZ'}\right|$ is the reciprocal of $\left|\frac{dZ'}{dZ}\right|$ given by (123). Then because $V_s'(r',\gamma) = V_s'(h_o,\beta)$ at corresponding points, the integral in (104) can be evaluated.

Actually it is more convenient to express the integral in (104) in terms of quantities in the (λ,σ) plane. From (131)

$$V_s'(r',\gamma) = V_s(\sigma)\frac{ds}{ds'_\xi} \tag{132}$$

But $V_s'(h_o,\beta) = V_s'(r',\gamma)$ and $ds_\xi = ds'_\xi$ because the z_o and Z' planes are identical except for a shift in origin (see Figure 7). Therefore by using (132) the term $V_s' ds_\xi$ in (104) can be written as

$$V_s' ds_\xi = V_s(\sigma)ds \tag{133}$$

Also, from Figures 7 and 8

$$z_o = Z' - (d+x)\sin\alpha \tag{134}$$

or with (124)

$$z_o = r_o e^{\Omega+i\gamma} - (d+x)\sin\alpha \tag{135}$$

Then (104) becomes

$$\frac{\bar{F}}{\frac{\bar{\rho}_\infty \bar{V}_\infty^2}{2} \bar{L}^2} = 2i \int_c [r_o e^{\Omega+i\gamma} - (d+x)\sin\alpha] V_s ds \tag{136}$$

From (133)

$$V_s ds = V_s' \, ds_\xi$$

But

$$\int_c V_s' \, ds_\xi = \Delta\phi_o = 0 \qquad \text{(See Equation (103))}$$

Therefore (136) is

$$\frac{\bar{F}}{\frac{\bar{\rho}_\infty \bar{V}_\infty^2}{2} \bar{L}^2} = 2i \, r_o \int_c e^{\Omega} (\cos\gamma + i \sin\gamma) \, V_s ds \tag{137}$$

or with $r_o e^{\Omega} = r'(\gamma)$ and $ds = \lambda d\sigma$

$$\frac{\bar{F}_Z}{\frac{\bar{\rho}_\infty \bar{V}_\infty^2}{2} L^2} = 2\lambda \int_c r' V_s \cos\gamma \, d\sigma \tag{138}$$

and

$$\frac{\bar{F}_Y}{\frac{\bar{\rho}_\infty \bar{V}_\infty^2}{2} L^2} = -2\lambda \int_o^{2\pi} r' V_s \sin\gamma d\sigma \tag{139}$$

where

$$\frac{r'}{r_o} = e^{\Omega} \quad \text{and} \quad \frac{\lambda}{r_o} = e^{\Omega_o} \tag{140}$$

and Ω and γ are known functions of σ because $\Omega=\Omega(\gamma)$ and $\gamma=\sigma-\varepsilon$.

The force $\bar{F}_Y$ is the Magnus force for the section of the body between the nose and the section x. The force $\bar{F}_Z$ lies in the plane through the free stream velocity vector and the axis of revolution of the body.

The Magnus moment about the nose of the body is given by the expression, with $\bar{L}$ taken as the body length,

$$\frac{\bar{M}_Y}{\frac{\bar{\rho}}{2}\bar{V}_\infty^2\bar{L}^3} = \int_{-d}^{0} (d+x) \frac{d\left(\frac{\bar{F}_Y}{\frac{\bar{\rho}}{2}\bar{V}_\infty^2\bar{L}^2}\right)}{dx} dx \tag{141}$$

where $\frac{\bar{F}_Y}{\frac{\bar{\rho}}{2}\bar{V}_\infty^2\bar{L}^2}$ is given by (139). By integration by parts

Equation (141) can be placed in the more convenient form

$$\frac{\bar{M}_Y}{\frac{\bar{\rho}}{2}\bar{V}_\infty^2\bar{L}^3} = d\left(\frac{\bar{F}_Y}{\frac{\bar{\rho}}{2}\bar{V}_\infty^2\bar{L}^2}\right)_{x=0} - \int_{-d}^{0} \frac{\bar{F}_Y}{\frac{\bar{\rho}}{2}\bar{V}_\infty^2\bar{L}^2} dx \tag{142}$$

Once the boundary layer displacement surface surrounding the body has been calculated, the Magnus force and moment can be calculated by a basically more exact method than slender-body theory, namely potential flow theory as applied in Reference 7. Although this method was not used in the present investigation because of a lack of funds, its use is discussed in Appendix C.

CALCULATION METHOD APPLIED TO FINENESS RATIO 5 HALF-ELLIPSOID

To begin the numerical integration the value of I in (100) and (101) is taken as 10^{-5} for all η except $\pm 95°$. For $\eta = \pm 95°$ I is taken as 10^{-3} in order to increase the spacing between the $\eta = \pm 90°$ and $\eta = \pm 95°$ streamlines (Figure 9).

The increments in θ and δ^* are calculated from (27) and (99) by use of the relations

$$\Delta\theta = \left(\frac{d\theta}{dx}\right)\Delta x$$

and

$$\Delta\delta^* = \frac{d\delta^*}{dx}\,\Delta x$$

The values of $\Delta\delta$ and $\Delta\psi$ are obtained from (62) and (63). The value of Δx used to calculate $\Delta\theta, \Delta\delta^*, \Delta\delta$ and $\Delta\psi$ is determined by the rate of change of $\frac{d\theta}{dx}$ between two succeeding values of x. The criterion is:

(a) if $.0002 < \left|1 - \frac{\left(d\theta/dx\right)_{x-\Delta x}}{\left(\frac{d\theta}{dx}\right)_x}\right| < .002$, then

Δx is left unchanged

(b) if $\left|1 - \frac{\left(\frac{d\theta}{dx}\right)_{x-\Delta x}}{\left(\frac{d\theta}{dx}\right)_x}\right| < .0002$, then Δx is doubled for the

next integration step

(c) if $\left|1 - \frac{\left(\frac{d\theta}{dx}\right)_{x-\Delta x}}{\left(\frac{d\theta}{dx}\right)_x}\right| > .002$, then Δx is halved for the

next integration step

In no case is Δx allowed to exceed 10^{-4}.

To calculate the derivatives of the J's (Equation 60, 61) $\Delta\theta$ and Δx are both taken as 10^{-4} and the derivatives are calculated by

$$\frac{\partial J_i}{\partial x} = \frac{J_{i,(x+\Delta x)} - J_{i,x}}{\Delta x}$$

$$\frac{\partial J_i}{\partial \theta} = \frac{J_{i,(\theta+\Delta\theta)} - J_{i,\theta}}{\Delta\theta}$$

When Equations (27), (60), (61) and (99) were integrated, it was found that rapidly diverging oscillations occurred at the start. This caused the computer to stop. Rather than spend time trying to eliminate the divergence, the values of δ, ψ, and δ^* were fixed at their stagnation point values until x became larger than -.998. They were then allowed to vary and no oscillations occurred. The stagnation point is at -.999910 so that δ, ψ, and δ^* were fixed for the first .001910 in x. For the largest value of η, namely $\pm 95°$, a calculation shows that the distance along the streamline is about .0057 compared with .00191 along x. Thus for the streamlines calculated (Figure 9), δ, ψ, and δ^* are fixed for distances along streamlines not greater than .0057 from the stagnation point. Consequently the results for δ^*, and so for the Magnus force on the portion of the body near the nose, may be inaccurate. Effects of changes in δ, ψ, and δ^* near the stagnation point decrease rapidly with increase in x. Thus, a change in δ at the stagnation point by a factor of 5 for $\eta = 95°$ makes only a change of 3 in the fourth significant figure in δ^* for x = -.600.

To evaluate the integral in (129) and (130) the method of Reference 11 is followed. Equation (129) is integrated by first noting that the integrand becomes infinite at $\gamma' = \gamma$. Consequently (129) is written as

$$\varepsilon(\gamma') = -\frac{1}{2\pi}\left[\int_0^{\gamma_1} \Omega(\gamma)\cot\frac{\gamma-\gamma'}{2}d\gamma + \int_{\gamma_2}^{2\pi} \Omega(\gamma)\frac{\gamma-\gamma'}{2}d\gamma + \right.$$

$$+\mathop{\mathcal{L}}_{\eta_o \to o} \left\{ \int_{\gamma_1}^{\gamma' - \eta_o} \Omega(\gamma) \cot \frac{\gamma - \gamma'}{2} d\gamma + \int_{\gamma' + \eta_o}^{\gamma_2} \Omega(\gamma) \cot \frac{\gamma - \gamma'}{2} d\gamma \right\} \tag{143}$$

Then near $\gamma = \gamma'$, $\Omega(\gamma)$ is written as

$$\Omega(\gamma) = \Omega(\gamma') + (\gamma - \gamma') \frac{d\Omega}{d\gamma}(\gamma') + \ldots$$

and substituted into

$$\mathop{\mathcal{L}}_{\eta_o \to o} \left\{ \int_{\gamma_1}^{\gamma' - \eta_o} \Omega(\gamma) \cot \frac{\gamma - \gamma'}{2} d\gamma + \int_{\gamma' + \eta_o}^{\gamma_2} \Omega(\gamma) \cot \frac{\gamma - \gamma'}{2} d\gamma \right\}$$

thereby giving $4\Delta \frac{d\Omega}{d\gamma}(\gamma')$, where $\gamma' - \gamma_1 = \Delta = \gamma_2 - \gamma'$.

Then equation (143) becomes

$$\varepsilon(\gamma') = -\frac{1}{2\pi} \left[\int_{o}^{\gamma' - \Delta} \Omega(\gamma) \cot \frac{\gamma - \gamma'}{2} d\gamma + \int_{\gamma' + \Delta}^{2\pi} \Omega(\gamma) \cot \frac{\gamma - \gamma'}{2} d\gamma \right.$$

$$\left. + 4\Delta \frac{d\Omega}{d\gamma}(\gamma') \right] \tag{144}$$

The integrals $\int_{0}^{\gamma'-\Delta} \Omega(\gamma)\cot\frac{\gamma-\gamma'}{2}d\gamma$ and $\int_{\gamma'+\Delta}^{2\pi} \Omega(\gamma)\cot\frac{\gamma-\gamma'}{2}d\gamma$ are evaluated

by dividing the interval of integration into equal lengths equal to Δ and taking Ω equal to the average of its values at the beginning and end of each interval of length Δ.

Then

$$\int_{k\Delta}^{(k+1)\Delta} \Omega(\gamma)\cot\frac{\gamma-\gamma'}{2}\,d\gamma = \Omega_{k+1}\ln\frac{\sin\frac{(k+1)\Delta-\gamma'}{2}}{\sin\frac{k\Delta-\gamma'}{2}}$$

where $\Omega_{k+1} = \Omega[(k+1)\Delta] + \Omega[(k\Delta)]$ (145)

By using (145) in (144) the expression for $\varepsilon(\gamma')$ becomes

$$\varepsilon(n) = -\frac{1}{2\pi}\left[4\Delta\frac{d\Omega}{d\gamma}(n) + \sum_{k=1}^{n-1}\Omega_k \ln\frac{\sin(k-n)\frac{\Delta}{2}}{\sin(k-1-n)\frac{\Delta}{2}}\right.$$
$$\left. + \sum_{k=n+2}^{N}\Omega_k \ln\frac{\sin(k-n)\frac{\Delta}{2}}{\sin(k-1-n)\frac{\Delta}{2}}\right] \qquad (146)$$
$$n\neq 0,N$$

where $N=\frac{2\pi}{\Delta}$. For n=0, instead of (146) the result is

$$\varepsilon(o) = -\frac{1}{2\pi}\left[4\Delta \frac{d\Omega}{d\gamma}(o) + \sum_{k=2}^{N-1} \Omega_k \ln \frac{\sin\frac{k\Delta}{2}}{\sin\frac{(k-1)\Delta}{2}} \right] \tag{147}$$

Also $\varepsilon(N)=\varepsilon(o)$. In the calculations, N was taken as 180. A test with N=360 showed a noticeable but negligible change in $\varepsilon(\gamma)$.

To evaluate the integrals in (138) and (139) the trapezoidal rule was used with the interval 2π divided into 180 equal parts.

The program for the numerical calculations for use on the CDC 6400 is given in Table IV.

RESULTS FOR FINENESS RATIO 5 HALF-ELLIPSOID

As an example, the Magnus force and moment on a fineness ratio 5 half-ellipsoid spinning at p=.25 and at $\alpha=4°$ is calculated. The boundary layer is turbulent and is characterized by n=1/5. The Reynolds number based on the length of the half-ellipsoid is 4.8×10^6.

The inviscid flow velocity distribution over the half-ellipsoid is assumed to be the same as over the forward half of a complete ellipsoid. Because of the wake this assumption is not exact, especially near the base, but is used in order to obtain an analytic expression for the velocity distribution in the example calculation which is of an exploratory nature. The velocity distribution is obtained from Chapter V of Reference 15. The parameter t (Figure 8) equals unity here. The result is

$$u_e = \left[\frac{1-x^2}{1-x^2(1-t^2)}\right]^{\frac{1}{2}} K_1 \cos\alpha - \frac{x}{[1-x^2(1-t^2)]^{\frac{1}{2}}} tK_2 \cos\theta \sin\alpha \tag{148}$$

and

$$v_e = -K_2 \sin\theta \sin\alpha \tag{149}$$

where

$$K_1 = \frac{2(1-t^2)^{3/2}}{2\sqrt{1-t^2} - t^2 \ln \frac{1+\sqrt{1-t^2}}{1-\sqrt{1-t^2}}} \tag{150}$$

and

$$K_2 = \frac{4(1-t^2)^{3/2}}{2\sqrt{1-t^2}(1-2t^2) + t^2 \ln \frac{1+\sqrt{1-t^2}}{1-\sqrt{1-t^2}}} \tag{151}$$

The half-ellipsoid for which the calculations are made has t=.1 so that K_1=1.02070 and K_2=1.96023. The shape of the half-ellipsoid is given by

$$r_o = t\sqrt{1-x^2}$$

Calculated streamlines on the half-ellipsoid are shown in Figure 9 for positive values of η. Each streamline shown in Figure 9 has a corresponding streamline which is its reflection in the line $\theta=\pi$ and which has a negative value of η.

The boundary layer displacement thickness δ^* along the streamlines shown in Figure 9 ($\eta>o$) are presented for $\eta>o$ in Figure 10a and for $\eta<o$ in Figure 10b.

In Figure 11a and 11b is given the distribution of the full boundary layer thickness δ along various streamlines.

In Figure 12a and 12b is shown the variation of δ^* with θ at $x=-.5$ and at $x=0$. The variation is slightly unsymmetric about $\theta=\pi$; it is this asymmetry that produces the Magnus force.

In Figure 13, (a)-(i) is shown the variation of ψ with x for all the streamlines calculated. The calculations were begun with $\psi=-1$ at the stagnation point instead of $\psi=-\infty$. A few trials showed that in the present example, $\alpha=4°$ and $p=.25$, when the initial value of ψ was less than -5 or so, the integration of the differential equations for δ^*, δ, and ψ could not be made because of divergent oscillations. The behavior of ψ near the stagnation point shown in Figure 13 indicates that the effect of the choice of the initial value of ψ soon disappears. Moreover, two calculations for $\alpha=6°$, $p=1$, $\eta=-10$, one with $\psi_s=-5$ and the other with $\psi_s=-10$ showed that when x had increased to -.985555 from the stagnation point value -.999796, the values of ψ for the two calculations differed by only 1 in the third significant figure. The difference then decreased as x increased.

In Figure 14 is shown the normal force coefficient C_N based on the local cross section area for the portion of the body between station x and the nose. The coefficient C_N is obtained from $\dfrac{\bar{F}_Z}{\frac{\bar{\rho}_\infty \bar{V}_\infty^2}{2}\bar{L}^2}$ (Equation (137)) by the relation

$$C_N = \frac{\bar{F}_Z}{\frac{\bar{\rho}_\infty \bar{V}_\infty^2}{2}\bar{L}^2}\left(\frac{\bar{L}^2}{\pi \bar{r}_o^2}\right) \tag{152}$$

In Figure 15 is shown the corresponding Magnus force coefficient C_Y obtained from $\dfrac{\bar{F}_Y}{\frac{\bar{\rho}_\infty \bar{V}_\infty^2}{2}\bar{L}^2}$ (Equation (138)) by

$$C_Y = \frac{\bar{F}_Y}{\frac{\bar{\rho}_\infty \bar{V}_\infty^2}{2}\bar{L}^2}\left(\frac{\bar{L}^2}{\pi \bar{r}_o^2}\right) \tag{153}$$

Although the sign of C_Y computed in the present method is positive along the +Y axis in Figure 6 for ω as shown in Figure 1, it is shown negative in Figure 15 in order to adhere to the sign convention given in Reference 16.

The curves for C_N and C_Y are shown dashed for $x<-.6$ because from calculations for $\eta=\pm 95°$, and a calculation for $\eta=+95°$ with δ_s equal to 5 times the correct value of δ_s, it was found that the change in δ^* for $x<-.600$ caused by using $5\delta_s$ instead of δ_s in the calculation for $\eta=+95°$ was greater than 10 percent of the difference between δ^* for $\eta=95°$ and δ^* for $\eta=-95°$. Thus the Magnus force for $x<-.600$ may be affected by more than 10 percent by inaccuracies in the initial values of δ and ψ and by the method of numerical integration; see section on "Numerical Calculations".

The results in Figures (14) and (15) indicate that because of the boundary layer, C_N decreases and C_Y increases as the fineness ratio increases. The decrease in C_N is almost linear with x for larger x but C_Y increases more rapidly than in a linear manner all the way to x=0, the body base.

The value of the moment coefficient of the entire body defined by (Reference 16),

$$C_n = \frac{\bar{M}_Y}{\frac{\bar{\rho}}{2}V_\infty^2 L^3}\left(\frac{1}{2\pi}\right)\left(\frac{\bar{L}}{r_M}\right)^3 \qquad (154)$$

is found to be 1.058×10^{-3}. (See Equation (142))

COMPARISON WITH EXPERIMENT

There do not seem to be any experimental data for a spinning half-ellipsoid of fineness ratio 5. Consequently, strictly speaking there can be no comparison of the calculated results with experiment. There are, however, some data for pointed shapes of near 5 fineness ratio in subsonic flow. One set of data is that of Reference 16. Tests were made of a model with a 2 cal. secant-ogive nose and a 3 cal. cylinder after-body. For $\alpha=4°$, M=.2, and $Re_L=4.8\times10^6$, the data in Figure 6 of Reference 16 indicate that C_Y was about -.0075. This value is about 24 times as large as the calculated value -3.11×10^{-4}. The experimental value of C_N was about .148 (Figure 11 of Reference 16); the calculated value is .1385. The calculated value is 93 percent of the experimental value. Slender-body theory, without any boundary layer, p. 67 of Reference 6, gives the value 2α or .1396. This is almost equal to the calculated value with boundary layer.

In Reference 17 the results of tests of a 4.9 caliber smooth body are presented. The nose is an almost flat surface of about .198 calibers; this is followed by a 16-degree half-angle cone for about .775 calibers; this in turn is followed by a tangent ogive for the next 2.5 calibers. The rear portion is a cylinder. The Reynolds number based on body length was about 3.4×10^6; at this Reynolds number the shape of the nose portion almost certainly ensures turbulent flow rearward from just behind the nose cap. For this body at a Mach number of .8, the lowest tested, the value of C_Y was found to be about -.0125. The change in body shape and Mach number from the tests of Reference 16 to those of Reference 17 resulted in a change in C_Y from -.0075 to -.0125. The value computed for the half-ellipsoid is -3.11×10^{-4}. Consequently it appears that the calculated value of C_Y for the half-ellipsoid is probably much too small. The half-ellipsoid may have a more favorable pressure distribution than the bodies tested and thus a thinner boundary layer. If so, it would have a smaller Magnus force. It is not, however, likely that this is the explanation of the large difference between the measured and calculated values of C_Y.

The calculated value of C_n, the Magnus yawing moment coefficient, Equation (154), is 1.058×10^{-3}. The value of C_n calculated by use of Figure 7 of Reference 16 is about -1.7×10^{-3}. The experimental values become zero at $\alpha=6°$ and positive for larger values of α. No values are shown for $\alpha<4°$. The value of C_n for the body of Reference 17 (Figure 42) is about 1.61×10^{-2}.

DISCUSSION OF METHOD

The present method computes a displacement surface by the use of boundary-layer theory. Consequently all the boundary layer approximations are inherent in the method. In order for boundary-layer theory to be applicable the boundary-layer thickness at a point on the surface should be much smaller than the distance from the point to the stagnation point. In the calculation for the half-ellipsoid the largest δ occurs at $x=0$, $\theta=0$. From Figure 11 it appears that δ is about 25 percent of r_o at $x=0$, $\theta=0$. Although δ is a large fraction of r_o, it is less than 2.5 percent of the distance to the stagnation point (see Figure 9). Therefore the boundary layer is thin as required by boundary-layer theory.

When the boundary layer approximations are made, it can be shown that

$$\frac{\partial P}{\partial y} = \frac{\rho v^2}{r_o} \cos \phi$$

When v is of the same order as u ($u=o(1)$), $\frac{\partial P}{\partial y}$ is of order unity instead of $o(\delta)$ as is usual without spin ($\delta<<1$). Therefore the static pressure difference across the boundary layer, which is proportional to $\frac{\partial P}{\partial y}$ can be of $o(\delta)$ for a body with spin instead of

$o(\delta^2)$ as is usual without spin. Although the difference in static pressure across the boundary layer is of $o(\delta)$ instead of $o(\delta^2)$, it is neglected in the present analysis because terms of $o(\delta)$ have been neglected in deriving the boundary layer equations from the complete equations of motion and because its inclusion would have made the method more complicated. Kelley and Thacker in their analysis for a cylinder with a laminar boundary layer find that the effect of the pressure gradient across the boundary layer changes the Magnus force by about 30 percent. Although this is appreciable, for the half-ellipsoid an effect of this amount would not change the impression that the calculated value of the Magnus force coefficient is much too small.

In the present metnod, the velocity profile shape parameter n is fixed before a calculation is made and does not vary along a streamline. If n were allowed to change by introducing an additional equation for the change of n, the displacement thicknes δ^* would respond more accurately to pressure gradients along the streamlines. The introduction of an equation for the change in n would, however, further complicate an already complicated method and introduce additional uncertainties associated with information needed for the n equation.

The assumption that the u and v velocity profiles have the same δ has been shown by Cooke (Reference 18) to be a source of inaccuracy. The use of two δ's would introduce another dependent variable and a partial differential equation for it. The feeling is that instead of introducing an equation for n and an equation for another δ it might be better to investigate the use of a finite difference method instead of the integral approach. Of course this introduces other problems, one of which is the effect on the turbulence of a spinning wall. Although this seems not to appear in the present analysis, it is hidden in the friction formula and velocity profile shape, both of which involve assumptions.

The use of slender-body theory, a theory for very thin bodies at very small angle of attack, to calculate the Magnus force further decreases the accuracy of the results. At first glance, it appears that more accurate results can be obtained by using the method of Reference 7 and 8. Although slender-body theory requires no information for the wake, the method of Reference 7 and 8 cannot be used unless the distribution of the displacement thickness behind the blunt base is known. The method of Reference 7 and 8 cannot be used to calculate the flow near the base of a body with a blunt base and zero wake displacement thickness; infinite velocities are obtained at the corner. Because the behavior of the wake is unknown and because the Magnus force is small, the inaccuracy caused by an inexact representation of the wake can be important. For a body with spin and angle of attack the wake is not axisymmetric. It seems that in order to get an accurate solution it may be necessary to solve the entire flow problem, boundary layer plus wake.

Another source of error is the lack of a reliable method for calculating where on the body the initial laminar boundary layer changes to a turbulent one. Consequently unless the transition point is fixed or known in some way, the initial conditions for the turbulent boundary layer and the location of its origin are also unknown. Therefore even if the entire flow field could be solved for exactly, the results might still be unreliable.

For tests of analytical methods for computing Magnus forces it would be desirable to test a simple shape such as a half-ellipsoid at a low Mach number. The advantage of a shape like a half-ellipsoid is that the potential flow velocity distribution over at least the forward portion is given by an analytic expression. This is a help in obtaining velocity derivatives and in finding the flow near the stagnation point at angle of attack.

REFERENCES

1. Martin, J. C., "On Magnus Effects Caused by the Boundary-Layer Displacement Thickness on Bodies of Revolution at Small Angles of Attack," Journal of the Aeronautical Sciences, Vol. 24, No. 6, p. 421, Jun 1957

2. Platou, A. S., "Magnus Characteristics of Finned and Nonfinned Projectiles," AIAA Journal 3, 83-90 (1965)

3. Kelly, H. R. and Thacker, G. R., "The Effect of High Spin on the Magnus Force on a Cylinder at Small Angles of Attack," Naval Ordnance Test Station, NAVORD Report 5036 (Feb 1956)

4. Sedney, R., "Laminar Boundary Layer on a Spinning Cone at Small Angles of Attack in a Supersonic Flow," Journal of the Aeronautical Sciences, Vol. 24, No. 6, p. 430, Jun 1957

5. Ward, G. N., "Linearized Theory of Steady High-Speed Flow," Cambridge Univ. Press (1955)

6. Nielsen, J. N., "Missile Aerodynamics," McGraw-Hill (1960)

7. Dawson, C. W., and Dean, J. S., "The XYZ Potential Flow Program," Tech. Note CMD-22-71, Jun 1971, NSRDC Bethesda, MD.

8. Hess, J. I. and Smith A. M. O., "Calculation of Potential Flow About Arbitrary Bodies," Progress in Aeronautical Sciences Vol. 8, Pergammon Press (1967)

9. Lighthill, M. J., "On Displacement Thickness," Journal of Fluid Mechanics, Vol. 14, Part 4, p. 383, Aug 1958

10. Rosenhead, L. (ed.), "Laminar Boundary Layers," Oxford Univ. Press (1963)

11. Theodorsen, T., "Theory of Wing Sections of Arbitrary Shape," NACA TR 411 (1931).

12. Theodorsen, T., and Garrick, I. E., "General Potential Theory of Arbitrary Wing Sections," NACA TR 452, (1933)

13. Millikan, C. B., "An Extended Theory of Thin Airfoils and its Application to the Biplane Problem," NACA TR 362, (1930)

14. Milne-Thomson, L. M., "Theoretical Hydrodynamics 5th ed. Macmillan, New York, (1968)

15. Lamb, H., "Hydrodynamics," 6th ed. Dover, New York (1945)

16. Carman, J. B., Uselton, J. C., and Summers, W. E., "Experimental Magnus Characteristics of Basic and Boattail Configurations of 3- and 5-Cal. Army-Navy Spinner Projectiles at Subsonic and Transonic Mach Numbers," AEDC-TR-70-36, Apr 1970

17. Regan F. J. Jr., and Schermerhorn, V. L., "Aeroballistic Evaluation and Computer Stability Analysis of the U. S. Navy 20-Millimeter General Purpose Projectile," NOLTR 71-95, Jun 1971

18. Cooke, J. C., "Pohlhausen's Method for Three-Dimensional Laminar Boundary Layers," Aeronaut. Quart. 3, 51-60

19. Shapiro, A. H., "The Dynamics and Thermodynamics of Compressible Fluid Flow," Vol. I Ronald Press, New York, (1953)

20. Pennington, R. H., "Introductory Computer Methods and Numerical Analysis," Macmillan Co., New York, (1965)

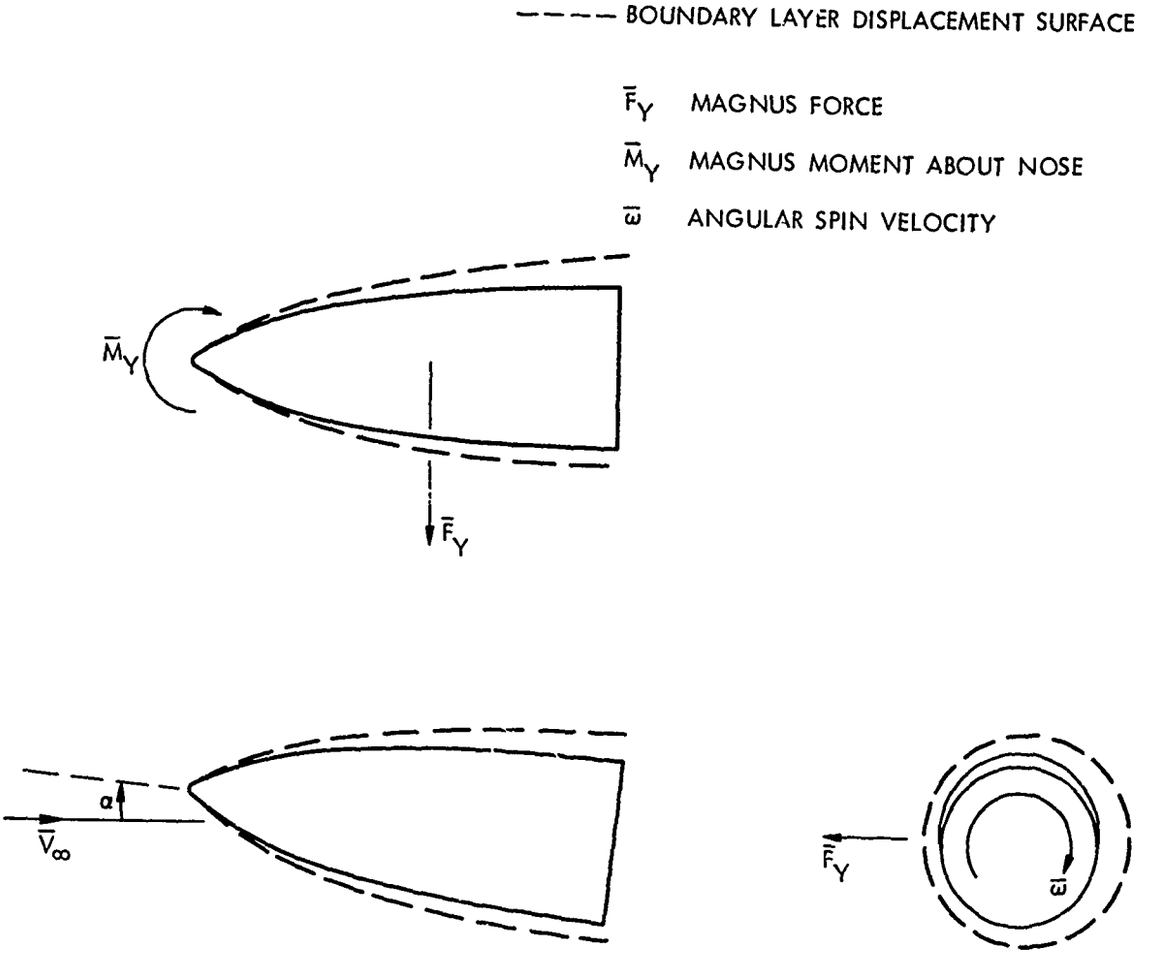

FIG. 1 FLOW ABOUT SPINNING AXISYMMETRIC BODY AT SMALL ANGLE OF ATTACK

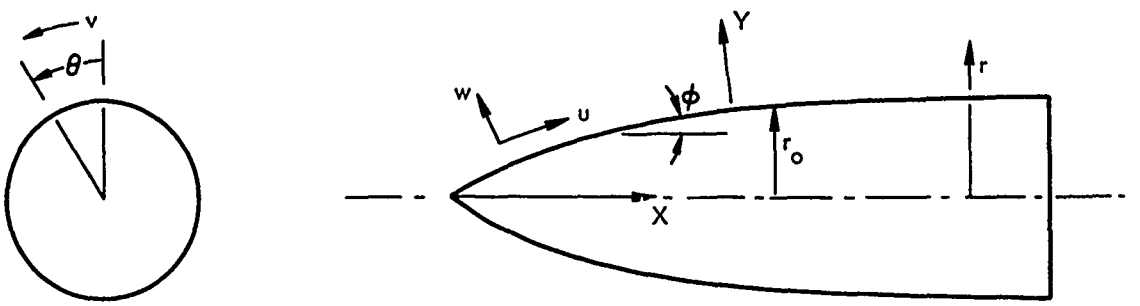

FIG. 2 COORDINATE SYSTEM

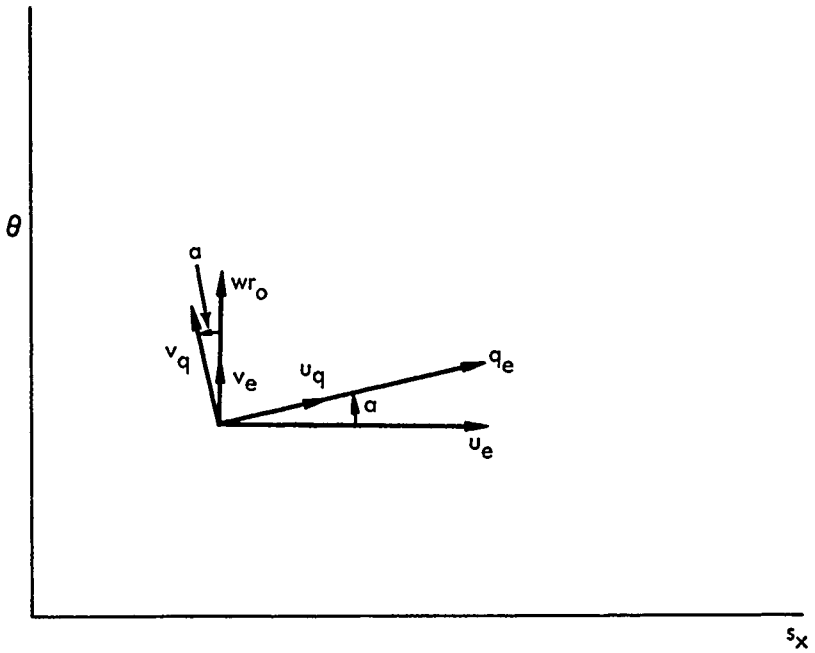

FIG. 3 VELOCITIES

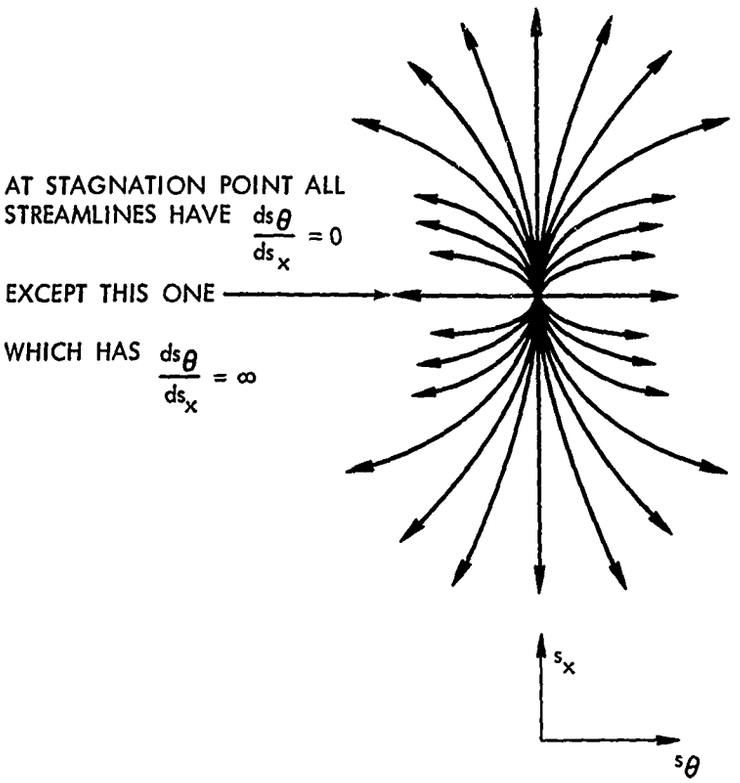

FIG. 4 STREAMLINES AT STAGNATION POINT

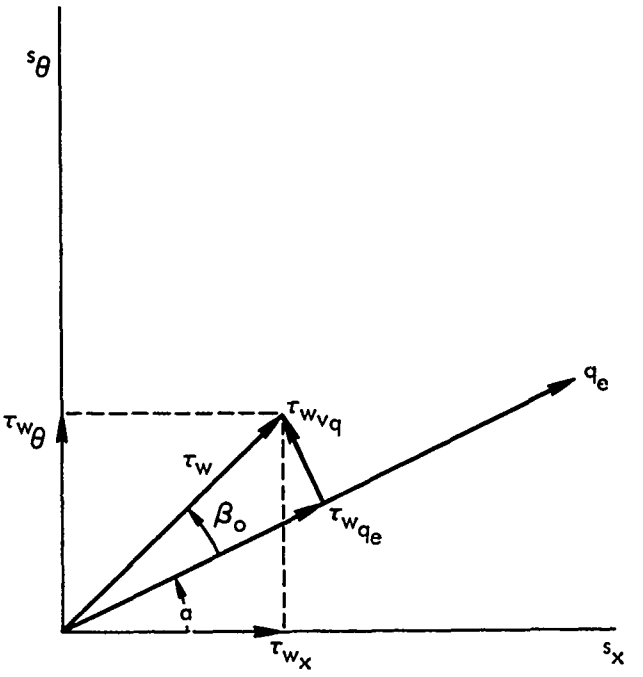

FIG. 5 SHEAR STRESS COMPONENTS

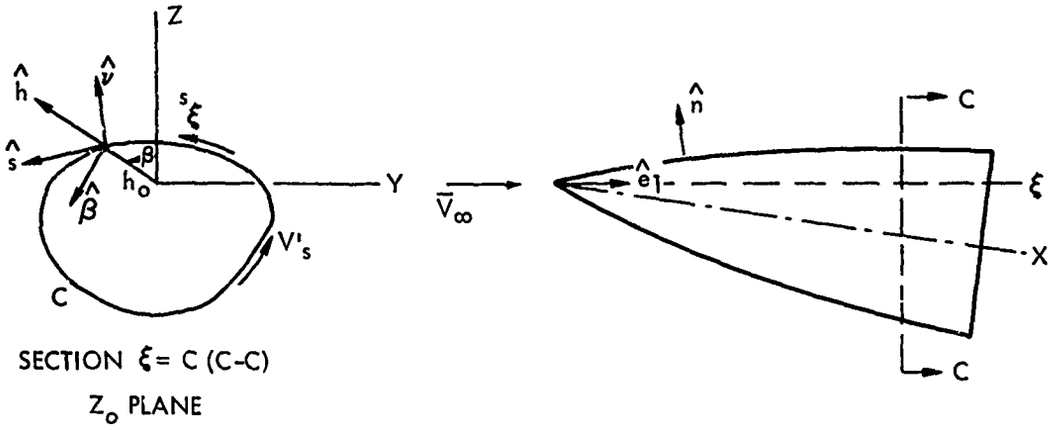

FIG. 6 COORDINATES FOR APPLICATION OF SLENDER-BODY THEORY

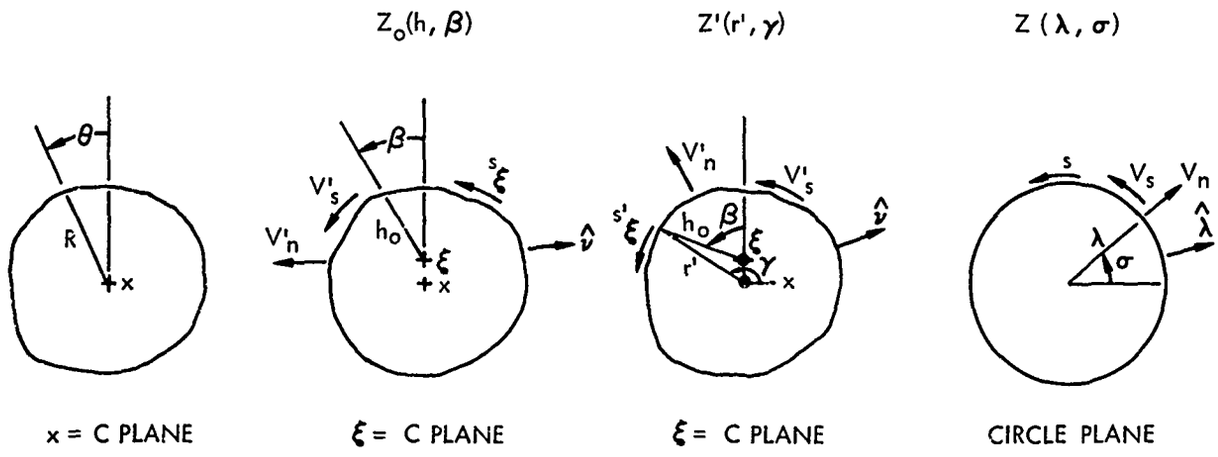

FIG. 7 CROSS SECTIONS USED TO FIND V'_s FOR USE IN SLENDER-BODY THEORY.

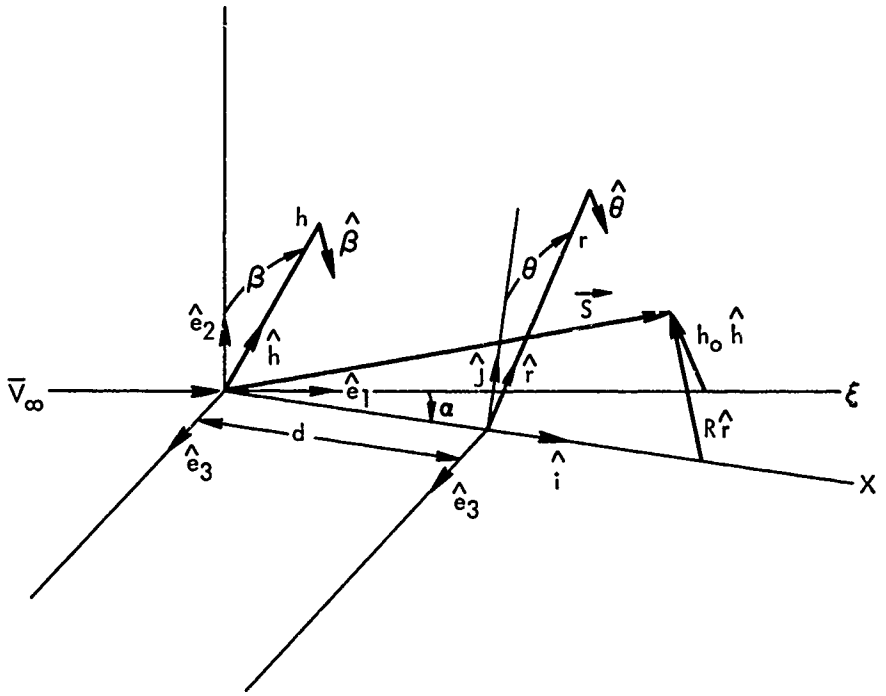

FIG. 8 COORDINATE SYSTEMS

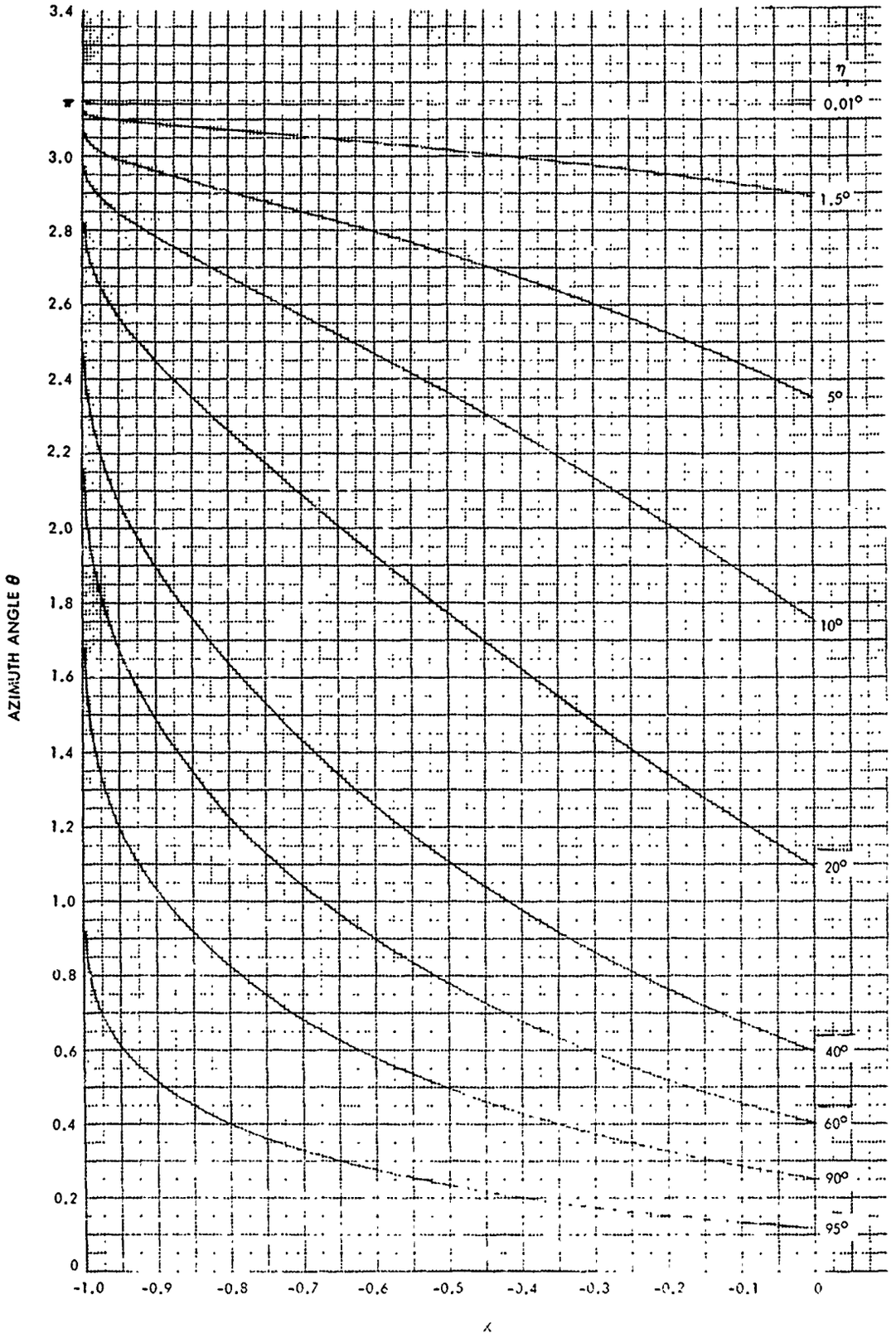

FIG. 9 STREAMLINES ON FINENESS RATIO 5 HALF-ELLIPSOID AT 4 DEGREES ANGLE OF ATTACK FOR VARIOUS STREAMLINE STARTING ANGLES η

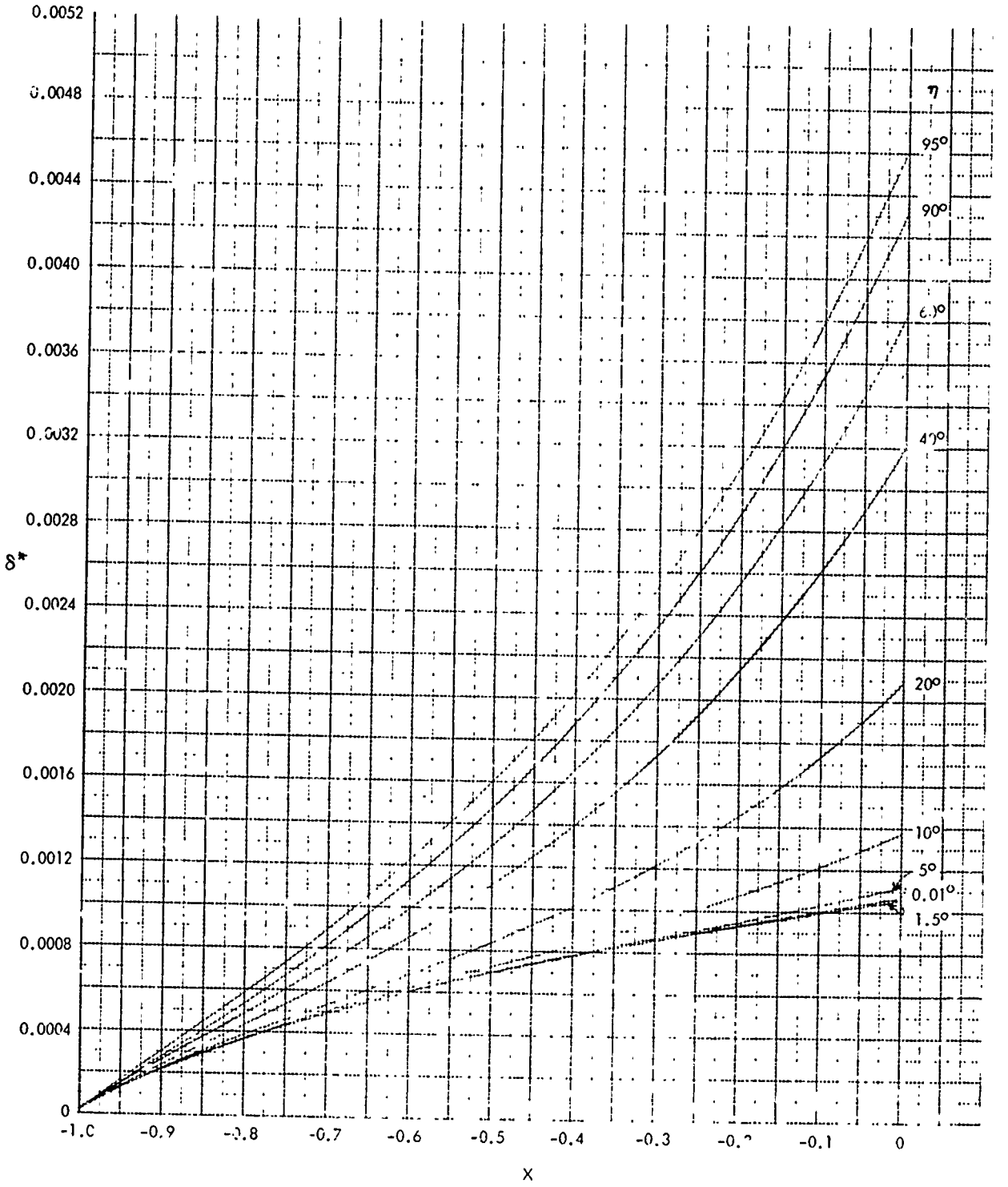

FIG. 10a BOUNDARY LAYER DISPLACEMENT THICKNESS δ^* ON HALF-ELLIPSOID ON VARIOUS STREAMLINES SPECIFIED BY STARTING ANGLE ($\eta > 0$).

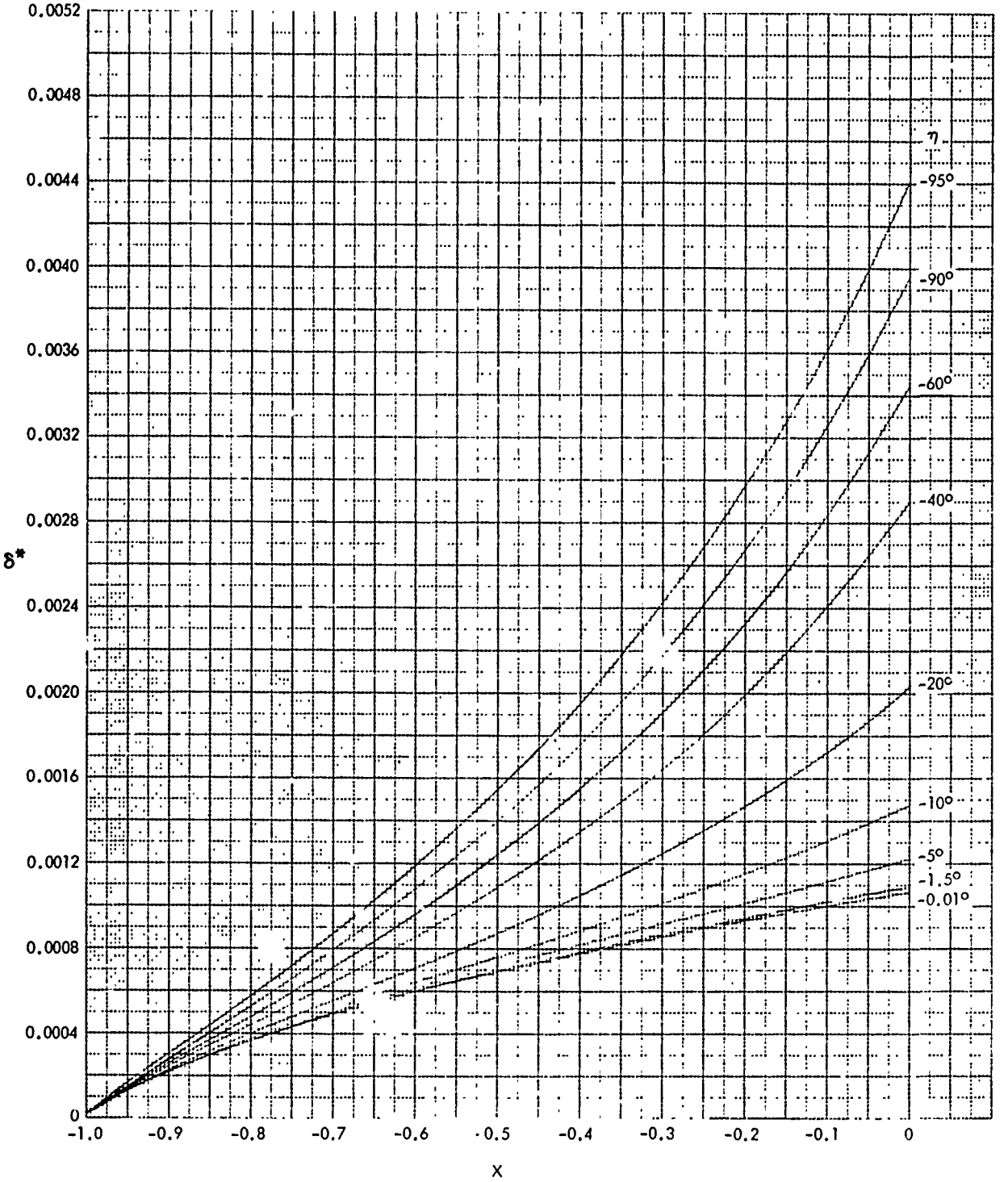

FIG. 10b BOUNDARY LAYER DISPLACEMENT THICKNESS δ^* ON HALF-ELLIPSOID ON VARIOUS STREAMLINES SPECIFIED BY STARTING ANGLE η ($\eta < 0$).

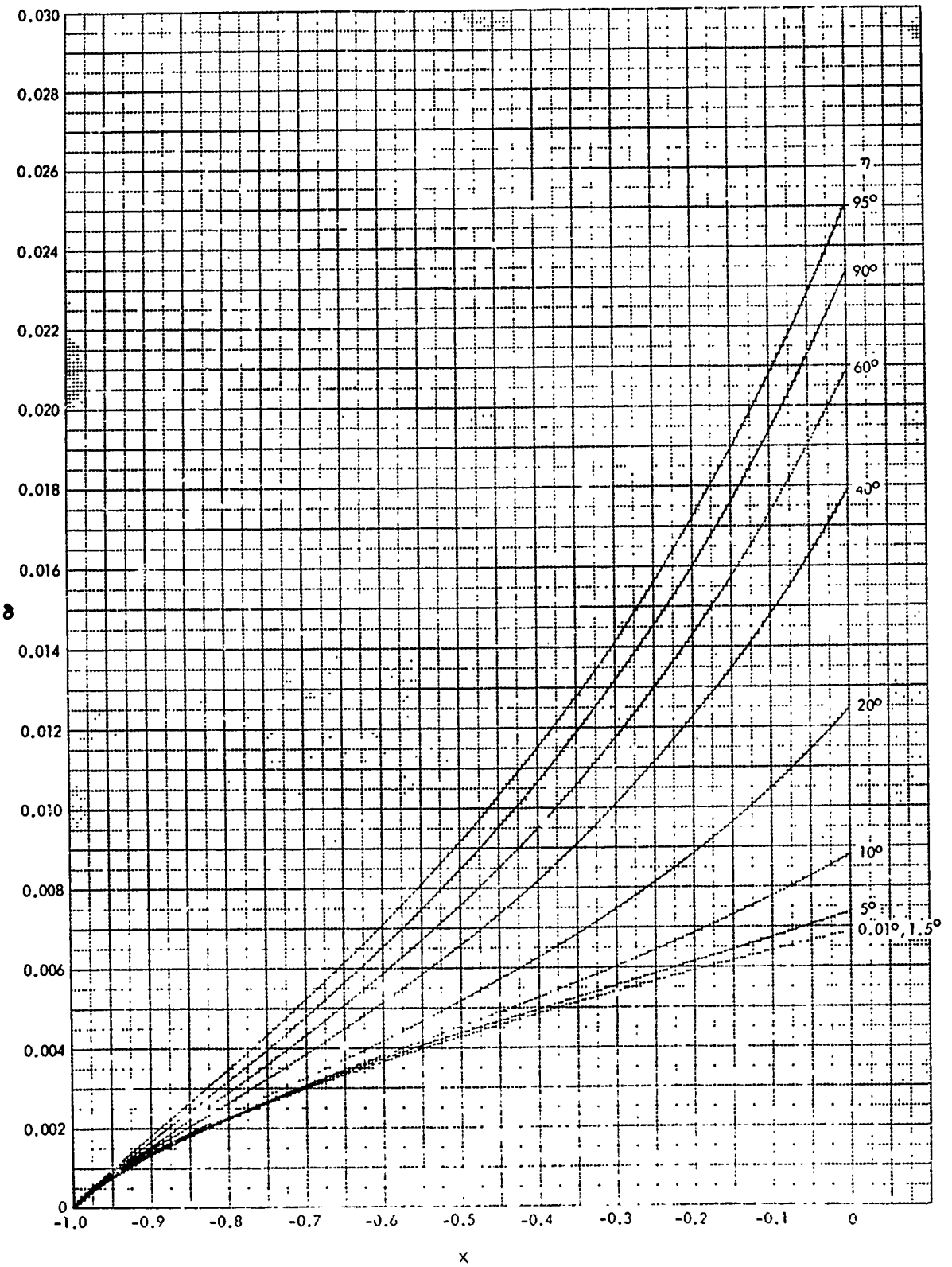

FIG. 11a BOUNDARY LAYER THICKNESS δ ON HALF-ELLIPSOID ON VARIOUS STPEAMLINES SPECIFIED BY STARTING ANGLE η ($\eta > 0$).

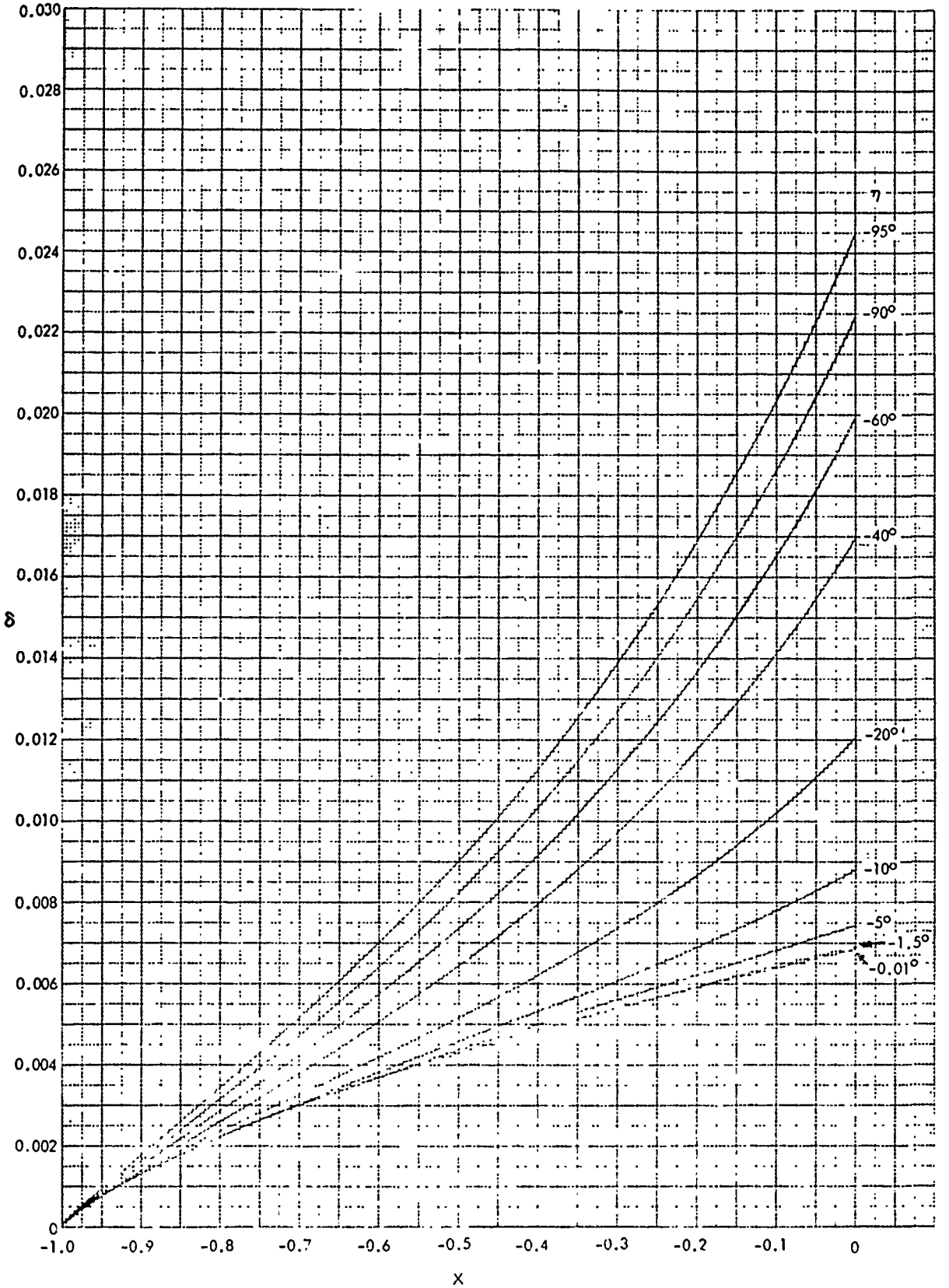

FIG. 11b BOUNDARY LAYER THICKNESS δ ON HALF-ELLIPSOID ON VARIOUS STREAMLINES SPECIFIED BY STARTING ANGLE η ($\eta < 0$).

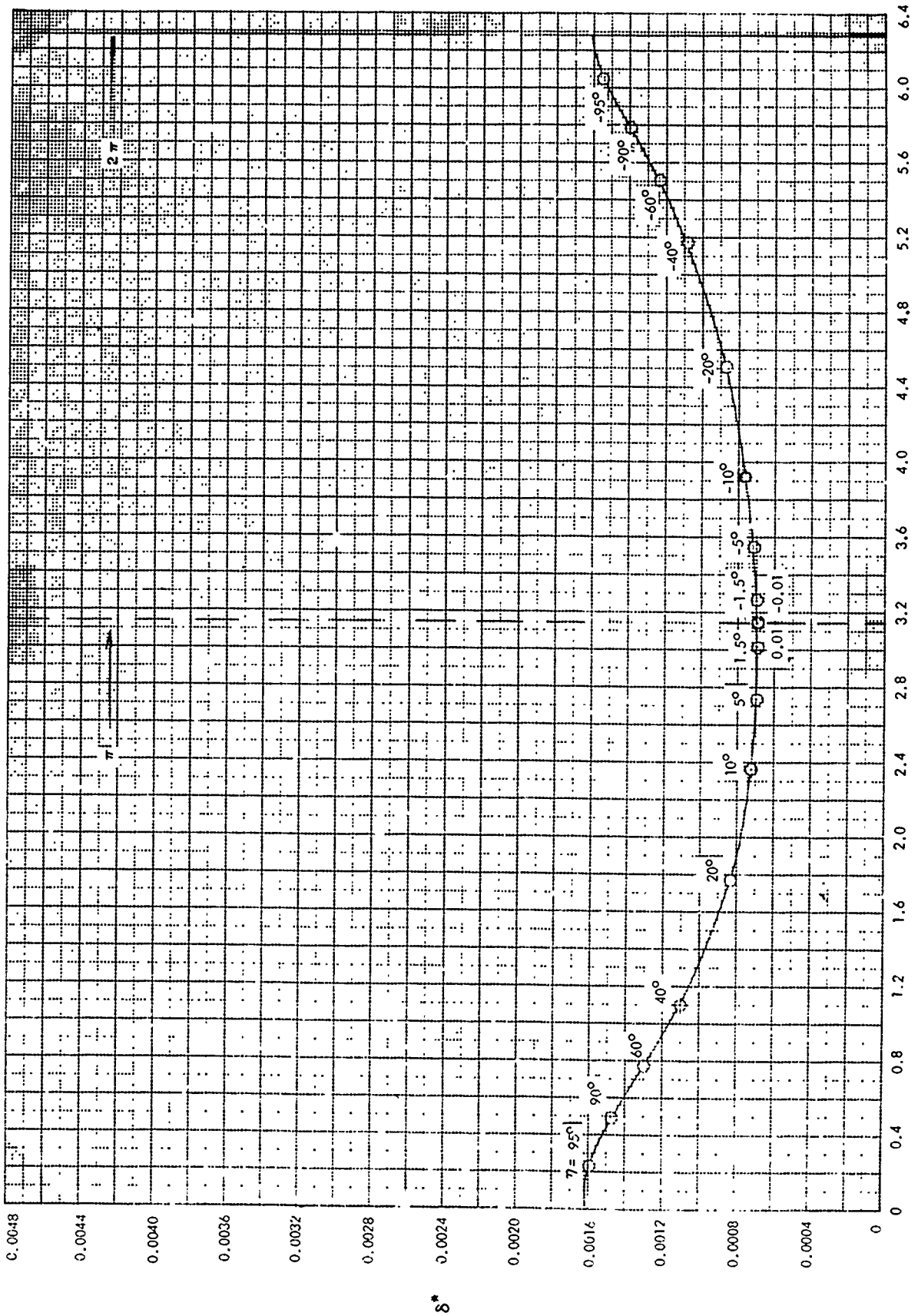

FIG. 12a BOUNDARY LAYER DISPLACEMENT THICKNESS δ* VERSUS AZIMUTHAL ANGLE θ AT X = -0.5.

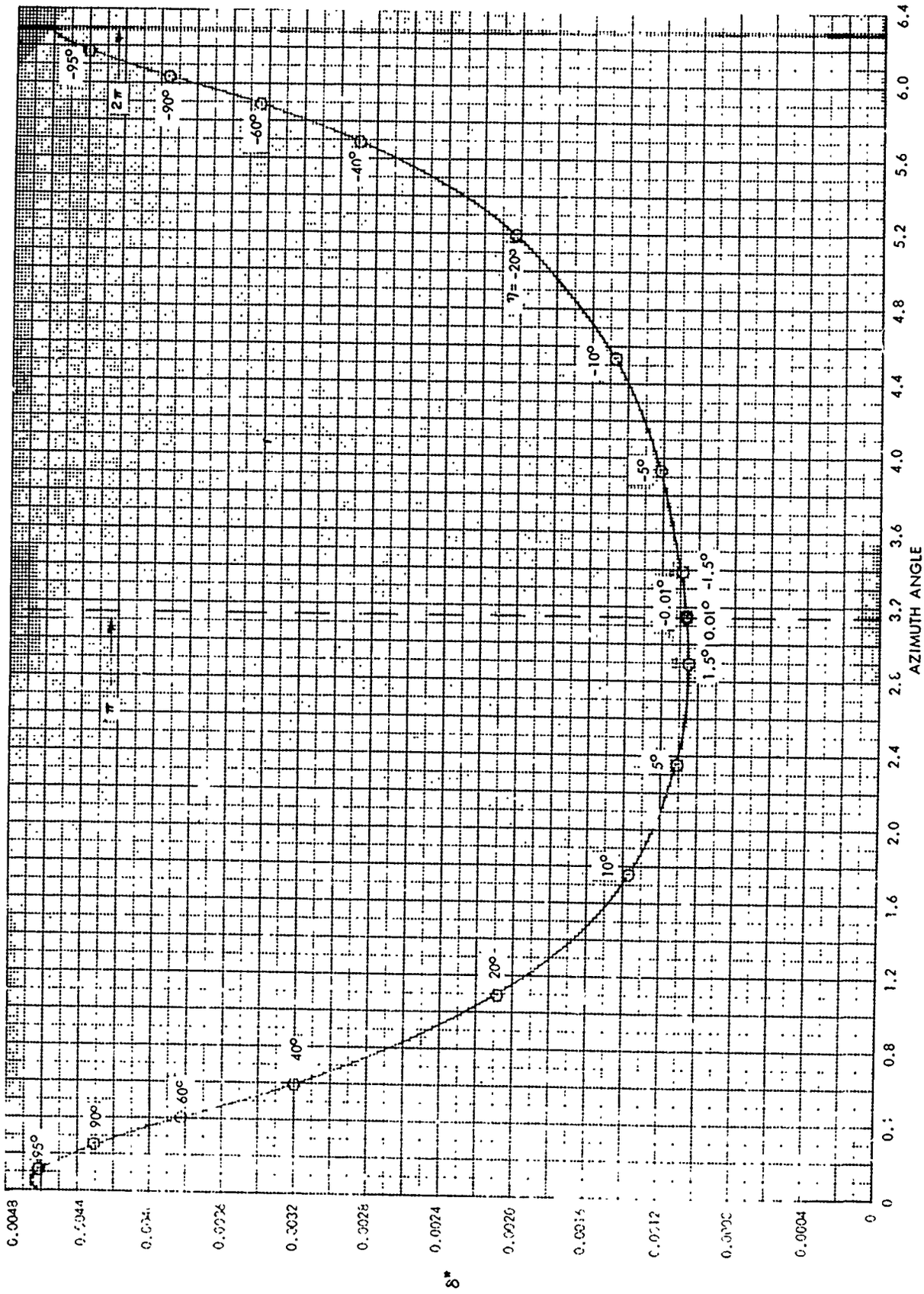

FIG. 12b BOUNDARY LAYER DISPLACEMENT THICKNESS δ^* VERSUS AZIMUTHAL ANGLE θ AT X = 0.

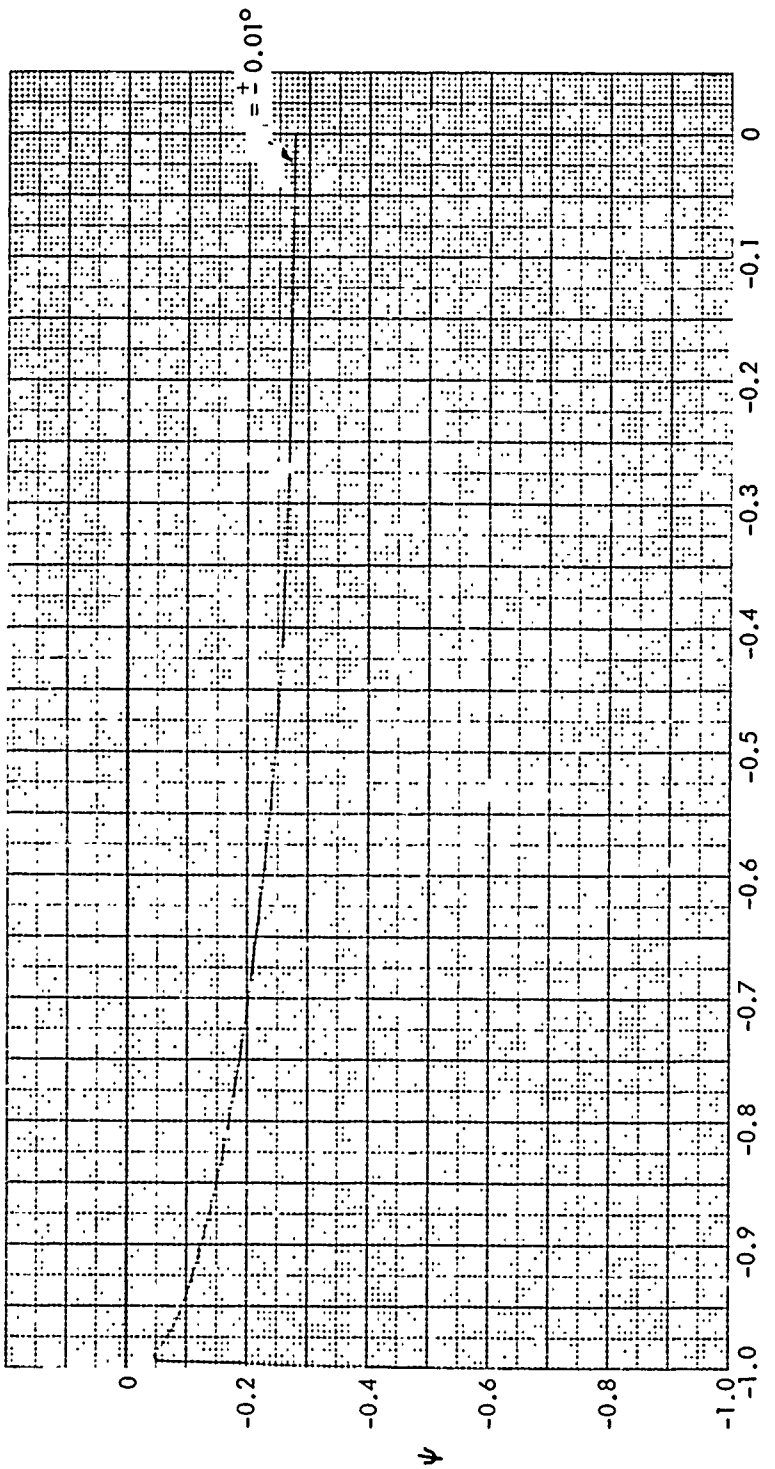

FIG. 13a Ψ, TANGENT OF ANGLE BETWEEN POTENTIAL FLOW STREAMLINE AND SURFACE SHEAR STRESS FOR STREAMLINES WITH STARTING ANGLES $\eta = \pm 0.01°$.

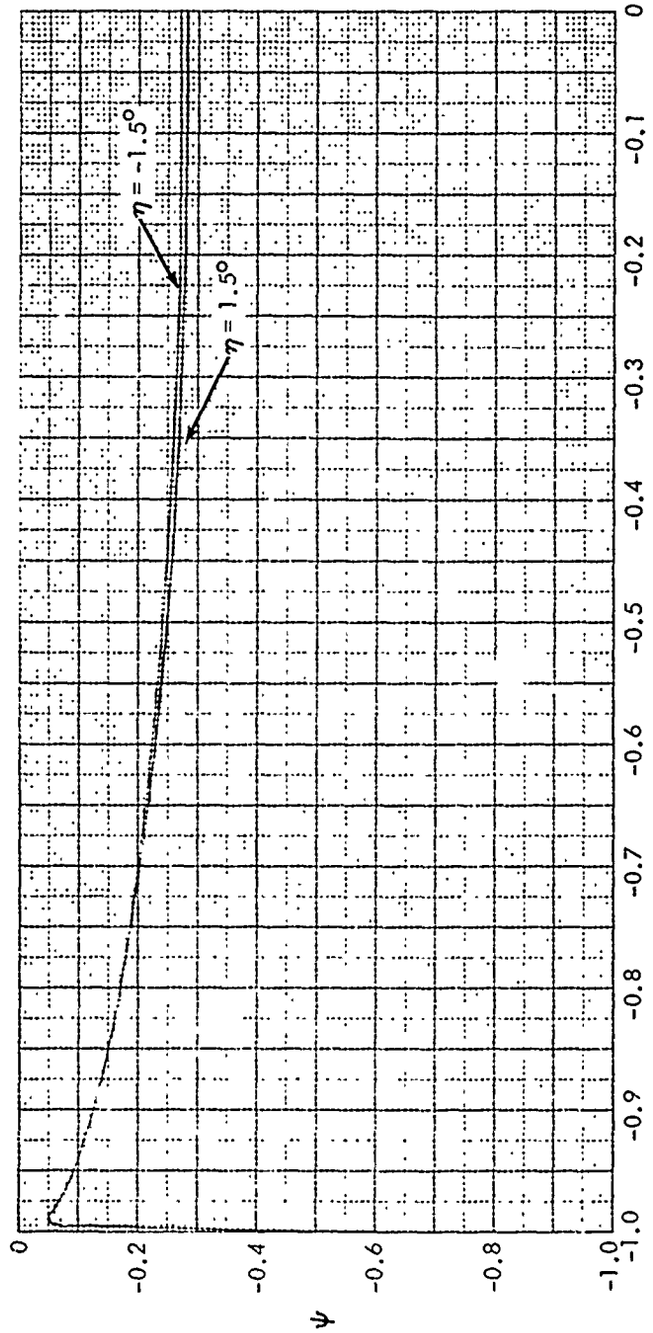

FIG. 13b ψ, TANGENT OF ANGLE BETWEEN POTENTIAL FLOW STREAMLINE AND SURFACE SHEAR STRESS FOR STREAMLINES WITH STARTING ANGLES $\eta = \pm 1.5°$.

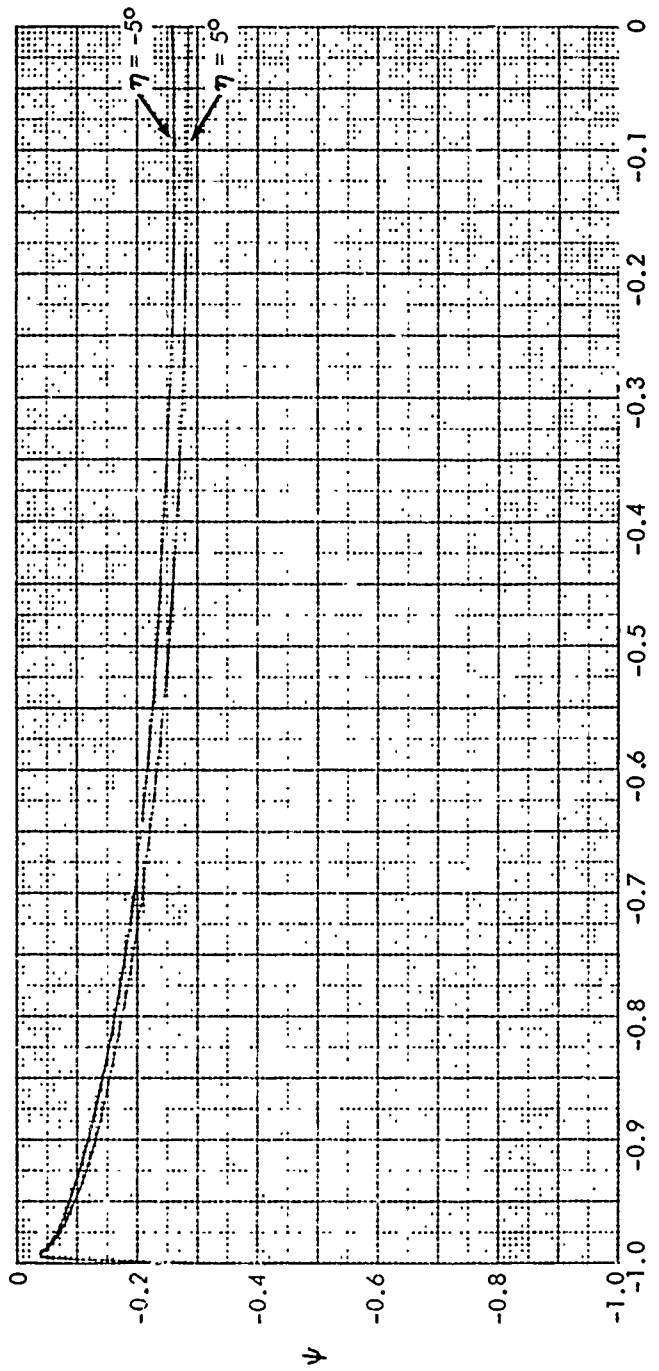

FIG. 13c Ψ, TANGENT OF ANGLE BETWEEN POTENTIAL FLOW STREAMLINE AND SURFACE SHEAR STRESS FOR STREAMLINES WITH STARTING ANGLES $\eta = \pm 5°$.

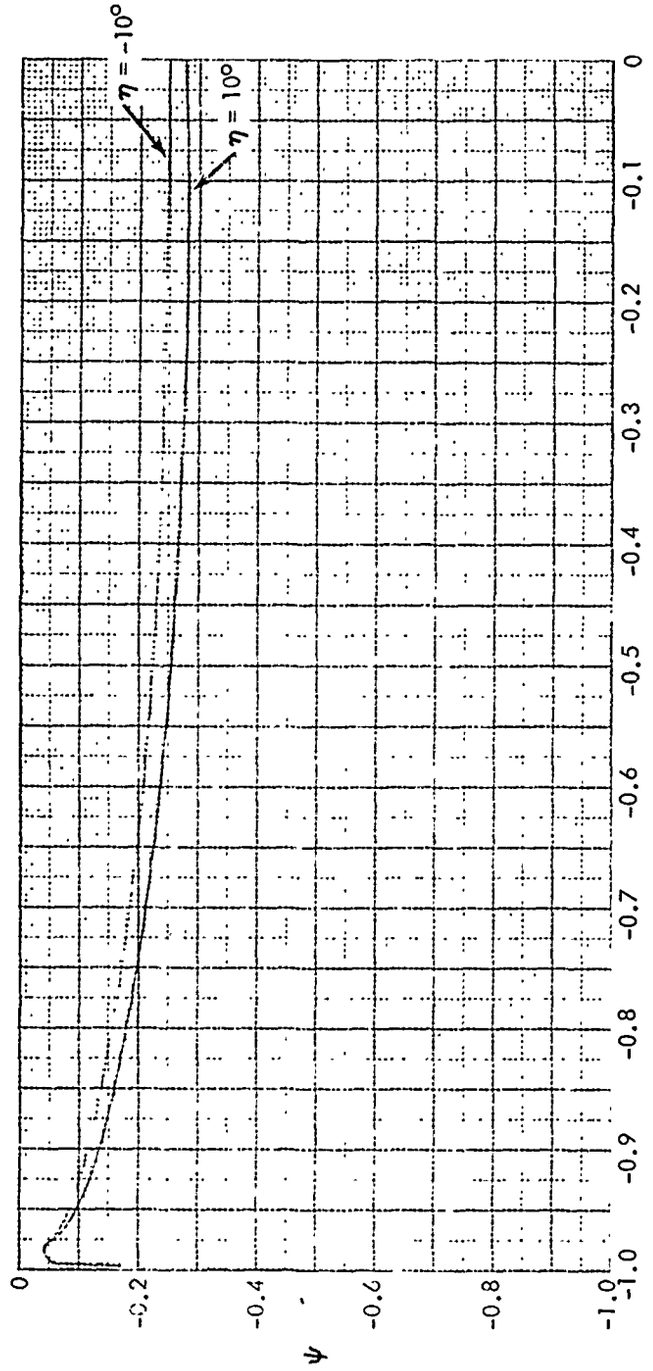

FIG. 13d Ψ, TANGENT OF ANGLE BETWEEN POTENTIAL FLOW STREAMLINE AND SURFACE SHEAR STRESS FOR STREAMLINES WITH STARTING ANGLES $\eta = \pm 10°$.

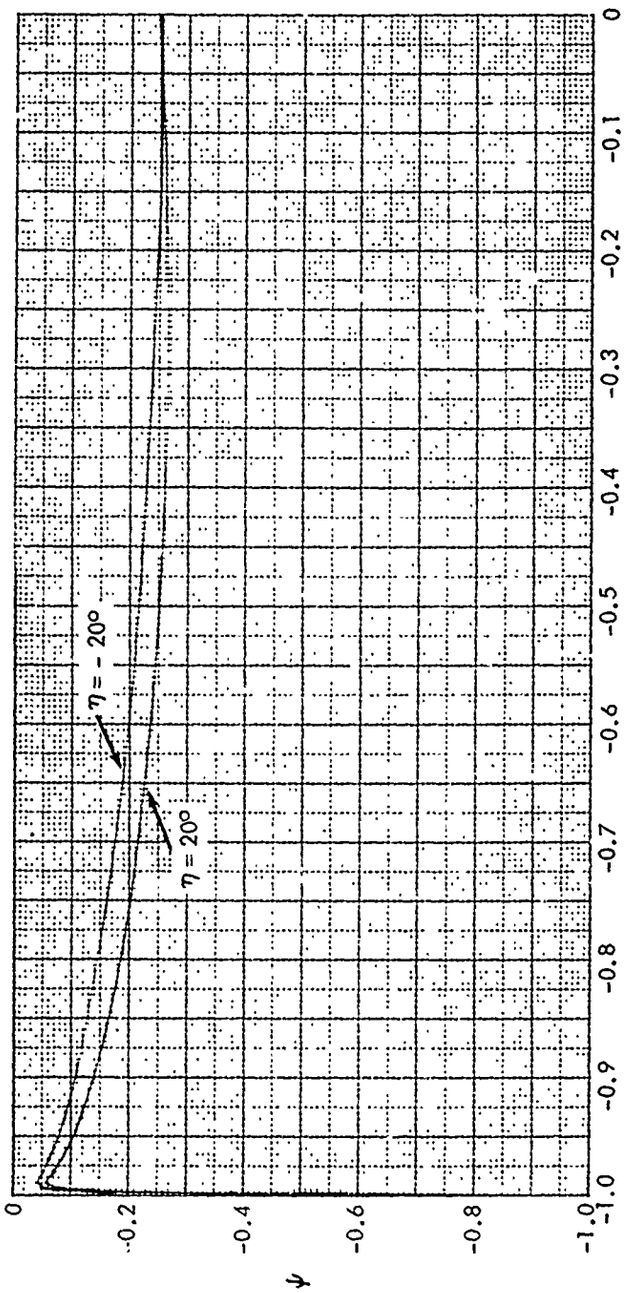

FIG. 13e ψ, TANGENT OF ANGLE BETWEEN POTENTIAL FLOW STREAMLINE AND SURFACE SHEAR STRESS FOR STREAMLINES WITH STARTING ANGLES $\eta = \pm 20°$.

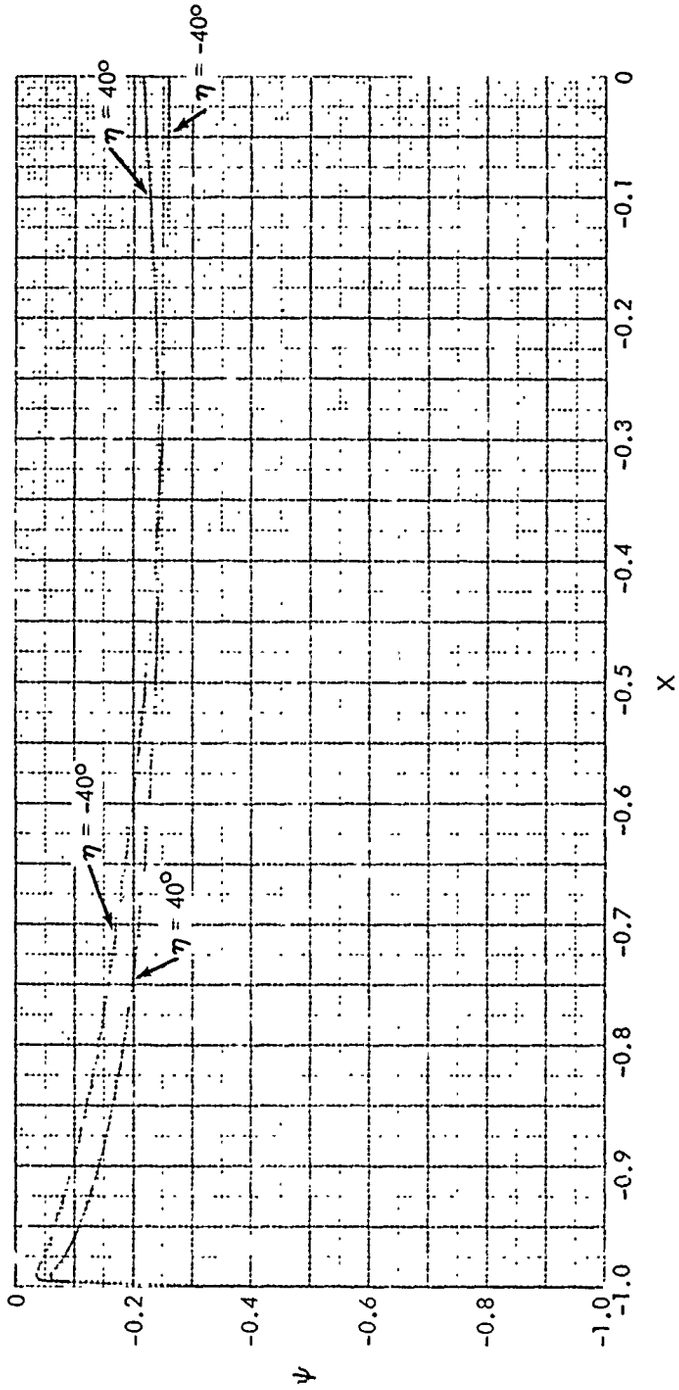

FIG. 13f ψ, TANGENT OF ANGLE BETWEEN POTENTIAL FLOW STREAMLINE AND SURFACE SHEAR STRESS FOR STREAMLINES WITH STARTING ANGLES $\eta = \pm 40°$.

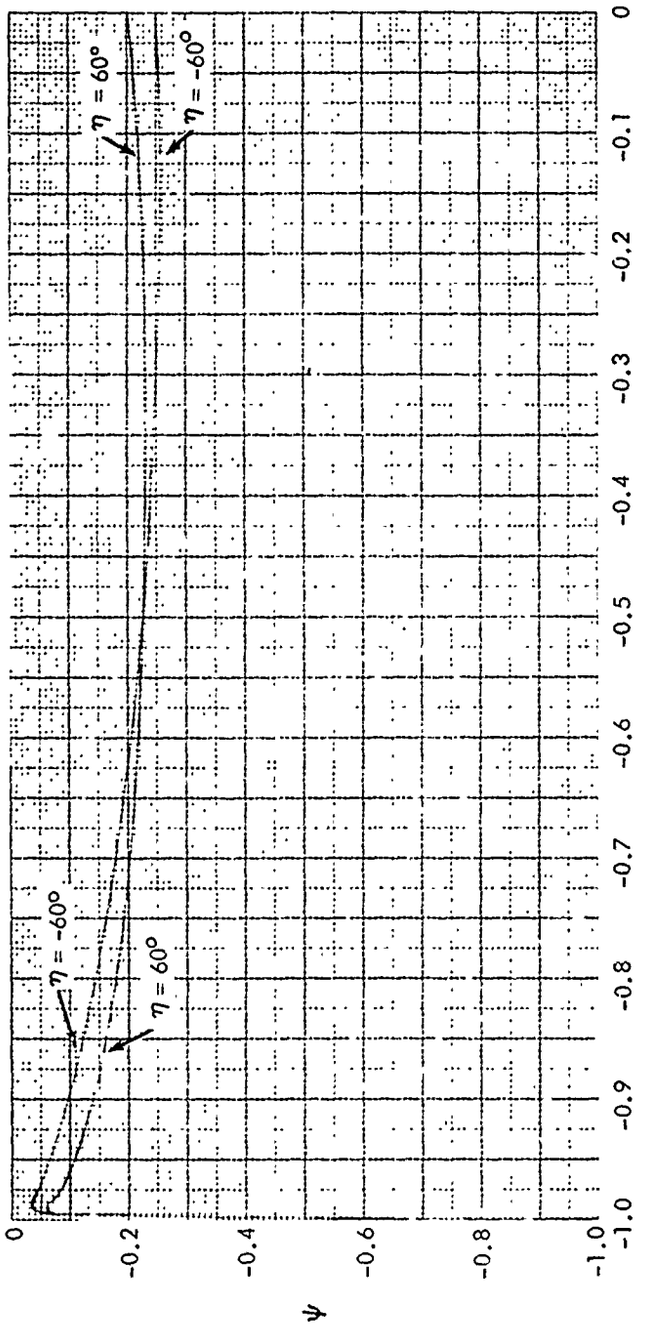

FIG. 13g ψ, TANGENT OF ANGLE BETWEEN POTENTIAL FLOW STREAMLINE AND SURFACE SHEAR STRESS FOR STREAMLINES WITH STARTING ANGLES $\eta = \pm 60°$.

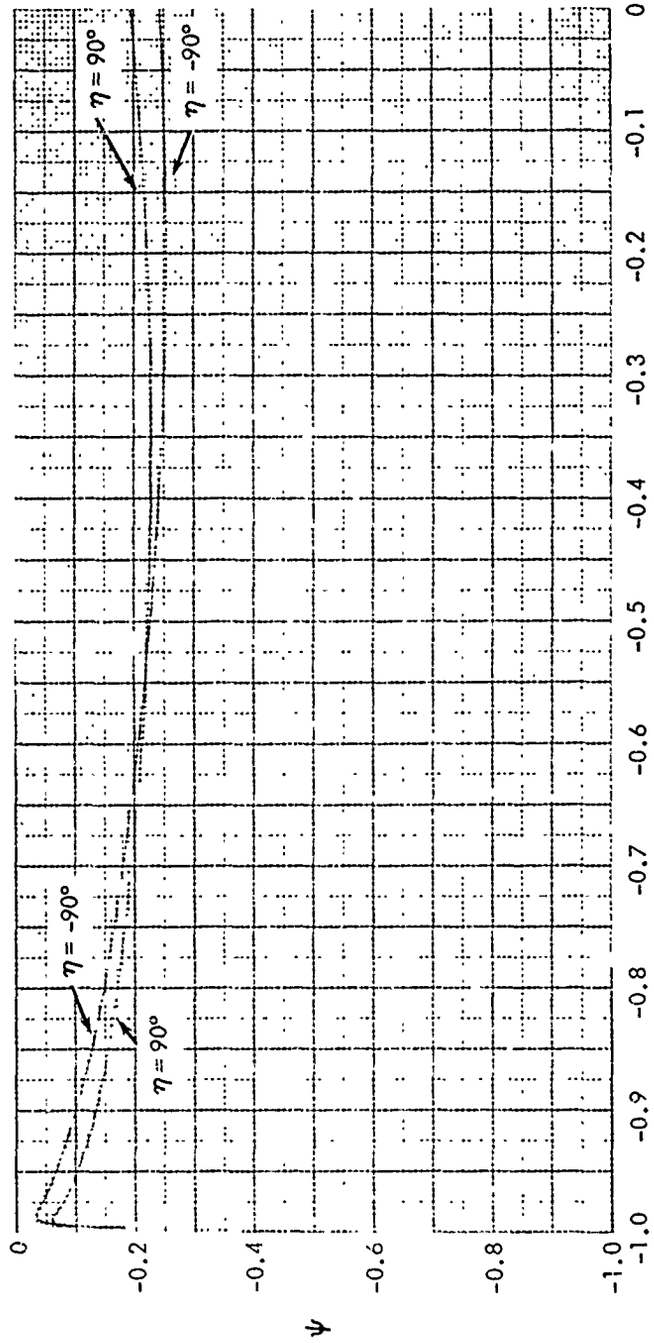

FIG. 13h ψ, TANGENT OF ANGLE BETWEEN POTENTIAL FLOW STREAMLINE AND SURFACE SHEAR STRESS FOR STREAMLINES WITH STARTING ANGLES $\eta = \pm 90°$.

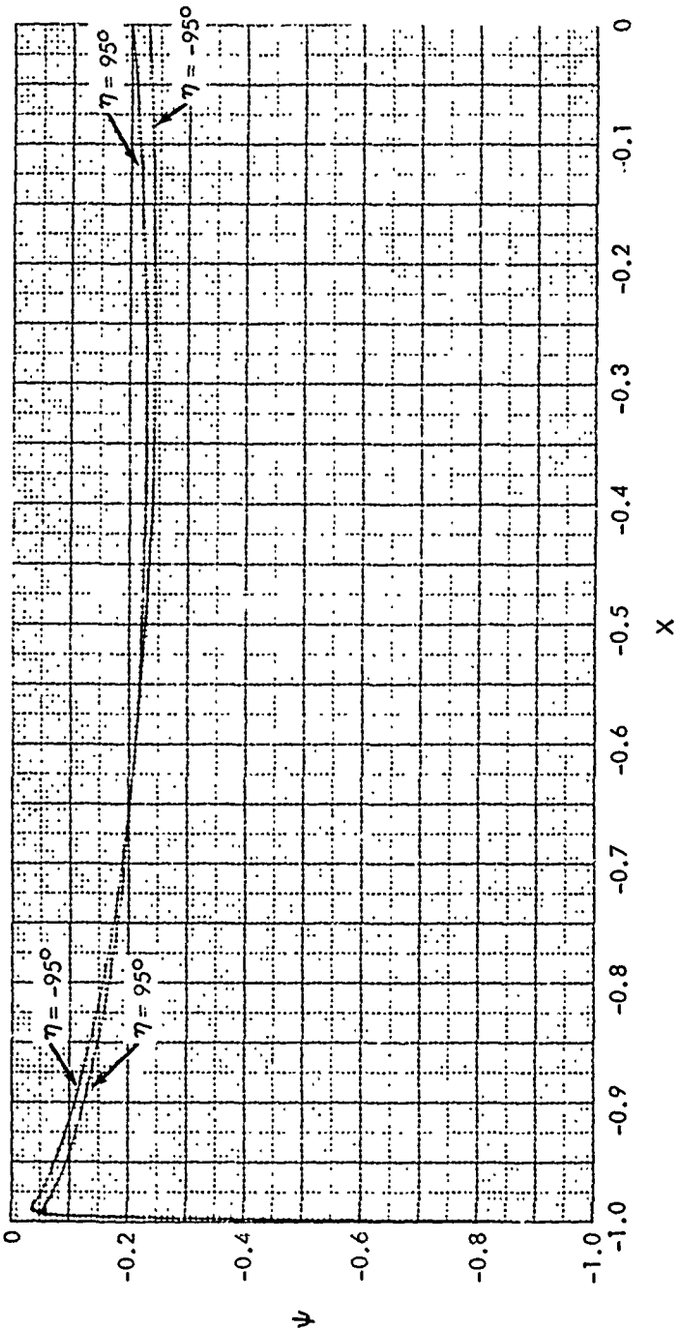

FIG. 13i ψ, TANGENT OF ANGLE BETWEEN POTENTIAL FLOW STREAMLINE AND SURFACE SHEAR STRESS FOR STREAMLINES WITH STARTING ANGLES $\eta = \pm$ 95°.

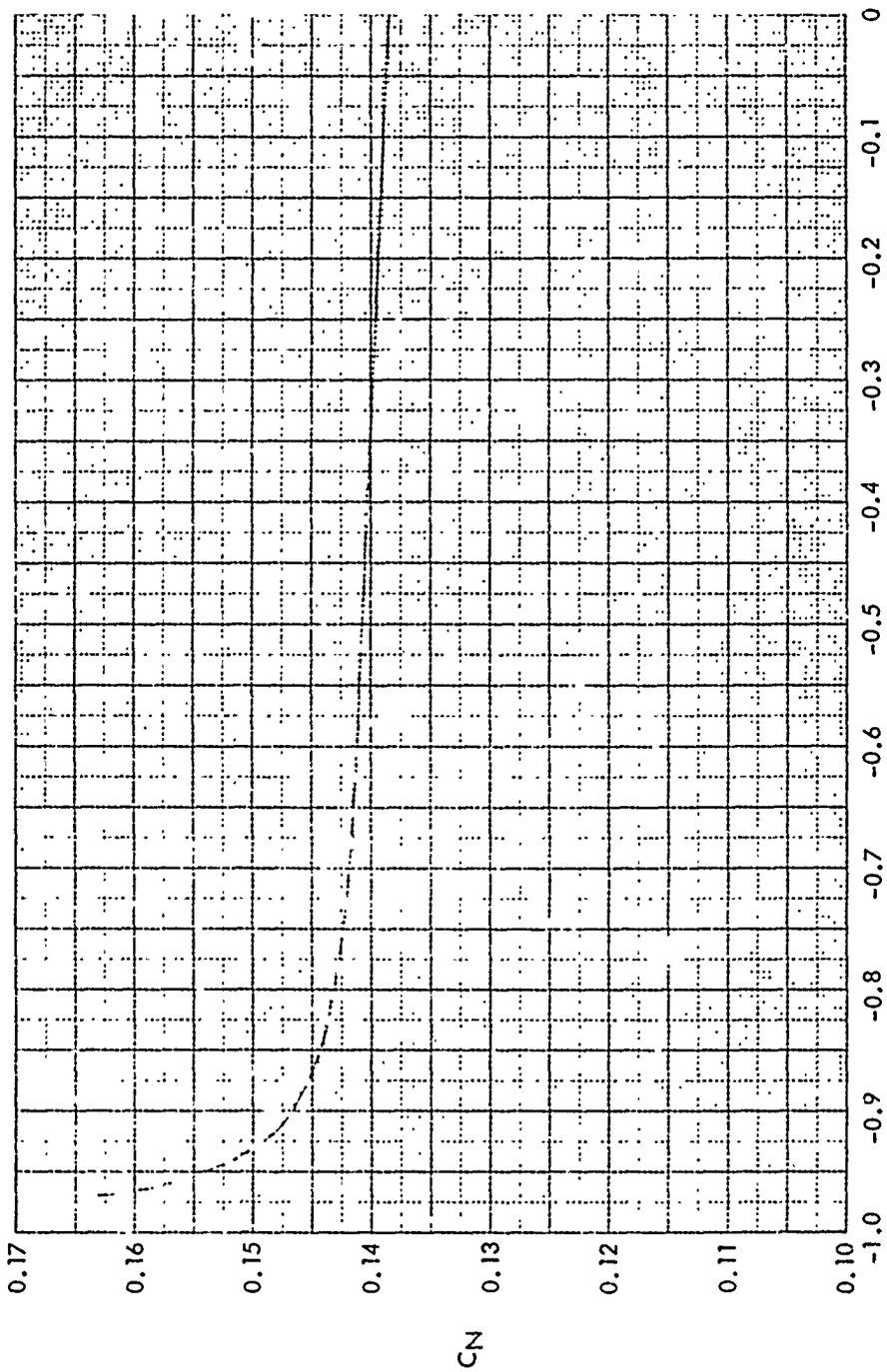

FIG. 14 NORMAL FORCE COEFFICIENT C_N BASED ON LOCAL CROSS SECTION AREA FOR PORTION OF BODY BETWEEN STATION X AND THE BODY NOSE.

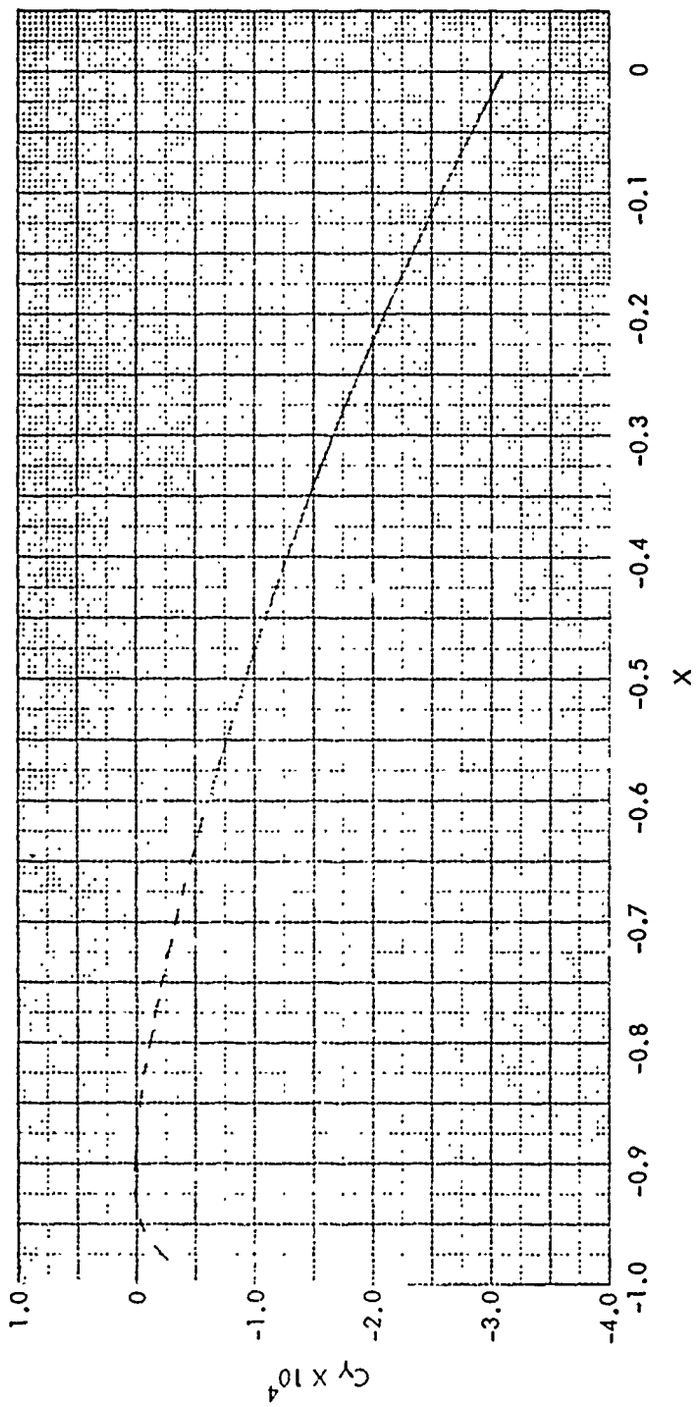

FIG. 15 MAGNUS FORCE COEFFICIENT C_Y BASED ON LOCAL CROSS SECTION AREA FOR PORTION OF BODY BETWEEN STATION X AND BODY NOSE.

APPENDIX A

To obtain an expression for $\frac{\partial a}{\partial x}$ at the stagnation point for $\alpha \neq 0$, the expression

$$\tan a = \frac{v_e}{u_e} \tag{A-1}$$

is used. By symmetry, the stagnation point lies on the curve $\theta = \pi$ and $v_e = 0$ on $\theta = \pi$ for all x. Therefore, $a = 0$ for $\theta = \pi$ for all x; therefore, $\frac{\partial a}{\partial x} = 0$ on $\theta = \pi$ and therefore at the stagnation point. Also $\frac{\partial v_e}{\partial x} = 0$ for all x so that the term

$$\frac{1}{u_e} \frac{\partial v_e}{\partial x} G_7 r_o \cos \phi \tag{A-2}$$

in (86) is zero for $\theta = \pi$.

To obtain an expression for $\frac{\partial a}{\partial \theta}$ at the stagnation point, use (A-1) to get

$$\frac{\partial a}{\partial \theta} = \frac{u_e \frac{\partial v_e}{\partial \theta} - v_e \frac{\partial u_e}{\partial \theta}}{u_e^2 + v_e^2} \tag{A-3}$$

For $x = x_s$ and θ near π,

$$u_e = \left(\frac{\partial u_e}{\partial \theta}\right)_s \Delta\theta + \left(\frac{\partial^2 u_e}{\partial \theta^2}\right)_s \frac{\Delta\theta^2}{2} + \ldots$$

$$v_e = \left(\frac{\partial v_e}{\partial \theta}\right)_s \Delta\theta + \left(\frac{\partial^2 v_e}{\partial \theta^2}\right)_s \frac{\Delta\theta^2}{2} + \cdots$$

$$\frac{\partial u_e}{\partial \theta} = \left(\frac{\partial u_e}{\partial \theta}\right)_s + \left(\frac{\partial^2 u_e}{\partial \theta^2}\right)_s \Delta\theta + \cdots$$

$$\frac{\partial v_e}{\partial \theta} = \left(\frac{\partial v_e}{\partial \theta}\right)_s + \left(\frac{\partial^2 v_e}{\partial \theta^2}\right)_s \Delta\theta + \cdots$$

Because u_e is symmetric with respect to $\theta = \pi$ it follows that $\left(\frac{\partial u_e}{\partial \theta}\right) = 0$ for $\theta = \pi$; therefore, $\left(\frac{\partial u_e}{\partial \theta}\right)_s = 0$. Also $\left(\frac{\partial^2 u_e}{\partial \theta^2}\right)_s \neq 0$ for $\alpha \neq 0$. Moreover, v_e is antisymmetric with respect to $\theta = \pi$. Therefore, $\left(\frac{\partial^2 v_e}{\partial \theta^2}\right) = 0$ for $\theta = \pi$; thus $\left(\frac{\partial^2 v_e}{\partial \theta^2}\right)_s = 0$. Also $\left(\frac{\partial v_e}{\partial \theta}\right)_s \neq 0$ for $\alpha \neq 0$. Then (A-3) becomes

$$\frac{\partial a}{\partial \theta} = \frac{\left(\frac{\partial^2 u_e}{\partial \theta^2}\right)_s \frac{\Delta\theta^2}{2} \left(\frac{\partial v_e}{\partial \theta}\right)_s - \left(\frac{\partial v_e}{\partial \theta}\right)_s \Delta\theta \left(\frac{\partial^2 u_e}{\partial \theta^2}\right)_s \Delta\theta}{\left(\frac{\partial^2 u_e}{\partial \theta^2}\right)_s^2 \frac{\Delta\theta^4}{4} + \left(\frac{\partial v_e}{\partial \theta}\right)_s^2 \Delta\theta^2}$$

or

$$\frac{\partial a}{\partial \theta} = \frac{-\frac{1}{2}\left(\frac{\partial^2 u_e}{\partial \theta^2}\right)_s \left(\frac{\partial v_e}{\partial \theta}\right)_s}{\left(\frac{\partial^2 u_e}{\partial \theta^2}\right)_s^2 \frac{\Delta\theta^2}{4} + \left(\frac{\partial v_e}{\partial \theta}\right)_s^2} \qquad \text{(A-4)}$$

As the stagnation point is approached $\Delta\theta \to o$ and (A-4) becomes

$$\left(\frac{\partial a}{\partial \theta}\right)_s = -\frac{1}{2} \frac{\left(\frac{\partial^2 u_e}{\partial \theta^2}\right)_s}{\left(\frac{\partial v_e}{\partial \theta}\right)_s} \qquad \text{(A-5)}$$

APPENDIX B

From Figure 8 the vector $\vec{S}$ to a point on the body is written, with all lengths non-dimensionalized by the body length $\bar{L}$, as

$$\vec{S} = \hat{i}(d+x) + R\hat{r} \tag{B-1}$$

also

$$\vec{S} = \hat{e}_1\xi + h_o\hat{h} \tag{B-2}$$

or, with (B-1) and (B-2)

$$\hat{i}(d+x) + R\hat{r} = \hat{e}_1\xi + h_o\hat{h} \tag{B-3}$$

Then

$$h_o = \hat{i}\cdot\hat{h}(d+x) + R\hat{h}\cdot\hat{r} \tag{B-4}$$

The unit vector $\hat{h}$ is given by

$$\hat{h} = \hat{e}_2 \cos\beta - \hat{e}_3 \sin\beta \qquad \text{(Figure 8)} \tag{B-5}$$

and the unit vector $\hat{r}$ is given by

$$\hat{r} = \hat{j} \cos\theta - \hat{e}_3 \sin\theta \qquad \text{(Figure 8)} \tag{B-6}$$

Then from (B-4), (B-5), and (B-6)

$$h_o = -(d+x)\sin\alpha\cos\beta + R(\cos\alpha\cos\beta\cos\theta + \sin\beta\sin\theta) \quad \text{(B-7)}$$

The expression for β is given later on.

To find $(\frac{\partial h_o}{\partial \xi})_\beta$ let the equation of the body plus the displacement surface be

$$H(x,R,\theta) = c \quad \text{(B-8)}$$

Also

$$x = x(\xi,h,\beta) \quad \text{(B-9)}$$

$$R = R(\xi,h,\beta) \quad \text{(B-10)}$$

$$\theta = \theta(\xi,h,\beta) \quad \text{(B-11)}$$

Then

$$dx = x_\xi d\xi + x_h dh + x_\beta d\beta \quad \text{(B-12)}$$

$$dR = R_\xi d\xi + R_h dh + R_\beta d\beta \quad \text{(B-13)}$$

$$d\theta = \theta_\xi d\xi + \theta_h dh + \theta_\beta d\beta \quad \text{(B-14)}$$

Also

$$dH = H_R dR + H_x dx + H_\theta d\theta = H_\xi d\xi + H_h dh + H_\beta d\beta \quad \text{(B-15)}$$

Then by using (B-12), (B-13), and (B-14) in the L.H.S. of (B-15) and equating the coefficients of $d\xi$, dh, and $d\beta$ there is obtained

$$H_\xi = H_R R_\xi + H_x x_\xi + H_\theta \theta_\xi \tag{B-16}$$

$$H_h = H_R R_h + H_x x_h + H_\theta \theta_h \tag{B-17}$$

$$H_\beta = H_R R_\beta + H_x x_\beta + H_\theta \theta_\beta \tag{B-18}$$

From $H(\xi, h_o, \beta) = c$ it follows that

$$\left(\frac{\partial h_o}{\partial \xi}\right)_\beta = - \frac{H_\xi}{H_h} \tag{B-19}$$

and

$$\left(\frac{\partial h_o}{\partial \beta}\right)_\xi = - \frac{H_\beta}{H_h} \tag{B-20}$$

When (B-16), (B-17), (B-18) are used in (B-19) and (B-20) the result is

$$\left(\frac{\partial h_o}{\partial \xi}\right)_\beta = - \frac{H_R R_\xi + H_x x_\xi + H_\theta \theta_\xi}{H_R R_h + H_x x_h + H_\theta \theta_h} \tag{B-21}$$

and

$$\left(\frac{\partial h_o}{\partial \beta}\right)_\beta = - \frac{H_R R_\beta + H_x x_\beta + H_\theta \theta_\beta}{H_R R_h + H_x x_h + H_\theta \theta_h} \tag{B-22}$$

The quantities on the R.H.S of (B-21) and (B-22) are obtained as follows. Equation (B-8) is written as

$$H(x,R,\theta) = R-R(x,\theta) = c \tag{B-23}$$

Then

$$H_R = 1 \tag{B-24}$$

$$H_x = \left(\frac{\partial R}{\partial x}\right)_\theta \tag{B-25}$$

$$H_\theta = \left(\frac{\partial R}{\partial \theta}\right)_x \tag{B-26}$$

From $R = r_o + \delta^*$ it follows that

$$\left(\frac{\partial R}{\partial x}_\theta\right) = \left(\frac{\partial r_o}{\partial x}\right)_\theta + \left(\frac{\partial \delta^*}{\partial x}\right)_\theta \tag{B-27}$$

Also

$$\frac{d\delta^*}{dx} = \left(\frac{\partial \delta^*}{\partial x}\right)_\theta + \left(\frac{\partial \delta^*}{\partial \theta}\right)_x \frac{d\theta}{dx} \tag{B-28}$$

Therefore

$$\left(\frac{\partial \delta^*}{\partial x}\right)_\theta = \frac{d\delta^*}{dx} - \left(\frac{\partial \delta^*}{\partial \theta}\right)_x \frac{d\theta}{dx} \tag{B-29}$$

The quantity $\frac{d\delta^*}{dx}$ is computed during the integration of the equation for the displacement surface. The quantity $\left(\frac{\partial \delta^*}{\partial \theta}\right)_x$ is found from the

computed values of δ^* at various θ for a fixed x by use of the spline-fit method of Reference 20. The quantity $\frac{d\theta}{dx}$ is the streamline direction. Equation (B-29) is used with (B-27) to get $(\frac{\partial R}{\partial x})_\theta$.

For $H_\theta = (\frac{\partial R}{\partial \theta})_x$ there is used

$$(\frac{\partial R}{\partial \theta})_x = (\frac{\partial r_o}{\partial \theta})_x + (\frac{\partial \delta^*}{\partial \theta})_x \qquad \text{(B-30)}$$

where $(\frac{\partial r_o}{\partial \theta})_x = 0$ because r_o is independent of θ.

From (B-3), (B-5), and (B-6) it follows that

$$R = \xi \sin \alpha \cos \theta + h_o(\cos \alpha \cos \beta \cos \theta + \sin \beta \sin \theta) \qquad \text{(B-31)}$$

Then

$$R_\xi = \sin \alpha \cos \theta \qquad \text{(B-32)}$$

$$R_{h_o} = \cos \alpha \cos \beta \cos \theta + \sin \beta \sin \theta \qquad \text{(B-33)}$$

$$R_\beta = h_o(-\cos \alpha \sin \beta \cos \theta + \cos \beta \sin \theta) \qquad \text{(B-34)}$$

Also from (B-3), (B-5) and (B-6) it follows that

$$x = \xi \cos \alpha - h_o \sin \alpha \cos \beta - d \qquad \text{(B-35)}$$

Then

$$x_\xi = \cos \alpha \qquad \text{(B-36)}$$

$$x_h = -\sin \alpha \cos \beta \qquad \text{(B-37)}$$

$$x_\beta = h \sin \alpha \sin \beta \qquad \text{(B-38)}$$

To find θ_ξ, θ_h, and θ_β multiply (B-3) by $\hat{e}_1 \cdot$. The result is

$$\xi = (d+x)\cos \alpha + R \sin \alpha \cos \theta \qquad \text{(B-39)}$$

Now multiply (B-3) by $\hat{e}_3 \cdot$. The result is

$$R \sin \theta = h_o \sin \beta \qquad \text{(B-40)}$$

By solving (B-39) for cos θ and (B-40) for sin θ there is obtained

$$\tan \theta = \frac{h_o \sin\beta}{\xi \sin \alpha + h_o \cos \beta \cos \alpha} \qquad \text{(B-41)}$$

Equation (B-3) is multiplied by $\hat{e}_2 \cdot$ with the result

$$-(d+x)\sin \alpha + R \cos \alpha \cos \theta = h_o \cos \beta \qquad \text{(B-42)}$$

From (B-40) and (B-42)

$$\tan \beta = \frac{R \sin \theta}{-(d+x) \sin \alpha + R \cos \alpha \cos \theta} \qquad \text{(B-43)}$$

From (B-41) there is found

$$\theta_\xi = \frac{-h_o \sin \beta \sin \alpha}{(\xi \sin \alpha + h_o \cos \beta \cos \alpha)^2 + (h_o \sin \beta)^2} \qquad \text{(B-44)}$$

$$\theta_h = \frac{\xi \sin \alpha \sin \beta}{(\xi \sin \alpha + h_o \cos \beta \cos \alpha)^2 + (h_o \sin \beta)^2} \qquad \text{(B-45)}$$

$$\theta_\beta = \frac{h_o (\xi \sin \alpha \cos \beta + h_c \cos \alpha)}{(\xi \sin \alpha + h_o \cos \beta \cos \alpha)^2 + (h_o \sin \beta)^2} \qquad \text{(B-46)}$$

APPENDIX C

Unlike slender-body theory the method of Reference 7 and 8 does not require the body to be slender or the angle of attack to be small. In contrast to slender-body theory, however, the contour on which the pressure is computed cannot have a blunt base because the pressure on the body near the base is affected by the shape of the wake behind it. A blunt base results in infinite velocities at the base corner and too high velocities in the entire region near the base. Consequently, the body must be extended beyond the base in a more or less realistic manner. As an approximation to the real flow the body can be extended beyond the base by use of the equation

$$\frac{R_w}{R_b} = \left[\frac{R^*_w}{R_b} - \frac{2}{\pi}\left(\frac{dR^*_w}{dx}\right)_b N\right] \sin^2 \frac{\pi}{2}\frac{x}{NR_b} + \cos^2\frac{\pi}{2}\frac{x}{NR_b}$$

$$+ \frac{2}{\pi}\left(\frac{dR^*_w}{dx}\right)_o \sin\frac{\pi}{2}\frac{x}{NR_b} \qquad \text{(C-1)}$$

where $R_b = R_b(0)$ and the distance x in (C-1) is zero at the body base and positive to the rear. The non-dimensional radius R^*_w is the wake displacement radius very far behind the body. It depends on the drag coefficient of the body; the relation is

$$\frac{R^*_w}{r_m} = \sqrt{\frac{C_D}{2}\left[1+(\kappa-1)M_\infty{}^2\right]} \qquad \text{(Appendix D)} \qquad \text{(C-2)}$$

The arbitrariness in the choice of N and in equation (C-1) itself make it inadvisable to introduce the additional complication of $R^*_w \neq 0$ and $(\frac{dR^*_w}{dx}) \neq 0$. Consequently, instead of (C-1), there can be used

$$\frac{R_w}{R_b} = \cos^2 \frac{\pi}{2} \frac{x}{NR_b} \qquad \text{(C-3)}$$

Calculations for tne body of reference 17 by a program of the method of Reference 8, prepared by Hess and Clissold of Douglas Aircraft showed that N=20 gave the most satisfactory velocity distribution over the rear portion of the body.

When the Mach number is not zero, the pressure coefficient C_p on the body is calculated by using Gotherts Rule (page 397 of Reference 19) together with the method of Reference 8 as programmed for an electronic computer in Reference 7. The velocity distribution is calculated first for a body of thickness ratio $t\sqrt{1-M_\infty^2}$ at an angle of attack of $\alpha\sqrt{1-M_\infty^2}$. The velocities are then multiplied by $\frac{1}{1-M_\infty^2}$. This velocity distribution is used to compute the boundary layer displacement surface δ^* which is added to r_o to get R. The resultant radius R is then multiplied by $\sqrt{1-M_\infty^2}$ and the program of Reference 7 used to compute C_p at $\alpha\sqrt{1-M_\infty^2}$; this C_p is then multiplied by $\frac{1}{1-M_\infty^2}$ to get the C_p distribution used to compute the Magnus force and moment.

The force in the Y direction is given by

$$\overline{F_Y} = -\int \overline{P}\,\hat{n}\cdot\hat{e}_3 d\overline{A} \tag{C-4}$$

where $\hat{n}$ is the outward unit normal to the body surface plus the displacement surface and $\hat{e}_3$ is a unit vector along the Y axis Figure 6. The unit vector $\hat{n}$ is given by

$$\hat{n} = \frac{\nabla H}{|\nabla H|} \tag{C-5}$$

where the equation of the body is

$$H(x,R,\theta) = R-R(x,\theta) = c \tag{C-6}$$

Then in the $\hat{i},\hat{r},\hat{\theta}$ system (Figure 8)

$$\nabla H = \hat{i}H_x + H_R\hat{r} + \frac{H_\theta}{R}\hat{\theta} \tag{C-7}$$

or

$$\nabla H = -\hat{i}R_x + \hat{r} - \frac{R_\theta}{R}\hat{\theta} \tag{C-8}$$

Then

$$\hat{n} = \frac{-\hat{i}R_x + \hat{r} - \frac{R_\theta}{R}\hat{\theta}}{\sqrt{R_x^2 + 1 + (\frac{R_\theta}{R})^2}} \tag{C-9}$$

therefore

$$\hat{n}\cdot\hat{e}_3 = \frac{-\sin\theta + \frac{R_\theta}{R}\cos\theta}{\sqrt{R_x^2 + 1 + (\frac{R_\theta}{R})^2}} \tag{C-10}$$

When the static pressure $\bar{P}$ is written as

$$\bar{P} = \frac{\bar{\rho}_\infty}{2} \bar{V}_\infty^2 C_p + \bar{P}_\infty \tag{C-11}$$

and when it is noted that

$$\int \bar{P}_\infty \hat{n} \cdot \hat{e}_3 d\bar{A} = 0 \tag{C-12}$$

it follows that (C-4) becomes

$$\frac{\bar{F}_y}{\frac{\bar{\rho}_\infty}{2} \bar{V}_\infty^2 \bar{L}^2} = \int_{-d}^{o} \int_{o}^{2\pi} C_p \frac{(\sin\theta - \frac{R_\theta}{R}\cos\theta)}{\sqrt{R_x^2 + 1 + (\frac{R_\theta}{R})^2}} R \frac{\sqrt{1 + (\frac{\partial \delta^*}{\partial x}\cos\phi)^2}}{\cos\phi} d\theta dx \tag{C-13}$$

where

$$dA = R \frac{\sqrt{1 + (\frac{\partial \delta^*}{\partial x}\cos\phi)^2}}{\cos\phi} d\theta dx \tag{C-14}$$

has been used. The non-dimensional area dA is on the body plus the displacement surface.

By using $\cos\phi \frac{\partial}{\partial x} = \frac{\partial}{\partial s_x}$, $R = \frac{\partial R}{\partial s_x} s_x = s_x$ and $\cos\phi \to o$ near the nose of a blunt body it can be shown that at the stagnation point the integrand becomes equal to $-C_{p_s} (\frac{\partial \delta^*}{\partial \theta})_s \cos\theta$. The value of $(\frac{\partial \delta^*}{\partial \theta})_s$ is zero because the δ^* surface is assumed to be continuous; therefore the integrand in (C-13) is zero at the nose of a blunt body.

The Magnus moment about the nose (x=-d) is given by

$$\frac{\bar{M}_y}{\frac{\bar{\rho}_\infty}{2}\bar{V}_\infty^2\bar{L}^3} = \int_{-d}^{o}\int_{o}^{2\pi} C_p \frac{\sin\theta - \frac{R_\theta}{R}\cos\theta}{\sqrt{R_x^2 + 1 + \left(\frac{R_\theta}{R}\right)^2}} R \frac{\sqrt{1 + \left(\frac{\partial \delta^*}{\partial x}\cos\phi\right)^2}}{\cos\phi}(d+x)\,d\theta dx \qquad \text{(C-15)}$$

where $\bar{M}_y$ is positive as shown in Figure 1.

APPENDIX D

Far behind the body the flow is parallel to $\bar{V}_\infty$. The wake displacement radius $\bar{R}_w^*$ far downstream is defined by

$$2\pi \int_{\bar{R}_w^*}^{\infty} \bar{\rho}_\infty \bar{V}_\infty \bar{y} d\bar{y} = 2\pi \int_0^{\infty} \bar{\rho}\bar{u}\bar{y} d\bar{y} \tag{D-1}$$

In (D-1) $\bar{y}$ is measured from the wake center line and $\bar{u}$ is parallel to $\bar{V}_\infty$.

Equation (D-1) can be written as

$$\int_0^{\infty} \bar{\rho}_\infty \bar{V}_\infty \bar{y} d\bar{y} - \int_0^{\bar{R}_w^*} \bar{\rho}_\infty \bar{V}_\infty \bar{y} d\bar{y} = \int_0^{\infty} \bar{\rho}\bar{u}\bar{y} d\bar{y}$$

or

$$\bar{\rho}_\infty \bar{V}_\infty \frac{\bar{R}_w^{*2}}{2} = \int_0^{\infty} (\bar{\rho}_\infty \bar{V}_\infty - \bar{\rho}\bar{u})\, \bar{y} d\bar{y} \tag{D-2}$$

Then

$$\left(\frac{R_w^*}{r_m}\right)^2 = 2 \int_0^{\infty} (1-\rho u) \frac{y}{r_M} \frac{dy}{r_M} \tag{D-3}$$

$$\frac{\bar{\rho}}{\bar{\rho}_\infty} = \frac{\bar{T}_\infty}{\bar{T}} = \frac{\bar{C}_p\bar{T}_s - \frac{\bar{V}_\infty^2}{2}}{\bar{C}_p\bar{T}_s - \frac{\bar{u}^2}{2}} \qquad \text{(D-8)}$$

where in (D-8) $\bar{C}_p$ is the specific heat at constant pressure.

Then with (D-7), (D-8) becomes

$$\frac{\bar{\rho}}{\bar{\rho}_\infty} = \frac{1}{1 - \frac{f_o\bar{V}_\infty^2}{\bar{C}_p\bar{T}_s - \bar{V}_\infty^2/2}} \qquad \text{(D-9)}$$

Let

$$C_o = \frac{\bar{V}_\infty^2}{\bar{C}_p\bar{T}_s - \frac{\bar{V}_\infty^2}{2}} = \frac{\bar{V}_\infty^2}{\bar{C}_p\bar{T}_\infty} = (\kappa-1)M_\infty^2$$

Then

$$\frac{\bar{\rho}}{\bar{\rho}_\infty} = \rho = \frac{1}{1 - f_oC_o} \qquad \text{(D-10)}$$

Also with $$1 - \rho u = \frac{-f_o}{1 - f_oC_o}(1+C_o)$$

and $$\rho u(1-u) = \frac{-f_o}{1 - f_oC_o}$$

Then (D-6) becomes

$$\frac{R_w^{*2}}{\beta_\infty} = 2 \frac{(1+C_o) \int_o^\infty \frac{f_o}{1 - f_o C_o} \frac{y}{r_M} d\frac{y}{r_M}}{\int_o^\infty \frac{f_o}{1 - f_o C_o} \frac{y}{r_M} d\frac{y}{r_M}}$$

or

$$\frac{R_w^{*2}}{\beta_\infty} = 2 \left[1+(\kappa-1)M_\infty^2\right] \qquad \text{(D-11)}$$

or with (D-5)

$$\frac{R_w^*}{r_M} = \sqrt{\frac{C_D}{2} \left[1 + (\kappa-1)M_\infty^2\right]} \qquad \text{(D-12)}$$

TABLE I
Expressions for the Gi(n)

$$G_1 = \frac{n-1}{(n+1)(n+2)(2n+1)}$$

$$G_2 = \frac{1}{(n+1)(n+2)}$$

$$G_3 = \frac{n^2 + n-1}{(n+1)(n+2)}$$

$$G_4 = \frac{n+1}{n+2}$$

$$G_5 = \frac{3n + 4}{2(n+1)(n+2)(2n+3)}$$

$$G_6 = \frac{-2(n+1)^2}{(n+2)(2n+3)}$$

$$G_7 = \frac{n}{n+1}$$

$$G_8 = \frac{1}{2n+1}$$

$$G_9 = \frac{1}{2(n+1)}$$

$$G_{10} = \frac{-n\ (2n+3)}{2(n+1)(n+2)}$$

$$G_{11} = \frac{-1}{(n+1)(2n+1)(2n+3)}$$

$$G_{12} = \frac{n}{(n+1)(2n+1)}$$

$$G_{13} = \frac{1}{2(n+1)(2n+1)}$$

$$G_{14} = \frac{3n}{2(n+1)(n+2)(2n+1)}$$

TABLE II
Integrals in Eq. (30) and (31)

$$\int_0^1 u(u_e-u)\,d\zeta = J_1\psi^2 + J_2\psi + J_3$$

$$\int_0^1 (u_e-u)\,d\zeta = J_4\psi + J_5$$

$$\int_0^1 v(u_e-u)\,d = J_6\psi^2 + J_7\psi + J_8$$

$$\int_0^1 (v_e-v)\,d\zeta = J_{18}\psi + J_{19}$$

$$\int_0^1 (v_e^2-v^2)\,d\zeta = J_9\psi^2 + J_{10}\psi + J_{11}$$

$$\int_0^1 v(v_e-v)\,d\zeta = J_9\psi^2 + J_{12}\psi + J_{13}$$

$$\int_0^1 u(v_e-v)\,d\zeta = J_6\psi^2 + J_{14}\psi + J_{15}$$

$$\int_0^1 (u_e v_e-uv)\,d\zeta = J_6\psi^2 + J_{16}\psi + J_{17}$$

TABLE III
Expressions for the Ji

$$J_1 = A^2G_{11}\sin^2 a$$

$$J_2 = A\left[-(AG_1-BG_2)\cos a \sin a - 2CG_5\sin^2 a\right]$$

$$J_3 = A(AG_8+B)G_7\cos^2 a + C(-AG_3+BG_4)\cos a \sin a + C^2G_6\sin^2 a$$

$$J_4 = AG_2\sin a$$

$$J_5 = AG_7\cos a + CG_4\sin a$$

$$J_6 = -A^2G_{11}\cos a \sin a$$

$$J_7 = A\left[(AG_{13}+BG_2)\sin^2 a + AG_{14}\cos^2 a + 2CG_5\cos a \sin a\right]$$

$$J_8 = \left[A(AG_{12}+BG_7)-C^2G_6\right]\cos a \sin a + C(AG_9+BG_4)\sin^2 a - ACG_{10}\cos^2 a$$

$$J_9 = A^2G_{11}\cos^2 a$$

$$J_{10} = A\left[AG_1-(q_e+B)G_2\right]\cos a \sin a - 2ACG_5\cos^2 a$$

$$J_{11} = A\left[AG_{12}+(q_e+B)G_7\right]\sin^2 a + C\left[AG_3-(q_e+B)G_4\right]\cos a \sin a + C^2G_6\cos^2 a$$

$$J_{12} = -A\left[(2AG_{13}+2G_2B-q_eG_2)\cos a \sin a + 2CG_5\cos^2 a\right]$$

$$J_{13} = \left[q_e(2AG_9+B) - (A^2G_8+4G_9AB+B^2)\right]\sin^2 a + C\left[q_eG_4-2(AG_9+BG_4)\right]\cos a \sin a + C^2G_6\cos^2 a$$

$$J_{14} = A\left[-(AG_{13}+BG_2)\cos^2 a + (AG_{13}+BG_2-q_eG_2)\sin^2 a + 2CG_5\cos a \sin a\right]$$

$$J_{15} = \left[q_e(2AG_9+B) - (A^2G_8+4ABG_9+B^2)-C^2G_6\right]\cos a \sin a - C(AG_9+BG_4)\cos^2 a + C(AG_9+BG_4-q_eG_4)\sin^2 a$$

$$J_{16} = A\left[-(AG_{13}+BG_2)(\cos^2 a-\sin^2 a) + 2CG_5\sin a \cos a\right]$$

$$J_{17} = \left[q_e^2-(A^2G_8+4ABG_9+B^2)-C^2G_6\right]\cos a \sin a - C(AG_9+BG_4)(\cos^2 a-\sin^2 a)$$

$$J_{18} = -AG_2\cos a$$

$$J_{19} = AG_7\sin a - CG_4\cos a$$

TABLE IV
Program for Computation of Magnus Force and Moment
For Half-Ellipsoid

Column I are symbols that occur in program
Column II are symbols in symbol list (page vi) that corresp[illegible] symbols in Column I

I	II
A	A
AK	k
AJN	J_i
Alpha	α
B	B
C	C
COS A	$\cos [\alpha \frac{\pi}{180}]$
COSMA	Cos a
COSPH	cos ϕ
COST	cos θ
DELTA	δ
DELTAI	δ_s
DELTAZ	δ_s for $\alpha \neq 0$, $\omega = 0$
DELTX	Δx
DDDX	$\frac{d\delta}{dx}$
DDSTAR	$\Delta\delta^*$
DDSTDX	$d\delta^*/dx$
DRDS	$\frac{dr_o}{ds}$
DSTARI	δ^*_s
DTHDX	$\frac{d\theta}{dx}$

DTHOLD	$\frac{d\theta}{dx}$ at $(x-\Delta x)$
DUEXSP	$(\frac{\partial u_e}{\partial x})_s$
EN	n
FN	G_i
G	K_1
GAMMA	η
H	K_2
P	p
PDT	$\frac{\partial \delta}{\partial \theta}$
PDX	$\frac{\partial \delta}{\partial x}$
PJNT	$\frac{\partial J_i}{\partial \theta}$
PJNX	$\frac{\partial J_i}{\partial x}$
PPT	$\frac{\partial \psi}{\partial \theta}$
PPX	$\frac{\partial \psi}{\partial x}$
PRT	$\frac{\overline{\omega r_o}}{\overline{V}_\infty}$
PRX	$\frac{\partial r_o}{\partial x}$
PRX1	$\frac{1}{r_o}\frac{\partial r_o}{\partial x}$

PSI	ψ
PSII	ψ_s
PUET	$\frac{\partial u_e}{\partial \theta}$
PUEX	$\frac{\partial u_e}{\partial x}$
PVET	$\frac{\partial v_e}{\partial \theta}$
PVEX	$\frac{\partial v_e}{\partial x}$
QVRAT	$\sqrt{u_e^2 + v_e^2}$
QDQN	$q_e \frac{\partial q_e}{\partial n}$
QDQS	$q_e \frac{\partial q_e}{\partial s}$
R	r_o
REL	Reynolds number $\frac{V_\infty \bar{L}}{\nu_\infty}$
RHO	I
RPDSTR	$r_c + \delta^*$
RUC	$r_o u_e \cos \phi$
SIN A	$\sin[\alpha \frac{\pi}{180}]$
SMA	a
SNSMA	Sin a
SINT	Sin θ

T	t
THETA	θ
TWQE	$\tau_{w_{q_e}}$
TWRT	τ_{w_θ}
TWXR	τ_{w_x}
URATIO	u_e
V RATIO	v_e
XEN	Value of n for $x=x_s$
XP	Values of x chosen for printout before run on computer
XSTAG	x_s

```
      PROGRAM JJTETV(INPUT,OUTPUT,TAPE5=INPUT,TAPE6=OUTPUT,TAPE15)
      COMMON /COEF/ H,SINA,COSA,T,P,G,REL,ALPHA,XSTAG
      COMMON /FTERMS/ F1,F2,F3,F4,F5,F6,F7,F8,F9,F10,F11,F12,F13,F14,
     1 F15,F16,F17,F18,F19,F20,F21,F22,F23,F24,F25,F26,F27,F28,F29
      COMMON /JTERMS/ AJ1,AJ2,AJ3,AJ4,AJ5,AJ6,AJ7,AJ8,AJ9,AJ10,AJ11,
     1 AJ12,AJ13,AJ14,AJ15,AJ16,AJ17,AJ18,AJ19,AJ1X,AJ2X,AJ3X,AJ6X,AJ7X,
     2 AJ8X,AJ9X,AJ12X,AJ13X,AJ14X,AJ15X,AJ4X,AJ5X,AJ18X,AJ19X
      DIMENSION PDX(50),PPX(50),PDT(50),PPT(50 )
      DIMENSION PSIDX(25),DELDX(25)
      NAMELIST/INPT1/ RHO,ALPHA,T,EM,AK,REL,EN,P,ERR,XEND,MPFREQ,GAMMA
     1, EZERO
      WRITE(6,100)
  100 FORMAT(1H1,10X14HNAMELIST INPT1 //)
      READ(5,2003) NFWD
 2003 FORMAT(18I4)
      WRITE(6,2) NFWD
    2 FORMAT(////*   FORWARDSPACE*I3* FILES ON TAPE*)
C     DOUBLE-CHECK NUMBER OF FILES TO SKIP
      JFWD=NFWD
    3 READ(5,2003) NCASE
      IF(NCASE.EQ.0) CALL REWIND(15)
      IF(NCASE.EQ.0) STOP
      NFWD=NFWD+1
      IF(NFWD.NE.NCASE) STOP
      IF(NCASE.EQ.1) GO TO 2004
      IF(JFWD.EQ.(NFWD-1)) CALL FSFILE(15,JFWD,0)
 2004 WRITE(15,2003) NCASE
      READ(5,INPT1)
      WRITE(6,INPT1)
      IPRINT=0
      MPRINT=1
      DDDX=0.
      DDSTDX=0.
      ERRX=2.*EZERO
      ERRX2=ERRX/10.
      CAMMAR=GAMMA*0.017453
      MFREQ2=MPFREQ/10
      PI=3.14159265358979
      PI2=PI/2.
    5 CALL FCALC(EN)
      SINA=SIN(ALPHA*0.017453)
      COSA=COS(ALPHA*0.017453)
      T2=T*T
      T3=SQRT(1.-T2)
   10 T4=ALOG( (1.+T3)/(1.-T3) )
      T5=2.*T3
      G=1.-T2*(T4-T5)/(T2*T4-T5)
      H=1.-(T2*T4-T5)/(T2*T4+T5*(1.-T2*2.))
      G2=G*G
      H2=H*H
      TANA2=(TAN(ALPHA*0.017453))**2
      QC=(G2+H2*TANA2)/(G2+H2*T2*TANA2)
```

```
      IF(ALPHA.EQ.0.) GO TO 11
      IF(ALPHA.NE.0.0.AND.P.EQ.0.) GO TO 1111
      PINPUT=P
      AINPUT=ALPHA
      UXS1=(G2*COSA*COSA-H2*SINA*SINA*(-1.))/(T2*COSA)
      UXS2=(G2+T2*H2*TANA2)**1.5/(G2+H2*TANA2)**2
      DUEXSP=UXS1*UXS2
      XEN=1.
      XEN1=XEN+1.
      XEN2=XEN+2.
      EN21=2.*XEN+1.
      XF10=1./EN21
      XF9=XEN/XEN1
      DELTAZ=SQRT(1./(DUEXSP*  REL*(2.*XF10+1.)*XF9))
      ALPHA=0.
      CALL QSUBR(PS,DET)
      DELZP=DET
      PSII=PS
      P=0.
      CALL QSUBR(PS,DET)
      DELZZ=DET
      DELTAI=DELZP+DELTAZ-DELZZ
**********
      IF(NCASE.EQ.1) DELTAI=DELTAI*5.0
      IF(NCASE.EQ.2) DELTAI=DELTAI*50.0
      P=PINPUT
      ALPHA=AINPUT
      GO TO 12
 1111 UXS1=(G2*COSA*COSA-H2*SINA*SINA*(-1.))/(T2*COSA)
      UXS2=(G2+T2*H2*TANA2)**1.5/(G2+H2*TANA2)**2
      DUEXSP=UXS1*UXS2
      XEN=1.
      XEN1=XEN+1.
      XEN2=XEN+2.
      EN21=2.*XEN+1.
      XF10=1./EN21
      XF9=XEN/XEN1
      DELTAI=SQRT(1./(DUEXSP*  REL*(2.*XF10+1.)*XF9))
      PSII=0.
      GO TO 12
   11 CALL QSUBR(PSIO,DELTO)
      PSII=PSIO
      DELTAI=DELTO
   12  DSTARI=DELTAI*.5
      XI=-1./ SQRT(1.+T2*H2*TANA2/G2)
      THETAI=3.14159265358979
      PSII=-1.
      XSTAG=XI
      XP=-.99
   13 ISTEP=1
      WRITE(6,1999) NCASE,ALPHA,P,REL,GAMMA,RHO
 1999 FORMAT(1H1,T10,*CASE*I4,T25,*ELLIPSOID*/T15,*ALPHA=*F6.1,T35,*P=*F6.3,
```

```
     1T50*REYNOLDS NO.=*E10.3,T80*GAMMA=*F7.2,          T99*RHO=*E9.2//
     1          T10*X*, T22*THETA*, T37*PSI*, T50*DELTA*, T63*UR*,
     1 T77*VR*, T91*TWRX*, T105*TWRT*, T119*DSTAR*/T22*DTH/DX*,
     2 T36*DELTX*,T51*SMA*,
     3 T65*A*, T79*B*, T92*C*,  T106*PRX*,  T119*COSPH*/
     4 T22*R*, T36*TWQE*, T51*QE*, T62*  DDDX  *, T78*QDQS*, T91*QDQN*,
     5 T105*DR/DS*, T118*STHETA* /T22*RPDSTR*,T35*DDSTDX*)
  14 X1=XI
  15 X=X1
     X2=X*X
     XT=1.-X2*(1.-T2)
     X21=1.-X2
     COSPH=SQRT(X21/XT)
  20 SINPH=COSPH*(-X*T/SQRT(X21))
     R=T*SQRT(X21)
     PRT=P*R/T
     TERM1=COSPH*G*COSA
     TERM2=X/SQRT(XT)*T*H*SINA
  26 PSI=PSII
     DELTA=DELTAI
     DSTAR=DSTARI
     RPDSTR=R+DSTAR
     BETA=ATAN(PSI)
     D2=DELTA**2
  30 THETA=THETAI
     IF(THETA.GE.0..AND.THETA.LE.PI2) STHETA=PI2-THETA
     IF(THETA.GT.PI2.AND.THETA.LE.2.*PI) STHETA=5.*PI2-THETA
     SINT=SIN(THETA)
     COST=COS(THETA)
     VRATIO=-H*SINT*SINA
     URATIO=TERM1-TERM2*COST
     IF(X.NE.XSTAG) GO TO 35
     QVRAT=0.
     SMA=0.
     SNSMA=0.
     COSMA=1.
     RUC=0.
     DTHDX=0.
     DRDS=-COSPH*X*T/SQRT(X21)
     QDQS=0.
     QDQN=0.
     DTHOLD=DTHDX
     DELTX=2.*RHO*COSPH*COS(GAMMAR)
     DCHECK=ABS(GAMMA)
     IF(DCHECK.GT.90.) DELTX=1.0E-8
     DELTAT=-2.*RHO*SIN(GAMMAR)/R
     GO TO 38
  35 QVRAT=SQRT(URATIO**2+VRATIO**2)
  36 IF(URATIO.NE.0.) GO TO 37
     SMA=0.
     SNSMA=0.
     COSMA=1.
```

```
      DTHDX=0.
      RUC=0.
      GO TO 38
   37 SMA=ATAN(VRATIO/URATIO)
      SNSMA=VRATIO/QVRAT
      COSMA=URATIO/QVRAT
      RUC=R*URATIO*COSPH
      DTHDX=VRATIO/RUC
   38 SINA2=SNSMA**2
      COSA2=COSMA**2
   41 B=PRT*SNSMA
      A=QVRAT-B
      C=PRT*COSMA
      IF(X21.GT.0.) GO TO 42
      PUEX=0.0
      PVET=0.0
      PUET=0.0
      PRX=0.
      PRX1=0.
      GO TO 43
   42 PUEX=-(X*T2*G*COSA/SQRT(X21)+T*H*SINA*COST)/XT**1.5
      PUET=X*T*H*SINA*SINT/SQRT(1.-X2*(1.-T2))
      PVET=-H*SINA*COST
      PVEX=0.
      PRX=-X*T/SQRT(X21)
      PRX1=-X/X21
      IF(X.EQ.XSTAG) GO TO 43
      BRAK1=(URATIO*PUEX+VRATIO*PVEX)*COSPH
      BRAK2=(URATIO*PUET+VRATIO*PVET)/R
      UQ=URATIO/QVRAT
      VQ=VRATIO/QVRAT
      QDQS=UQ*BRAK1+VQ*BRAK2
      QDQN=-VQ*BRAK1+UQ*BRAK2
      DRDS=PRX*COSPH/SQRT(1.+R*R*DTHDX**2*COSPH**2)
   43 CALL JAYS(A,B,C,COSMA,SNSMA,SINA2,COSA2,QVRAT)
      AJ1X=AJ1
      AJ2X=AJ2
   50 AJ3X=AJ3
      AJ4X=AJ4
      AJ5X=AJ5
      AJ6X=AJ6
      AJ7X=AJ7
   55 AJ8X=AJ8
      AJ9X=AJ9
      AJ10X=AJ10
      AJ11X=AJ11
      AJ12X=AJ12
   60 AJ13X=AJ13
      AJ14X=AJ14
      AJ15X=AJ15
      AJ16X=AJ16
      AJ17X=AJ17
```

```
   AJ18X=AJ18
   AJ19X=AJ19
   CALL PARTLS(X,THETA,                PJ1X,PJ2X,PJ3X,PJ6X,PJ14X,PJ15X,
  1PJ6T,PJ7T,PJ8T,PJ9T,PJ12T,PJ13T,PJ4X,PJ5X,PJ18T,PJ19T)

   TWQE=AK*ABS(A)**(2-EM)/(REL**EM*DELTA**EM)
   TWXR=TWQE*(COSMA-PSI*SNSMA)
   TWTR=TWQE*(SNSMA+PSI*COSMA)
   RCOS=R*COSPH
   C0=RCOS*(PSI*PSI*AJ1X+PSI*AJ2X+AJ3X)
   C1=RCOS*DELTA*(2.*PSI*AJ1X+AJ2X)
   C2=PSI*PSI*AJ6X+PSI*AJ7X+AJ8X
   C3=DELTA*(2.*PSI*AJ6X+AJ7X)
   PART1=(PSI*PSI*PJ1X+PSI*PJ2X+PJ3X)*RCOS
   PART2=(PSI*PSI*AJ1X+PSI*AJ2X+AJ3X)*SINPH
   PART3=RCOS*PVEX*(PSI*AJ4X+AJ5X)
   PART4=PSI*PSI*PJ6T+PSI*PJ7T+PJ8T
   PART5=PVET*(PSI*AJ18X+AJ19X)
   PART6=(PSI*PSI*AJ9X+PSI*AJ10X+AJ11X)*SINPH
   C4=DELTA*(PART1+PART2+PART3+PART4+PART5-PART6)
   C5=RCOS*(PSI*PSI*AJ6X+PSI*AJ14X+AJ15X)
   C6=RCOS*DELTA*(2.*PSI*AJ6X+AJ14X)
   C7=PSI*PSI*AJ9X+PSI*AJ12X+AJ13X
   C8=DELTA*(2.*PSI*AJ9X+AJ12X)
   P91=(PSI*PSI*PJ6X+PSI*PJ14X+PJ15X)*RCOS
   P92=(PSI*PSI*AJ6X+PSI*AJ14X+AJ15X)*SINPH
   P93=PSI*PSI*PJ9T+PSI*PJ12T+PJ13T
   P94=PVET*(PSI*AJ18X+AJ19X)
   P95=(PSI*PSI*AJ6X+PSI*AJ16X+AJ17X)*SINPH
   P96=RCOS*PVEX*(PSI*AJ4X+AJ5X)
   C9=DELTA*(P91+P92+P93+P94+P95+P96)
   DEN1=C0*C6-C1*C5
   DEN2=C2*C8-C3*C7
   CON1=R*TWXR-C4
   CON2=R*TWTR-C9
   IF(ABS(X).LT.0.95) MPFREQ=MFREQ2
   IF(X.EQ.XSTAG) GO TO 89
   IF(X-XP)92,91,92
91 IF(X.LT.-.9) XP=XP+.01
   IF(X.GE.-.9) XP=XP+.025
   IPRINT=IPRINT+1
   IF(IPRINT.LT.11) GO TO 93
   WRITE(6,1999) NCASE,ALPHA,P,REL,GAMMA,RHO
   IPRINT=1
   GOTO93
92 MPRINT=MPRINT+1
   IF(MPRINT.LT.MPFREQ) GO TO 94
   MPRINT=0
89 IPRINT=IPRINT+1
   IF(IPRINT.LT.11) GO TO 93
   WRITE(6,1999) NCASE,ALPHA,P,REL,GAMMA,RHO
   IPRINT=1
```

```
   93 WRITE(6,2000) X,THETA,PSI,DELTA,URATIO,VRATIO,TWXR,TWTR,DSTAR,
     1 DTHDX,DELTX,SMA,A,B,C,PRX,COSPH,R,TWQE,QVRAT,DDDX,QDQS,QDQN,DRDS
     2 ,STHETA,RPDSTR,DDSTDX
 2000 FORMAT(1H0,1P9E14.5/15X1P8E14.5/15X1P8E14.5/15X1P2E14.5)
      WRITE(15,2001) X,THETA,PSI,DELTA,URATIO,VRATIO,TWXR,TWTR,DSTAR
      WRITE(15,2001) DTHDX,DELTX,SMA,A,B,C,PRX,COSPH
      WRITE(15,2001) R,TWQE,QVRAT,DDDX,QDQS,QDQN,DRDS,STHETA
      WRITE(15,2001) RPDSTR,DDSTDX
 2001 FORMAT(1P9E14.5)
C  VARIABLE A IN MAIN PROGRAM IS VELOCITY RATIO
   94 K=1
      IF(X.NE.XSTAG) GO TO 95
      DELDX(K)=DELTA
      PSIDX(K)=PSI
      GO TO 130
   95 PDX(1)=(C6*CON1-C1*CON2)/DEN1
      PPX(1)=(C0*CON2-C5*CON1)/DEN1
      IF(P.NE.0.) GO TO 96
      PDT(1)=0.
      PPT(1)=0.
      GO TO 97
   96 PDT(1)=(C8*(CON1-C0*PDX(1)-C1*PPX(1))-C3*(CON2-C5*PDX(1)-C6*PPX(1)
     1))/DEN2
      PPT(1)=(C2*(CON2-C5*PDX(1)-C6*PPX(1))-C7*(CON1-C0*PDX(1)-C1*PPX(1)
     1 ))/DEN2
   97 DELDX(1)=DELTA+(PDX(1)+PDT(1)*DTHDX)*DELTX
      PSIDX(1)=PSI+(PPX(1)+PPT(1)*DTHDX)*DELTX
C*****ITERATION
  102 DO 128 K=2,25
      E1=C2*PDT(K-1)
      E2=C3*PPT(K-1)
  105 E3=C7*PDT(K-1)
      E4=C8*PPT(K-1)
      E5=C0*PDX(K-1)
      E6=C1*PPX(K-1)
      E7=C5*PDX(K-1)
  110 E8=C6*PPX(K-1)

      IF(P.NE.0.) GO TO 111
      PDT(K)=0.
      PPT(K)=0.
      GO TO 112
  111 PDT(K)=(C8*(CON1-E5-E6)-C3*(CON2-E7-E8))/DEN2
      PPT(K)=(C2*(CON2-E7-E8)-C7*(CON1-E5-E6))/DEN2
  112 PDX(K)=(C6*(CON1-E1-E2)-C1*(CON2-E3-E4))/DEN1
      PPX(K)=(C0*(CON2-E3-E4)-C5*(CON1-E1-E2))/DEN1
      DDDX=PDX(K)+PDT(K)*DTHDX
      DELDX(K)=DELTA+DDDX*DELTX
      PSIDX(K)=PSI+(PPX(K)+PPT(K)*DTHDX)*DELTX
  115 TEST1=(DELDX(K)-DELDX(K-1))/DELDX(K-1)
      IF(ABS(TEST1).LE.ERR) GO TO 118
      GO TO 128
```

```
  118 IF(P.EQ.0.) GO TO 130
      TEST2=(PSIDX(K)-PSIDX(K-1))/PSIDX(K-1)
      IF(ABS(TEST2).LE.ERR) GO TO 130
  128 CONTINUE
      WRITE(6,500)
  500 FORMAT(1H1,10X31HNO CONVERGENCE IN, 25 ITERATIONS )
      STOP
  130 GO TO (135,140),ISTEP
  135 THETAI=THETA+DELTAT
      DELTAI=DELDX(K)
      PSII=PSIDX(K)
      DSTARI=DELTAI*.5
      XI=X+DELTX
      ISTEP=2
      GO TO 14
  140 IF(ALPHA.EQ.0.)GOTO144
      IF(THETA.EQ.0.)GOTO144
      IF(THETA.EQ.PI)GOTO144
      DXTERM=ABS(1.-DTHOLD/DTHDX)
      IF(DXTERM.GE.ERRX2.AND.DXTERM.LE.ERRX) GO TO 144
      IF(DXTERM.LT.ERRX2) DELTX=2.*DELTX
      IF(DXTERM.GT.ERRX) DELTX=0.5*DELTX
  144 IF(DELTX.GT.0.0001) DELTX=0.0001
      DELTAT=DTHDX*DELTX
      THETI=THETA+DELTAT
      IF(URATIO.NE.0.) GO TO 145
      DDSTAR=-DSTAR*DELTX*PRX1
      GO TO 150
  145 DDS1=-(PUEX/URATIO+PRX1+PVET/RUC)*DSTAR*DELTX
      DDS2=DELTA*DELTX/URATIO*(PJ4X*PSI+AJ4X*PPX(K)+PJ5X)
      DDS3=DELTX/URATIO*(PDX(K)+DELTA/R*PRX)*(PSI*AJ4X+AJ5X)
      DDS4=DELTA*DELTX/RUC*(AJ18X*PPT(K)+PJ18T*PSI+PJ19T)
      DDS5=DELTX*PDT(K)/RUC*(AJ18X*PSI+AJ19X)
      DDSTAR=DDS1+DDS2+DDS3+DDS4+DDS5
  150 PSIX=PSI+(PPX(K)+PPT(K)*DTHDX)*DELTX
***********
      XLIM=-.9980
      IF(NCASE.EQ.2) XLIM=-.950
      IF(X.GT.XLIM) GO TO 174
      DELTAI=DELTA
      DSTARI=DSTAR
      PSII=PSI
      GO TO 176
  174 IF(DDDX.LT.0.) DDDX=0.
      DELTAX=DELTA+DDDX*DELTX
  175 PSII=PSIX
      DELTAI=DELTAX
      DSTARI=DSTAR+DDSTAR
  176 THETAI=THETI
  177 XI=X+DELTX
      IF(ABS(X-XP).GT.DELTX) GO TO 178
      DELTX=ABS(X-XP)
```

```
      XI=XP
      DELTAI=DELTA+DDDX*DELTX
      PSII=PSI+(PPX(K)+PPT(K)*DTHDX)*DELTX
      THETAI=THETA+DTHDX*DELTX
      IF(URATIO.NE.0.) GO TO 1450
      DDSTAR=-DSTAR*DELTX*PRX1
      GO TO 1500
 1450 DDS1=-(PUEX/URATIO+PRX1+PVET/RUC)*DSTAR*DELTX
      DDS2=DELTA*DELTX/URATIO*(PJ4X*PSI+AJ4X*PPX(K)+PJ5X)
      DDS3=DELTX/URATIO*(PDX(K)+DELTA/R*PRX)*(PSI*AJ4X+AJ5X)
      DDS4=DELTA*DELTX/RUC*(AJ18X*PPT(K)+PJ18T*PSI+PJ19T)
      DDS5=DELTX*PDT(K)/RUC*(AJ18X*PSI+AJ19X)
      DDSTAR=DDS1+DDS2+DDS3+DDS4+DDS5
      DDSTDX=DDSTAR/DELTX
 1500 DSTARI=DSTAR+DDSTAR
  178 IF(XI.GT.XEND) ENDFILE 15
      IF(XI.GT.XEND) GO TO 3
      DTHOLD=DTHDX
      GO TO 14
       END
```

```
      SUBROUTINE JAYS(A,B,C,COSMA,SINSMA,SINA2,COSA2,QVRAT)
      COMMON /COEF/ H,SINA,COSA,T,P,G,REL,ALPHA,XSTAG
      COMMON /FTERMS/ F1,F2,F3,F4,F5,F6,F7,F8,F9,F10,F11,F12,F13,F14,
     1 F15,F16,F17,F18,F19,F20,F21,F22,F23,F24,F25,F26,F27,F28,F29
      COMMON /JTERMS/ AJ1,AJ2,AJ3,AJ4,AJ5,AJ6,AJ7,AJ8,AJ9,AJ10,AJ11,
     1 AJ12,AJ13,AJ14,AJ15,AJ16,AJ17,AJ18,AJ19,AJ1X,AJ2X,AJ3X,AJ6X,AJ7X,
     2 AJ8X,AJ9X,AJ12X,AJ13X,AJ14X,AJ15X,AJ4X,AJ5X,AJ18X,AJ19X
    1 A2=A*A
      COSNA=COSMA*SINSMA
      AJ1=A2*F18*SINA2
      AJ2=A*(-(A*F1-B*F2)*COSNA-2.*C*F7*SINA2)
    5 AJ3=A*(A*F10+B)*F9*COSA2+C*(-A*F3+B*F4)*COSNA+C*C*F8*SINA2
      AJ4=A*F2*SINSMA
      AJ5=A*F9*COSMA+C*F4*SINSMA
      AJ6=-A2*F18*COSNA
      AJ7=A*((A*F22+B*F2)*SINA2+A*F23*COSA2+2.*C*F7*COSNA)
   10 AJ8=(A*(A*F21+B*F9)-C*C*F8)*COSNA+C*(A*F11+B*F4)*SINA2
     1-A*C*F14*COSA2
      AJ9=A2*F18*COSA2
      AJ10=A*(A*F1-(QVRAT+B)*F2)*COSNA-2.*A*C*F7*COSA2
      AJ11=A*(A*F21+(QVRAT+B)*F9)*SINA2+C*(A*F3-(QVRAT+B)*F4)*COSNA+C*C*
     1 F8*COSA2
      AJ12=-A*(COSNA*(2.*A*F22+2.*F2*B-QVRAT*F2)+2.*C*F7*COSA2)
   15 AJ13=(QVRAT*(2.*A*F11+B)-(A2*F10+4.*F11*A*B+B*B))*SINA2
     1+C*(QVRAT*F4-2.*(A*F11+B*F4))*COSNA+C*C*F8*COSA2
      AJ14=A*(-COSA2*(A*F22+B*F2)+(A*F22+B*F2-QVRAT*F2)*SINA2+2.*C*F7*
     1COSNA)
      AJ15=(QVRAT*(2.*A*F11+B)-(A2*F10+4.*A*B*F11+B*B)-C*C*F8)*COSNA-
     1C*(A*F11+B*F4)*COSA2+C*(A*F11+B*F4-QVRAT*F4)*SINA2
      AJ16=A*(-(COSA2-SINA2)*(A*F22+B*F2)+2.*C*F7*COSNA)
      AJ17=(QVRAT*QVRAT-(A2*F10+4.*A*B*F11+B*B)-C*C*F8)*COSNA-C*(A*F11+
     1 B*F4)*(COSA2-SINA2)
   20 AJ18=-A*F2*COSMA
      AJ19=A*F9*SINSMA-C*F4*COSMA

      RETURN
       END
```

```
      SUBROUTINE FCALC (EN)
      COMMON /FTERMS/ F1,F2,F3,F4,F5,F6,F7,F8,F9,F10,F11,F12,F13,F14,
     1 F15,F16,F17,F18,F19,F20,F21,F22,F23,F24,F25,F26,F27,F28,F29
      EN1=EN+1.
      EN2=EN+2.
      EN21=2.*EN+1.
      F1=(EN-1.)/(EN1*EN2* EN21)
      F2=1./(EN1*EN2)
      F3=(EN**2+EN-1.)/(EN1*EN2)
      F4=EN1/EN2
      F5=3./(2.*EN2*EN21)
      F6=(2.*EN+3.)/(2.*EN2)
      F7=(3.*EN+4.)/(2.*EN1*EN2*(2.*EN+3.))
      F8=(-2.*EN1**2)/(EN2*(2.*EN+3.))
      F9=EN/EN1
      F10=1./EN21
      F11=1./(2.*EN1)
      F12=1./(2.*EN2)
      F13=EN1/((2.*EN+3.)*EN2)
      F14=-EN*(2.*EN+3.)/(2.*EN1*EN2)
      F15=-F3
      F16=F1
      F17=-F2
      F18=-1./(EN1*EN21*(2.*EN+3.))
      F19=-F7
      F20=-2.*F7
      F21=EN/(EN1*EN21)
      F22=1./(2.*EN1*EN21)
      F23=3.*EN/(2.*EN1*EN2*EN21)
      F24=-F18
      F25=F23-2.*F7
      F26=F21-F9
      F27=F3+F4
      F28=F26
      WRITE(6,40) F1,F2,F3,F4,F5,F6,F7,F8,F9,F10,F11,F12,F13,F14,F15,
     1 F16,F17,F18,F19,F20,F21,F22,F23,F24,F25,F26,F27,F28
   40 FORMAT(1H0,10X10HFTERMS ,,,/ (10X1P8E15.5))

      RETURN
       END
```

```
      SUBROUTINE PARTLS(X,THETA,                PJ1X,PJ2X,PJ3X,PJ6X,PJ14X,
     1 PJ15X,PJ6T,PJ7T,PJ8T,PJ9T,PJ12T,PJ13T,PJ4X,PJ5X, PJ18T,PJ19T)
      COMMON /COEF/ H,SINA,COSA,T,P,G,REL,ALPHA,XSTAG
      COMMON /JTERMS/ AJ1,AJ2,AJ3,AJ4,AJ5,AJ6,AJ7,AJ8,AJ9,AJ10,AJ11,
     1 AJ12,AJ13,AJ14,AJ15,AJ16,AJ17,AJ18,AJ19,AJ1X,AJ2X,AJ3X,AJ6X,AJ7X,
     2 AJ8X,AJ9X,AJ12X,AJ13X,AJ14X,AJ15X,AJ4X,AJ5X,AJ18X,AJ19X
      DIMENSION Z1(2,2), Z2(2,2), Z3(2,2), Z6(2,2), Z7(2,2), Z8(2,2),
     1 Z9(2,2), Z12(2,2), Z13(2,2), Z14(2,2), Z15(2,2)
     2, Z4(2,2), Z5(2,2), Z18(2,2), Z19(2,2)

      DELTX=0.0001
      DELTAT=0.0001
    1 T2=T*T
      XK=X
      TK=THETA
      NT=2
    5 XKEEP=XK-DELTX
      DO 61 I=1,2
      XKEEP=XKEEP+DELTX
      X2=XKEEP**2
      XT=1.-X2*(1.-T2)
   10 X21=1.-X2
      COSPH=SQRT(X21/XT)
      SINPH=COSPH*(-X*T/SQRT(X21))
      R=T*SQRT(X21)
      PRT=P*R/T
   15 TERM1=COSPH*G*COSA
      TERM2=XKEEP/SQRT(XT)*T*H*SINA
      TK=TK-DELTAT
      DO 58 J=1,NT
      IF(I.EQ.1.AND.J.EQ.1) GO TO 46
   20 TK=TK+DELTAT
      SINT=SIN(TK)
      COST=COS(TK)
      VR=-H*SINT*SINA
      UR=TERM1-TERM2*COST
      IF(XKEEP.NE.XSTAG) GO TO 30
      OVRAT=0.
      SMA=0.
      SNSMA=0.
      COSMA=1.
      GO TO 33
   30 OVRAT=SQRT(UR**2+VR**2)
      IF(UR.NE.0.) GO TO 32
      SMA=0.
      SNSMA=0.
      COSMA=1.
      GO TO 33
   32 SMA=ATAN(VR/UR)
      SNSMA=VR/OVRAT
      COSMA=UR/OVRAT
   33 SINA2=SNSMA**2
```

```
      Z9(I,J)=AJ9
      Z12(I,J)=AJ12
      Z13(I,J)=AJ13
      Z14(I,J)=AJ14
      Z15(I,J)=AJ15
      Z18(I,J)=AJ18
      Z19(I,J)=AJ19
      GO TO 58
   46 Z1(1,1)=AJ1X
      Z2(1,1)=AJ2X
      Z3(1,1)=AJ3X
      Z4(1,1)=AJ4X
      Z5(1,1)=AJ5X
      Z6(1,1)=AJ6X
   50 Z7(1,1)=AJ7X
      Z8(1,1)=AJ8X
      Z9(1,1)=AJ9X
      Z12(1,1)=AJ12X
      Z13(1,1)=AJ13X
      Z14(1,1)=AJ14X
      Z15(1,1)=AJ15X
      Z18(1,1)=AJ18X
      Z19(1,1)=AJ19X
      TK=THETA
      IF(ALPHA.EQ.0.) GO TO 59
   58 CONTINUE
   59 NT=1
      TK=THETA
   61 CONTINUE

C     PARTIALS WITH RESPECT TO X

      PJ1X=(Z1(2,1)-Z1(1,1))/DELTX
      PJ2X=(Z2(2,1)-Z2(1,1))/DELTX
      PJ3X=(Z3(2,1)-Z3(1,1))/DELTX
      PJ4X=(Z4(2,1)-Z4(1,1))/DELTX
      PJ5X=(Z5(2,1)-Z5(1,1))/DELTX
   65 PJ6X=(Z6(2,1)-Z6(1,1))/DELTX
      PJ14X=(Z14(2,1)-Z14(1,1))/DELTX
      PJ15X=(Z15(2,1)-Z15(1,1))/DELTX

C     PARTIALS WITH RESPECT TO THETA

      IF(ALPHA.NE.0.) GO TO 68
      PJ6T=0.0
      PJ7T=0.0
      PJ8T=0.0
      PJ9T=0.0
      PJ12T=0.0
      PJ13T=0.0
      PJ18T=0.
```

```
      PJ19T=0.
      GO TO 72
   68 PJ6T=(Z6(1,2)-Z6(1,1))/DELTAT
      PJ7T=(Z7(1,2)-Z7(1,1))/DELTAT
   70 PJ8T=(Z8(1,2)-Z8(1,1))/DELTAT
      COSA2=COSMA**2
      B=PRT*SNSMA
      A=QVRAT-B
      C=PRT*COSMA
      CALL JAYS(A,B,C,COSMA,SNSMA,SINA2,COSA2,QVRAT)
      Z1(I,J)=AJ1
      Z2(I,J)=AJ2
      Z3(I,J)=AJ3
      Z4(I,J)=AJ4
      Z5(I,J)=AJ5
      Z6(I,J)=AJ6
      Z7(I,J)=AJ7
   40 Z8(I,J)=AJ8
      PJ9T=(Z9(1,2)-Z9(1,1))/DELTAT
      PJ12T=(Z12(1,2)-Z12(1,1))/DELTAT
      PJ13T=(Z13(1,2)-Z13(1,1))/DELTAT
      PJ18T=(Z18(1,2)-Z18(1,1))/DELTAT
      PJ19T=(Z19(1,2)-Z19(1,1))/DELTAT
   72 RETURN
       END
```

```
      SUBROUTINE QSUBR(PSII,DELTAI)
      COMMON /COEF/ H,SINA,COSA,T,P,G,REL,ALPHA
      DIMENSION Q(25),E(25)
      EN=1.
      EN1=EN+1.
      EN2=EN+2.
      EN21=2.*EN+1.
      F7=(3.*EN+4.)/(2.*EN1*EN2*(2.*EN+3.))
      F8=(-2.*EN1**2)/(EN2*(2.*EN+3.))
      F9=EN/EN1
      F10=1./EN21
      F11=1./(2.*EN1)
      F18=-1./(EN1*EN21*(2.*EN+3.))
      F22=1./(2.*EN1*EN21)
      C1=(3.*F10+1.)*F9
      C2=((P*T)/G)**2
      C3=16.*F18*F11**2
      Q(1)=1.0
      Q(2)=0.95
      DO 20 I=1,25
      E(I)=Q(I)-C1+C2*(C3/(Q(I)+4.*F22)**2+(8.*F11*F7)/(Q(I)+4.*F22)
     1 +F8)
      IF(ABS(E(I)).LE.0.00001) GO TO 25
      IF(I.LT.2) GO TO 20
      Q(I+1)=Q(I)-E(I)*(Q(I)-Q(I-1))/(E(I)-E(I-1))
   20 CONTINUE
      STOP
   25 PSII=(-4.*F11*(P*T)/G)/(Q(I)+4.*F22)
      DELTAI=(T**2)/(Q(I)*1.*G*REL)
      DELTAI=SQRT(DELTAI)
      WRITE(6,10) PSII,DELTAI,Q(I)
   10 FORMAT(1H0,11HQSUB--PSII=1PE13.5,5X7HDELTAI=1PE13.5,5X2HQ=1PE13.5)
      RETURN
       END
```

```
      SUBROUTINE FSBSFL(IP1,IP2,IP3)
      DIMENSION IUTAB(100)
       DATA IFLAG/0/
      DATA IUTAB/100*1/
C
C     SUBROUTINE TO BE USED WITH MULTIFILE FORTRAN TAPES.  ALL FILE
C     POSITIONING AND END-OF-FILE TESTS ON MULTIFILE TAPES MUST BE
C     HANDLED THROUGH THIS ROUTINE
C
C       THE SUBROUTINE IS USED AS FOLLOWS
C
C       1.  CALL REWIND(UNIT)
C           REWIND SPECIFIED LOGICAL UNIT
C
C       2.  CALL FSFILE(UNIT,NFILES,MODE)
C           FORWARD SKIP SPECIFIED NO. OF FILES
C
C       3.  CALL BSFILE(UNIT,NFILES,MODE)
C           BACK SPACE SPECIFIED NUMBER OF FILES
C
C       4.  CALL RWFILE(UNIT,MODE)
C           REWIND CURRENT FILE
C
C       5.  CALL ENDFIL(UNIT,STATUS)
C           TEST FOR EOF
C               IF STATUS = 1 -- EOF FOUND
C               IF STATUS = 2 -- EOF NOT FOUND
C
C     THE INPUT AND OUTPUT PARAMETERS ARE
C
C         UNIT = LOGICAL UNIT NO. ON WHICH TO PERFORM OPERATION
C
C         NFILES = NUMBER OF FILES TO SKIP
C
C         MODE = MODE OF OPERATIONS ON UNIT
C           0 - BCD
C           1 - BINARY
C
C         STATUS = RETURN PARAMETER FOR END- OF-FILE TEST (DEFINED ABOVE)
C
C     ***********************************************
C     *NOTE --- ALL PARAMETERS MUST BE TYPE INTEGER*
C     ***********************************************
C
C
C       ***** REWIND SECTION
C
       ENTRY REWIND
C
         IF(LOCF(IP1).EQ. 0) GO TO 9999
        IUNIT = IP1
        IF(IUNIT.LE.0.OR. IUNIT.GT. 99) GO TO 9999
```

```
      REWIND IUNIT
       IUTAB(IUNIT) = 1
      RETURN
C
C     SKIP FILES FORWARD
      ENTRY FSFILE
       N=1
       GO TO 1000
C    BACKSPACE FILE
      ENTRY BSFILE
       N=2
       GO TO 1000
C   REWIND FILE
      ENTRY RWFILE
       N=3
       GO TO 1000
C     TEST FOR EOF
      ENTRY ENDFIL
       GO TO 5000
C
 1000 IF(IFLAG.NE.0) GO TO 1999
       IFLAG = 1
       ISTAT = 0
       ICUFIL = 1
 1999 ITEST = LOCF(IP1)
      IF(ITEST .EQ. 0) GO TO 9999
       IUNIT = IP1
      IF(IUNIT .LE. 0 .OR. IUNIT .GT. 99) GO TO 9999
       ICUFIL = IUTAB(IUNIT)
       ITEST = LOCF(IP2)
       IF(ITEST.EQ. 0) GO TO 1001
       NFILES = IP2
       GO TO 1002
 1001  NFILES = 1
 1002  ITEST = LOCF(IP3)
       IF(ITEST .EQ. 0) GO TO 1003
       MODE = IP3
       GO TO 1004
C
C ASSUME BCD IF MODE NOT SPECIFIED
 1003  MODE = 0
C
 1004 IF(N.EQ. 3) MODE = NFILES
C
      GO TO (2000,3000,4000)    ,N
C
C
C         FORWARD SKIP NFILES
C
 2000 IF (MODE.NE. 0) GO TO 2500
 2001 READ(IUNIT,6000)
 6000 FORMAT(13A10,A6)
```

```
      IF(EOF(IUNIT)) 2002,2001,2002
 2002 ICUFIL= ICUFIL+1
      NFILES = NFILES-1
      IF(NFILES.LE.0) GO TO 7777
      GO TO 2001
C         BINARY MODE
C
C
C
C
 2500 READ(IUNIT)
      IF(EOF(IUNIT)) 2502,2500,2502
 2502  ICUFIL = ICUFIL+1
       NFILES = NFILES-1
       IF(NFILES.LE.0) GO TO 7777
       GO TO 2500
C
C        BACK SPACE FILES
C
 3000 IF(NFILES.LE.0) GO TO 9999
 3010  CONTINUE
       REWIND IUNIT
       NSKIP = ICUFIL-NFILES-1
       ICUFIL = NSKIP+1
       IF(NSKIP .LE. 0) GO TO 7777
       IF(MODE.NE.0) GO TO 3500
 3001 READ(IUNIT,6000)
      IF(EOF(IUNIT)) 3100,3001,3100
 3100 CONTINUE
       NSKIP = NSKIP-1
       IF(NSKIP.LE.0) GO TO 7777
       GO TO   3001
C
C      BINARY MODE
C
 3500  DO 3502 I=      1,NSKIP
 3501 READ(IUNIT)
      IF(EOF(IUNIT)) 3502,3501,3502
 3502 CONTINUE
       GO TO 7777
C
C       END FILE TEST
C
 5000 CONTINUE
       ITEMP = LOCF(IP1)
       IF(ITEMP.EQ. 0) GO TO 9999
       IUNIT = IP1
       ICUFIL = IUTAB(IUNIT)
      IF(EOF(IUNIT)) 5001,5050,5001
 5001  ICUFIL = ICUFIL+1
       IP2 = 1
       GO TO 7777
 5050  IP2      =2
```

```
      GO TO 7777
C
C    REWIND CURRENT FILE
C
 4000  NFILES = 0
       GO TO 3010
C
CC     COMMON RETURN POINT
CC      RESET FILE IN PROPER SLOT
C
 7777 IF(ICUFIL .LE. 0) ICUFIL = 1
       IUTAB(IUNIT)= ICUFIL
      RETURN
C
CC
CC
C       ERROR MESSAGE
C
 9999 PRINT 9000
 9000 FORMAT(////,* $$$ ILLEGAL OR NO PARAMETER IN CALL TO FSBSFL $$$*,//
     X/)
      CALL EXIT
      END
```

```
      PROGRAM VNPRSPL(INPUT,OUTPUT,TAPE5=INPUT,TAPE6=OUTPUT,TAPE15,
     1TAPE16)
      DIMENSION XPICK(50),JORDER(50),AA(300,27),ZTHETA(45,35),ZX(45,35),
     1 ZDTHDX(45,35),ZDSTAR(45,35),ZRPDSTR(45,35),XSPLIN(181),
     1YSPL1(181),YSPL2(181),YSPL3(181),YSPL4(181),YSPL5(181),C1(4,40),
     1C2(4,40),C3(4,40),C4(4,40),C5(4,40),XIN(181),ZDDSTDX(45,35),
     1ZPRX(45,35)
      WRITE(6,302)
  302 FORMAT(1H1*    VALUES READ FROM TAPE*/T7*CASE*,T21*X*,T25*ORDER*,
     1T39*THETA*,T53*DSTAR*,T69*PRX*,T81*DTHDX*,T94*RPDSTR*,T108*DDSTDX*
     1/)
C     JPICKS=NUMBER OF X VALUES TO BE PROCESSED
      READ(5,301) JPICKS
      READ(5,501) (XPICK(J),J=1,JPICKS)
  501 FORMAT(12F6.3)
      NOMIT=0
      PI=3.14159265358979
      TWOPI=2.*PI
C     NCASES=TOTAL NUMBER OF CASES ON TAPE
C     JORDER(N) IS SEQUENCING OF CASES IN ASCENDING VALUES OF GAMMA FOR
C           ASCENDING VALUES OF THETA
C     JORDER(N) INPUT AS 0 IF CASE IS NOT TO BE PROCESSED
      READ(5,301) NCASES
      READ(5,301) (JORDER(N),N=1,NCASES)
  301 FORMAT(24I3)
      CALL FSFILE(16,27,0)
    1 READ(15,9) NCASE
      N=0
    9 FORMAT(14I4)
   12 N=N+1
      IF(N.GT.300) STOP4
      READ(15,20)(AA(N,I),I=1,9)
   20 FORMAT(9E14.5)
      CALL ENDFIL(15,ISTAT)
C     ISTAT=1 IF END OF FILE.   ISTAT=2 IF NO END OF FILE
      IF(ISTAT.EQ.1) GO TO 30
   25 READ(15,21)(AA(N,I),I=10,27)
   21 FORMAT(8E14.5)
      GO TO 12
   30 NN=JORDER(NCASE)
      IF(NN)22,22,23
   22 NOMIT=NOMIT+1
      IF(NCASE.EQ.NCASES) GO TO 37
      GO TO 1
   23 NLINES=N-1
      DO 35 J=1,JPICKS
      DO 40 N=1,NLINES
*** XDIFF CHECK AT VALUE OF X=0.0
      XDIFF=ABS(AA(N,1)-XPICK(J))
      IF(XDIFF.GE.1.0E-11) GO TO 40
      ZTHETA(J,NN)=AA(N,2)
      ZPRX(J,NN)=AA(N,16)
```

```
      ZDDSTDX(J,NN)=AA(N,27)
      ZDTHDX(J,NN)=AA(N,10)
      ZDSTAR(J,NN)=AA(N,9)
      ZRPDSTR(J,NN)=AA(N,26)
      ZX(J,NN)=AA(N,1)
      WRITE(6,303) NCASE,ZX(J,NN),NN,ZTHETA(J,NN),ZDSTAR(J,NN),
     1ZPRX(J,NN),ZDTHDX(J,NN),ZRPDSTR(J,NN),ZDDSTDX(J,NN)
  303 FORMAT(I10,1PE14.5,I5,6E14.5)
      GO TO 35
   40 CONTINUE
      STOP1
   35 CONTINUE
      IF(NCASE.LT.NCASES) GO TO 1
   37 NPTS=NCASES-NOMIT
      DO 70 J=1,JPICKS
      DO 311 I=1,3
      II=NPTS-(3-I)
      XSPLIN(I)=-(TWOPI-ZTHETA(J,II))
      YSPL1(I)=ZDSTAR(J,II)
      YSPL2(I)=ZPRX(J,II)
      YSPL3(I)=ZDTHDX(J,II)
      YSPL4(I)=ZRPDSTR(J,II)
      YSPL5(I)=ZDDSTDX(J,II)
      XSPLIN(NPTS+3+I)=TWOPI+ZTHETA(J,I)
      YSPL1(NPTS+3+I)=ZDSTAR(J,I)
      YSPL2(NPTS+3+I)=ZPRX(J,I)
      YSPL3(NPTS+3+I)=ZDTHDX(J,I)
      YSPL4(NPTS+3+I)=ZRPDSTR(J,I)
      YSPL5(NPTS+3+I)=ZDDSTDX(J,I)
  311 CONTINUE
      DO 312 NN=1,NPTS
      XSPLIN(NN+3)=ZTHETA(J,NN)
      YSPL1(NN+3)=ZDSTAR(J,NN)
      YSPL2(NN+3)=ZPRX(J,NN)
      YSPL3(NN+3)=ZDTHDX(J,NN)
      YSPL4(NN+3)=ZRPDSTR(J,NN)
  312 YSPL5(NN+3)=ZDDSTDX(J,NN)
      MPAIR=NPTS+6
      WRITE(6,310)XPICK(J),(NN,XSPLIN(NN),YSPL1(NN),YSPL2(NN),YSPL3(NN),
     1YSPL4(NN),YSPL5(NN),NN=1,MPAIR)
  310 FORMAT(1H1,*  ORDERED VALUES GOING INTO SPLINE FIT.    X=*F7.4/T7,
     1*NN*,T18*THETA*,T32*DSTAR*,T48*PRX*,T60*DTHDX*,T73*RPDSTR*,T87,
     1*DDSTDX*/(I8,1P6E14.5))
      CALL SPLICON(XSPLIN,YSPL1,MPAIR,C1)
      CALL SPLICON(XSPLIN,YSPL2,MPAIR,C2)
      CALL SPLICON(XSPLIN,YSPL3,MPAIR,C3)
      CALL SPLICON(XSPLIN,YSPL4,MPAIR,C4)
      CALL SPLICON(XSPLIN,YSPL5,MPAIR,C5)
      XINCR=2.*PI/180.
      XIN(1)=0.
      DO 314 NN=2,181
```

```
  314 XIN(NN)=XIN(NN-1)+XINCR
      WRITE(6,200)
  200 FORMAT(1H1,T8*ALPHA*,T25*X*,T37*RPDSTR*,T53*THETA*,T68*DSTAR*,T82,
     1*DDSTDX*,T97*PDSTDX*/T7*DSTART*,T24*PRX*,T39*CSE*,T54*BTA*,T70,
     1*RO*,T82*DRODBT*,T97*DRODCS*/T9*VNPR*,T23*GAMA*,T39*CPR*)
      IPRINT=0
      DO 60 NN=1,181
      THETA=XIN(NN)
      CALL SPLINE(XSPLIN,YSPL1,MPAIR,C1,THETA,DSTAR,DERIV,IOK)
      IF(IOK.EQ.0) WRITE(6,320) THETA
  320 FORMAT(///*   OUT OF RANGE FOR SPLINE FIT*/*THETA=*E14.5)
      IF(IOK.EQ.0) STOP3
      CALL SPLINE(XSPLIN,YSPL2,MPAIR,C2,THETA,PRX,DUM,IOK)
      IF(IOK.EQ.0) STOP3
      CALL SPLINE(XSPLIN,YSPL3,MPAIR,C3,THETA,DTHDX,DUM,IOK)
      IF(IOK.EQ.0) STOP3
      CALL SPLINE(XSPLIN,YSPL4,MPAIR,C4,THETA,RPDSTR,DUM,IOK)
      IF(IOK.EQ.0) STOP3
      CALL SPLINE(XSPLIN,YSPL5,MPAIR,C5,THETA,DDSTDX,DUM,IOK)
      IF(IOK.EQ.0) STOP3
      X=XPICK(J)
      DSTART=DERIV
      ALPHA=4.
      A=1.
      T=.1
      ALPH=ALPHA*PI/180.
      FR=1.
      R=T *SQRT(1.-X*X)
      PDSTDX=DDSTDX-DTHDX*DSTART
      FX=-PRX-PDSTDX
      FTHTA=-A*DSTART
      DRDCSE=SIN(ALPH)*COS(THETA)
      Z1=(R+DSTAR)*SIN(THETA)/(-(1.+X)*SIN(ALPH)+(R+DSTAR)*
     1COS(ALPH)*COS(THETA))
C     Z1 IS NOT USED
      XK1=-(A+X)*SIN(ALPH)+(R+DSTAR)*COS(ALPH)*COS(THETA)
      XK2=(R+DSTAR)*SIN(THETA)
      XK2K1=ABS(XK2/XK1)
      BTA1=ATAN(XK2K1)
   50 FORMAT(     5X*NUMERATOR XK2 =*E13.5/5X,*DENOMINATOR XK1 =*E13.5/
     15X,*ATAN(XK2/XK1)=BTA1 =*E13.5)
      CSINAL=SIN(ALPH)
      CCOSAL=COS(ALPH)
      CSINTH=SIN(THETA)
      CCOSTH=COS(THETA)
  401 FORMAT(5X*SIN(ALPH)=*E13.5/5X*COS(ALPH)=*E13.5/5X*SIN(THETA)=*,
     1E13.5/5X*COS(THETA)=*E13.5)
      IF(XK2.GT.0..AND.XK1.GT.0.) BTA=BTA1
      IF(XK2.GT.0..AND.XK1.LT.0.) BTA=PI-BTA1
      IF(XK2.LT.0..AND.XK1.LT.0.) BTA=PI+BTA1
      IF(XK2.LT.0.AND.XK1.GT.0.) BTA=2.*PI-BTA1
      IF(THETA.EQ.0.) BTA=0.
```

```
      IF(THETA.EQ.PI) BTA=PI
      RO=-(1.+X)*SIN(ALPH)*COS(BTA)+(R+DSTAR)*(COS(ALPH)*COS(BTA)
     1*COS(THETA)+SIN(BTA)*SIN(THETA))
      DRDB=A*RO*(-COS(ALPH)*SIN(BTA)*COS(THETA)+COS(BTA)*SIN(THETA))
      DRDRO=COS(ALPH)*COS(BTA)*COS(THETA)+SIN(BTA)*SIN(THETA)
      DXDCSE=COS(ALPH)
      CSE=(1.+X)*COS(ALPH)+(R+DSTAR)*SIN(ALPH)*COS(THETA)
      DXDBTA=A*RO*SIN(ALPH)*SIN(BTA)
      DXDRO=-SIN(ALPH)*COS(BTA)
      DEN=(CSE*SIN(ALPH)+RO*COS(BTA)*COS(ALPH))**2+(RO*SIN(BTA))**2
      DTDCSE=-(RO*SIN(BTA)*SIN(ALPH))/(DEN*A)
      DTHTDB=(RO*CSE*SIN(ALPH)*COS(BTA)+RO*RO*COS(ALPH))/DEN
      DTHDRO=(CSE*SIN(ALPH)*SIN(BTA))/(DEN*A)
      DEN1=FR*DRDRO+FX*DXDRO+FTHTA*DTHDRO
      DRDCS=-(FR*DRDCSE+FX*DXDCSE+FTHTA*DTDCSE)/DEN1
      DRDBT=-(FR*DRDB+FX*DXDBTA+FTHTA*DTHTDB)/(DEN1*A)
  405 FORMAT(5X*DEN=*E13.5)
  404 FORMAT(T5*DRDRO=*E13.5/T5*DXDRO=*E13.5/T5*DTHDRO=*E13.5)
  402 FORMAT(/T5*DRDCSE=*E13.5/T5*FX=*E13.5/T5*DXDCSE=*E13.5/T5*FTHTA=*,
     1E13.5/T5*DTDCSE=*E13.5/T5*DEN1=*E13.5)
  403 FORMAT(/T5*DRDB=*E13.5/T5*DXDBTA=*E13.5/T5*DTHTDB=*E13.5)
      VNPR=DRDCS/SQRT(1.+(DRDBT/RO)**2)
  242 FORMAT(*  RO=*1PE13.5,*   X=*1PE13.5,*   SIN(ALPH)=*1PE13.5,*   BT
     1A=*1PE13.5)
      CHEC4=RO**2+2.*RO*(1.+X)*COS(BTA)*SIN(ALPH)+((1.+X)*SIN(ALPH))**2
      IF(CHEC4.LE.0.) WRITE(6,420) CHEC4
      IF(CHEC4.LE.0.) STOP6
  420 FORMAT(//*   CHEC4=*1PE15.5)
      RPR=SQRT(RO**2+2.*RO*(1.+X)*COS(BTA)*SIN(ALPH)
     1+((1.+X)*SIN(ALPH))**2)
      IF(RPR.LE.1.0E-6) WRITE(6,421) RPR
      IF(RPR.LE.1.0E-6) STOP6
  421 FORMAT(//*   RPR=*1PE15.5)
  406 FORMAT(*   RPR=*1PE13.5,4X,*RO=*1PE13.5,4X,*X=*1PE13.5)
      PIHALF=PI/2.
      TWOPI=2.*PI
      PI15=1.5*PI
      IF(BTA.GE.0..AND.BTA.LE.PIHALF) GO TO 600
      IF(BTA.GT.PI15.AND.BTA.LT.TWOPI) GO TO 605
      IF(BTA.EQ.PI) GAMA=PI15
      IF(BTA.EQ.TWOPI) GAMA=PIHALF
      IF(BTA.EQ.PI) GO TO 450
      IF(BTA.EQ.TWOPI) GO TO 450
      TARG=(1.0+X)*SIN(ALPH)/RO
      IF(ABS(TARG).GT.1.0) WRITE(6,445)
  445 FORMAT(51H   CALCULATION OF TERM = ASIN((1.0+X)*SIN(ALPH)/RO))
      IF(ABS(TARG).GT.1.0) CALL CHECS(TARG)
      TERM=ASIN(TARG)
      IF(TARG.EQ.1.0) WRITE(6,446) TERM
  446 FORMAT(*   TERM=*1PE13.5)
      IF(BTA.GT.PIHALF.AND.BTA.LT.(PIHALF+TERM)) GO TO 601
      IF(BTA.GT.(PIHALF+TERM).AND.BTA.LT.PI) GO TO 602
```

```
      IF(BTA.GT.PI.AND.BTA.LT.(PI15-TERM)) GO TO 603
      IF(BTA.GT.(PI15-TERM).AND.BTA.LE.PI15) GO TO 604
      IF(BTA.EQ.(PIHALF+TERM)) GAMA=PI
      IF(BTA.EQ.(PI15-TERM)) GAMA=TWOPI
      IF(BTA.EQ.(PIHALF+TERM)) GO TO 450
      IF(BTA.EQ.(PI15-TERM)) GO TO 450
      WRITE(6,447) BTA,TERM
  447 FORMAT(/*   BTA =*1PE13.5,4X*TERM =*1PE13.5/*   NO CONDITIONS SATI
     1SFIED FOR GAMA---STOP.*)
      STOP7
  600 ARG=RO*SIN(BTA)/RPR
      IF(ABS(ARG).GT.1.0) CALL CHECS(ARG)
      GAMA=PIHALF+ASIN(ARG)
      GO TO 450
  601 ARG=RO*COS(BTA-PIHALF)/RPR
      IF(ABS(ARG).GT.1.0) CALL CHECS(ARG)
      GAMA=PIHALF+ASIN(ARG)
      GO TO 450
  602 ARG=(RO*SIN(BTA-PIHALF)-(1.0+X)*SIN(ALPH))/RPR
      IF(ABS(ARG).GT.1.0) CALL CHECS(ARG)
      GAMA=PI+ASIN(ARG)
      GO TO 450
  603 ARG=(RO*SIN(PI15-BTA)-(1.0+X)*SIN(ALPH))/RPR
      IF(ABS(ARG).GT.1.0) CALL CHECS(ARG)
      GAMA=TWOPI-ASIN(ARG)
      GO TO 450
  604 ARG=RO*COS(PI15-BTA)/RPR
      IF(ABS(ARG).GT.1.0) CALL CHECS(ARG)
      GAMA=PIHALF-ASIN(ARG)
      GO TO 450
  605 ARG=(RO*SIN(BTA-PI15)+(1.0+X)*SIN(ALPH))/RPR
      IF(ABS(ARG).GT.1.0) CALL CHECS(ARG)
      GAMA=ASIN(ARG)
C     PRINT HEADER AND 14 BLOCKS OF DATA ON EACH PAGE
  450 IPRINT=IPRINT+1
      IF(IPRINT.GT.14) WRITE(6,200)
      IF(IPRINT.GT.14) IPRINT=1
      WRITE(6,201)ALPHA,X,RPDSTR,THETA,DSTAR,DDSTDX,PDSTDX,DSTART,PRX,
     1CSE,BTA,RO,DRODBT,DRODCS,VNPR,GAMA,RPR
  201 FORMAT(/(1P7E15.5))
      WRITE(16,2) ALPHA,X,RPDSTR,THETA,DSTAR,DDSTDX,PDSTDX
      WRITE(16,2)  DSTART,PRX,CSE,BTA,RO,DRODBT,DRODCS
      WRITE(16,2) VNPR,GAMA,RPR
    2 FORMAT(1P7E15.5)
   60 CONTINUE
      ENDFILE 16,
   70 CONTINUE
      STOP
       END
```

```
      SUBROUTINE CHECS(ARG)
      DIFF=ABS(ARG)-1.0
      WRITE(6,10) ARG,DIFF
   10 FORMAT(/*   ABSOLUTE VALUE OF ARGUMENT FOR ASIN IS GREATER THAN 1.
     10 FOR COMPUTATION OF GAMA.*/*    ARG=*1PE17.10,6X*(ABS(ARG)-1.0)=*,
     16PE22.10)
      IF(DIFF.LT.1.0E-5) ARG=1.0
      IF(DIFF.LT.1.0E-5) RETURN
      STOP10
       END
```

```
      SUBROUTINE SPLICON(X,Y,M,C)
C     INPUT X AND Y TABLE ARRAYS IN ASCENDING VALUES OF X
C     INPUT M = NUMBER OF (X,Y) PAIRS IN TABLE
C     OUTPUT C ARRAY OF CONSTANTS
C     DIMENSION X(N),Y(N),D(N),P(N),E(N),C(4,N),A(N,3),B(N),Z(N) WHERE N.GE.M
      DIMENSION X(40),Y(40),D(40),P(40),E(40),C(4,40),A(40,3),B(40),Z(40
     1)
      MM=M-1
   20 FORMAT(1H1,T9*SUBROUTINE SPLICON DIFFERENCES,*/T11*D(K)=X(K+1)-X(K
     1)*/T11*E(K)=(Y(K+1)-Y(K))/D(K)*/T10*D(K)*,T25*E(K)*)
      DO 2 K=1,MM
      D(K)=X(K+1)-X(K)
C     RLB CHECK.  GUESSING AT 1.0E-8 AS A LIMIT.
      IF(D(K).LT.1.0E-8) STOP5
      P(K)=D(K)/6.
      E(K)=(Y(K+1)-Y(K))/D(K)
   21 FORMAT(2F15.8)
    2 CONTINUE
      DO 3 K=2,MM
    3 B(K)=E(K)-E(K-1)
      A(1,2)=-1.-D(1)/D(2)
      A(1,3)=D(1)/D(2)
      A(2,3)=P(2)-P(1)*A(1,3)
      A(2,2)=2.*(P(1)+P(2))-P(1)*A(1,2)
      A(2,3)=A(2,3)/A(2,2)
      B(2)=B(2)/A(2,2)
      DO 4 K=3,MM
      A(K,2)=2.*(P(K-1)+P(K))-P(K-1)*A(K-1,3)
      B(K)=B(K)-P(K-1)*B(K-1)
      A(K,3)=P(K)/A(K,2)
    4 B(K)=B(K)/A(K,2)
      Q=D(M-2)/D(M-1)
      A(M,1)=1.+Q+A(M-2,3)
      A(M,2)=-Q-A(M,1)*A(M-1,3)
      B(M)=B(M-2)-A(M,1)*B(M-1)
      Z(M)=B(M)/A(M,2)
      MN=M-2
      DO 6 I=1,MN
      K=M-I
    6 Z(K)=B(K)-A(K,3)*Z(K+1)
      Z(1)=-A(1,2)*Z(2)-A(1,3)*Z(3)
   50 FORMAT(    /,T5*SUBROUTINE SPLICON*/,
     1T8*X INPUT*,T22*Y INPUT*,T32*Z=2ND DERIV*/(1P3E14.5))
      DO 7 K=1,MM
      Q=1./(6.*D(K))
      C(1,K)=Z(K)*Q
      C(2,K)=Z(K+1)*Q
      C(3,K)=Y(K)/D(K)-Z(K)*P(K)
    7 C(4,K)=Y(K+1)/D(K)-Z(K+1)*P(K)
      RETURN
       END
```

```
      SUBROUTINE SPLINE(X,Y,M,C,XINT,YINT,DERIV,IOK)
C     INPUT X AND Y TABLE ARRAYS IN ASCENDING VALUES OF X
C     INPUT M = NUMBER OF (X,Y) PAIRS IN TABLE
C     INPUT C ARRAY OF CONSTANTS FROM SPLICON SUBROUTINE
C     INPUT XINT TO INTERPOLATE
C     OUTPUT YINT = INTERPOLATED VALUE
C     OUTPUT IOK, IOK=1 IF (XINT.GE.X(1).AND.XINT.LT.X(M))
C                 IOK=0 IF XINT OUTSIDE RANGE.  YINT AND DERIV SET EQUAL TO 0.0
      DIMENSION X(40),Y(40),C(4,40)
      IF(XINT-X(1))7,1,2
    1 YINT=Y(1)
      GO TO 8
    2 K=1
    3 IF(XINT-X(K+1))6,4,5
    4 YINT=Y(K+1)
      GO TO 8
    5 K=K+1
      IF(M-K)7,7,3
    6 YINT=(X(K+1)-XINT)*(C(1,K)*(X(K+1)-XINT)**2+C(3,K))
      YINT=YINT+(XINT-X(K))*(C(2,K)*(XINT-X(K))**2+C(4,K))
C   COMPUTATION OF DSTART FOR TETERVIN = VALUE OF FIRST DERIVATIVE
C   DERIVATIVE IS CALCULATED OVER SAME RANGE AS YINT
    8 DERIV=-3.*C(1,K)*(X(K+1)-XINT)**2+3.*C(2,K)*(XINT-X(K))**2-C(3,K)+
     1C(4,K)
      IOK=1
      RETURN
    7 IOK=0
      YINT=0.
      DERIV=0.
      RETURN
      END
```

```
      PROGRAM CABEPSL(INPUT,OUTPUT,TAPE5=INPUT,TAPE6=OUTPUT,TAPE16,
     1TAPE17)
      DIMENSION A(17),JFILE(45),XVNPR(200),XGAMA(200),XRPR(200),
     1XSPLIN(400),YSPL1(400),YSPL2(400),XTEMP(400),YT1(400),YT2(400),
     1C1(4,200),C2(4,200),GAMA(400),RPR(400),SIGMA(400),EPS(400),
     1DEPSDG(400),DSIGDG(400),DZPRDZ(400),VN(400),PHI(400),VNPR(400)
*** NOTE USE OF FSBSFL ROUTINE ***************
      CALL FSFILE(17,32,0)
      NTHRU=0
      READ(5,110) NFILES
      READ(5,110) (JFILE(N),N=1,NFILES)
  110 FORMAT(24I3)
      PI=3.14159265358979
      TWOPI=2.*PI
      NF=0
  111 N=0
      NF=NF+1
  112 N=N+1
      READ(16,120) (A(I),I=1,7)
  120 FORMAT(7E15.5)
      CALL ENDFIL(16,ISTAT)
C     ISTAT = 1 FOR EOF,  ISTAT = 2 FOR NO EOF.
      IF(ISTAT.EQ.1) GO TO 130
  125 READ(16,120) (A(I),I=8,14),XVNPR(N),XGAMA(N),XRPR(N)
      X=A(2)
      GO TO 112
  130 DO 132 I=1,NFILES
      IF(NF.EQ.JFILE(I)) GO TO 135
  132 CONTINUE
      GO TO 111
  135 NPTS=N-1
      DO 140 N=1,NPTS
      IF(XGAMA(N).GT.1.0) GO TO 140
      GO TO 142
  140 CONTINUE
      STOP1
  142 MIN=N
      MAX=N-1
      II=0
      NBAD=0
      DO 145 N=MIN,NPTS
      II=II+1
      XTEMP(II)=XGAMA(N)
      YT1(II)=XRPR(N)
      YT2(II)=XVNPR(N)
      IF(II.EQ.1) GO TO 145
      IF(XTEMP(II).GT.XTEMP(II-1)) GO TO 145
      NBAD=NBAD+1
      II=II-1
      WRITE(6,143) N,XGAMA(N),XRPR(N),XVNPR(N)
  143 FORMAT(///*  BAD VALUES FOR SPLINE FIT.  GAMA NOT INCREASING AT N=
     1*I3/*  GAMA=*1PE15.5,3X,*RPR=*1PE15.5,3X,*VNPR=*1PE15.5)
```

```
  145 CONTINUE
      DO 150 N=1,MAX
      II=II+1
      XTEMP(II)=XGAMA(N)
      YT1(II)=XRPR(N)
      YT2(II)=XVNPR(N)
      IF(XTEMP(II).GT.XTEMP(II-1)) GO TO 150
      NBAD=NBAD+1
      II=II-1
      IF(N.EQ.1) GO TO 150
      WRITE(6,143) N,XGAMA(N),XRPR(N),XVNPR(N)
  150 CONTINUE
      M=XPTS-NBAD
      DO 160 I=1,3
      NN=M-(3-I)
      XSPLIN(I)=-(TWOPI-XTEMP(NN))
      YSPL1(I)=YT1(NN)
      YSPL2(I)=YT2(NN)
      XSPLIN(M+3+I)=TWOPI+XTEMP(I)
      YSPL1(M+3+I)=YT1(I)
      YSPL2(M+3+I)=YT2(I)
  160 CONTINUE
      DO 165 I=1,M
      XSPLIN(I+3)=XTEMP(I)
      YSPL1(I+3)=YT1(I)
  165 YSPL2(I+3)=YT2(I)
      MPAIR=M+6
**** NOTE PRINT-OUT ******
      WRITE(6,170) X,(XSPLIN(I),YSPL1(I),YSPL2(I),I=1,MPAIR)
  170 FORMAT(1H1,*  ORDERED VALUES GOING INTO SPLINE FIT.  X=*F6.3/T12*G
     1AMA*,T28*RPR*,T42*VNPR*/(1P3E15.5))
      CALL SPLICON(XSPLIN,YSPL1,MPAIR,C1)
      CALL SPLICON(XSPLIN,YSPL2,MPAIR,C2)
      NBIG=180
      N1=NBIG+1
      DELTGA=2.*PI/(FLOAT(NBIG))
      D2=2.*DELTGA
      DELT2=DELTGA/2.
      DO 105 N=1,N1
      GAMA(N)=DELTGA*FLOAT(N-1)
      XINT=GAMA(N)
      CALL SPLINE(XSPLIN,YSPL1,MPAIR,C1,XINT,YINT,DUM,IOK)
      IF(IOK.EQ.0) WRITE(6,115) XINT
  115 FORMAT(///*  OUT OF RANGE FOR SPLINE FIT*/*  GAMA=*1PE15.5)
      IF(IOK.EQ.0) STOP2
      RPR(N)=YINT
      CALL SPLINE(XSPLIN,YSPL2,MPAIR,C2,XINT,YINT,DUM,IOK)
      IF(IOK.EQ.0) STOP2
      VNPR(N)=YINT
  105 CONTINUE
      T=.1
      R=T*SQRT(1.-X**2)
```

```
      DO 108 N=1,N1
  108 SIGMA(N)=ALOG(RPR(N)/R)
      DSIGDG(1)=(SIGMA(2)-SIGMA(NBIG))/D2
      DO 10 N=2,NBIG
      DSIGDG(N)=(SIGMA(N+1)-SIGMA(N-1))/D2
   10 CONTINUE
      DO 25 N=2,NBIG
      EN=N
      P1=4.*DELTGA*DSIGDG(N)
      SUM1=0.
      NM1=N-2
      IF(N.EQ.2) GO TO 20
      DO 15 K=1,NM1
      AK=K
      SIGK=SIGMA(K+1)+SIGMA(K)
      S1=SIN(DELT2*(AK-EN+1.))
      S2=SIN(DELT2*(AK-EN))
      SUM1=SUM1+SIGK*ALOG(S1/S2)
   15 CONTINUE
   20 SUM2=0.
      IF (N.GE.NBIG) GO TO 23
      NK=N+1
      DO 24 K=NK,NBIG
      AK=K
      SIGK=SIGMA(K+1)+SIGMA(K)
      S1=SIN(DELT2*(AK-EN+1.))
      S2=SIN(DELT2*(AK-EN))
      SUM2=SUM2+SIGK*ALOG(S1/S2)
   24 CONTINUE
   23 EPS(N)=-(P1+SUM1+SUM2)/(2.*PI)
   25 CONTINUE
      SUM3=0.
      NM2=NBIG-1
      DO 30 K=2,NM2
      SIGK=SIGMA(K+1)+SIGMA(K)
      S1=SIN(DELT2*FLOAT(K))
      S2=SIN(DELT2*FLOAT(K-1))
      SUM3=SUM3+SIGK*ALOG(S1/S2)
   30 CONTINUE
      EPS(1)=-(4.*DELTGA*DSIGDG(1)+SUM3)/(2.*PI)
      EPS(N1)=EPS(1)
      DSIGDG(N1)=DSIGDG(1)
      DO 50 K=1,N1
      PHI(K)=GAMA(K)+EPS(K)
   50 CONTINUE
      SUM 4=0
      DO 60 K=1,NM2
      SUM4=SUM4+SIGMA(K+1)
   60 CONTINUE
      SIGMAZ=(SIGMA(1)+SUM4)*DELTGA/(2.*PI)
      DO 70 K=2,N
```

```
      DEPSDG(K)=(EPS(K+1)-EPS(K-1))/D2
70    CONTINUE
      DEPSDG(1)=(EPS(2)-EPS(NBIG))/D2
      DEPSDG(N1)=DEPSDG(1)
      DO 80 N=1,N1
      DZPRDZ(N)=(EXP(SIGMA(N)-SIGMAZ))*(SQRT(1.+DSIGDG(N)**2))/
     1(1.+DEPSDG(N))
      VN(N)=VNPR(N)*DZPRDZ(N)
80    CONTINUE
      WRITE(6,200) X,SIGMAZ
200   FORMAT(1H1*  X=*F7.3,4X,*SIGMAZ=*,1PE14.5//T4*N*,T11*GAMA*,T26,
     1*RPR*,T38*SIGMA*,T54*EPS*,T65*DEPSDG*,T79*DSIGDG*,T93*DZPRDZ*,
     1T111*VN*,11X*PHI*)
      WRITE(6,201)(N,GAMA(N),RPR(N),SIGMA(N),EPS(N),DEPSDG(N),DSIGDG(N),
     1DZPRDZ(N),VN(N),PHI(N),N=1,N1)
201   FORMAT(I4,1P9E14.5)
      WRITE(17,202) X,SIGMAZ
202   FORMAT(1P2E14.5)
      WRITE(17,201)(N,GAMA(N),RPR(N),SIGMA(N),EPS(N),DEPSDG(N),
     1DSIGDG(N),DZPRDZ(N),VN(N),PHI(N),N=1,N1)
      ENDFILE 1,
      NTHRU=NTHRU+1
      IF(NTHRU.LT.NFILES) GO TO 111
      STOP
       END
```

```
      PROGRAM CABVINT(INPUT,OUTPUT,TAPE5=INPUT,TAPE6=OUTPUT,TAPE17)
      DIMENSION XGAMA(800),XRPR(800),XVN(800),XPHI(800),C1(4,200),
     1C2(4,200),C3(4,200),XSPLIN(200),YSPL1(200),YSPL2(200),YSPL3(200),
     1GAMA(800),RPR(800),PHI(800),VS(800),DVNDPH(800),VN(800),Z1(800),
     1Z2(800),FY(50),FZ(50),XX(50)
      PI=3.14159265358979
      TWOPI=2.*PI
***
      READ(5,500) (XX(ICNT),FZ(ICNT),FY(ICNT),ICNT=1,35)
  500 FORMAT(F6.3,2E11.5)
      ICNT=35
  201 READ(17,202) X,SIGMAZ
  202 FORMAT(2E14.5)
      N=0
  125 N=N+1
      READ(17,120) M,XGAMA(N),XRPR(N),DUM,DUM,DUM,DUM,DUM,XVN(N),XPHI(N)
  120 FORMAT(I4,9E14.5)
      IF(EOF(17)) 130,125
  130 NPTS=N-1
****
      IF(X.LT.-.120) GO TO 201
      DO 160 I=1,2
      NN=NPTS-(3-I)
      XSPLIN(I)=XPHI(NN)-TWOPI
      YSPL1(I)=XVN(NN)
      YSPL2(I)=XRPR(NN)
      YSPL3(I)=XGAMA(NN)-TWOPI
      XSPLIN(NPTS+2+I)=XPHI(I+1)+TWOPI
      YSPL1(NPTS+2+I)=XVN(I+1)
      YSPL2(NPTS+2+I)=XRPR(I+1)
      YSPL3(NPTS+2+I)=XGAMA(I+1)+TWOPI
  160 CONTINUE
      DO 165 I=1,NPTS
      XSPLIN(I+2)=XPHI(I)
      YSPL1(I+2)=XVN(I)
      YSPL2(I+2)=XRPR(I)
  165 YSPL3(I+2)=XGAMA(I)
      MPAIR=NPTS+4
      WRITE(6,168) X
  168 FORMAT(1H1*   ORDERED VALUES GOING INTO SPLINE FIT AT X=*F6.3/
     1T10*PHI*,T34*VN*,T48*RPR*,T62*GAMA*)
      DO 170 N=1,MPAIR
      WRITE(6,169) XSPLIN(N),YSPL1(N),YSPL2(N),YSPL3(N)
  169 FORMAT(5X,1P4E15.5)
      IF(N.EQ.1) GO TO 170
      IF(XSPLIN(N).LE.XSPLIN(N-1)) STOP1
  170 CONTINUE
      CALL SPLICON(XSPLIN,YSPL1,MPAIR,C1)
      CALL SPLICON(XSPLIN,YSPL2,MPAIR,C2)
      CALL SPLICON(XSPLIN,YSPL3,MPAIR,C3)
      MBIG=180
      JJ=0
  175 MI=MBIG+1
```

```
      DLTPHI=2.*PI/FLOAT(MBIG)
      D3=2.*DLTPHI
      DELT3=DLTPHI/2.
      DO5M=1,MI
      PHI(M)=DLTPHI*FLOAT(M-1)
    5 CONTINUE
      DO 6 M=1,MI
      XINT=PHI(M)
      CALL SPLINE(XSPLIN,YSPL1,MPAIR,C1,XINT,YINT,DERIV,IOK)
      IF(IOK.EQ.0)  WRITE(6,115) XINT
  115 FORMAT(///*  OUT OF RANGE FOR SPLINE FIT.  PHI=*1PE14.5)
      IF(IOK.EQ.0) STOP2
      VN(M)=YINT
      CALL SPLINE(XSPLIN,YSPL2,MPAIR,C2,XINT,YINT,DERIV,IOK)
      IF(IOK.EQ.0) STOP2
      RPR(M)=YINT
      CALL SPLINE(XSPLIN,YSPL3,MPAIR,C3,XINT,YINT,DERIV,IOK)
      IF(IOK.EQ.0) STOP2
      GAMA(M)=YINT
    6 CONTINUE
      DVNDPH(1)=(VN(2)-VN(MBIG))/D3
      DO10 M=2,MBIG
      DVNDPH(M)=(VN(M+1)-VN(M-1))/D3
   10 CONTINUE
      DO 25 M=2,MBIG
      EM=M
      P1=4.*DLTPHI*DVNDPH(M)
      SUM1=0
      MA1=M-2
      IF(M.EQ.2) GO TO 20
      DO 15 K=1,MA1
      AK=K
      VNK=VN(K+1)+VN(K)
      S1=SIN(DELT3*(AK-EM+1.))
      S2=SIN(DELT3*(AK-EM))
      SUM1=SUM1+VNK*ALOG(S1/S2)
   15 CONTINUE
   20 SUM2=0
      IF(M.GE.MBIG) GO TO 23
      MK=M+1
      DO 24 K=MK,MBIG
      AK=K
      VNK=VN(K+1)+VN(K)
      S1=SIN(DELT3*(AK-EM+1.))
      S2=SIN(DELT3*(AK-EM))
      SUM2=SUM2+VNK*ALOG(S1/S2)
   24 CONTINUE
   23 VS(M)=-(P1+SUM1+SUM2)/(2.*PI)
   25 CONTINUE
      SUM3=0
      MA2=MBIG-1
      DO30K=2,MA2
      VNK=VN(K+1)+VN(K)
      S1=SIN(DELT3*FLOAT(K))
```

```
      S2=SIN(DELT3*FLOAT(K-1))
      SUM3=SUM3+VNK*ALOG(S1/S2)
   30 CONTINUE
      VS(1)=-(4.*DLTPHI*DVNDPH(1)+SUM3)/(2.*PI)
      VS(M1)=VS(1)
      DVNDPH(M1)=DVNDPH(1)
      WRITE(6,310) X
  310 FORMAT(1H1,T5*X=*F6.3/T5*N*,T14*PHI*,T30*VN*,T45*VS*,T59*RPR*,T73,
     1*GAMA*,7X16HRPR*VS*COS(GAMA),4X16HRPR*VS*SIN(GAMA))
      DO 330 N=1,M1
      Z1(N)=RPR(N)*VS(N)*COS(GAMA(N))
      Z2(N)=RPR(N)*VS(N)*SIN(GAMA(N))
      WRITE(6,320) N,PHI(N),VN(N),VS(N),RPR(N),GAMA(N),Z1(N),Z2(N)
  320 FORMAT(I5,1P5E15.5,E17.5,E20.5)
  330 CONTINUE
      SUM1=(Z1(1)+Z1(M1))/2.
      SUM2=(Z2(1)+Z2(M1))/2.
      DO 340 N=2,MBIG
      SUM1=SUM1+Z1(N)
  340 SUM2=SUM2+Z2(N)
      Z1INT=SUM1*DLTPHI
      WRITE(6,345) Z1INT
  345 FORMAT(///39H   INTEGRAL OF (RPR*VS*COS(GAMA)DPHI) =,1PE13.5)
      Z2INT=SUM2*DLTPHI
      WRITE(6,346) Z2INT
  346 FORMAT(39H   INTEGRAL OF (RPR*VS*SIN(GAMA)DPHI) =,1PE13.5)
      T=.1
      R=T*SQRT(1.0-X**2)
      CONST=2.*R*EXP(SIGMA2)
      WRITE(6,350) CONST
  350 FORMAT(*   CONSTANT =*1PE13.5)
      ICNT=ICNT+1
      FZ(ICNT)=CONST*Z1INT
      FY(ICNT)=-CONST*Z2INT
      XX(ICNT)=X
      WRITE(6,355) FZ(ICNT),FY(ICNT)
  355 FORMAT(/*   FZ =*1PE13.5/*   FY =*1PE13.5)
      IF(X.GT..045) GO TO 420
      IF(ABS(X-0.).GT.1.0E-8) GO TO 201
C     X=-.970,-.950,-.920,-.900,-.875,-.825,ETC.
      FTRAP=.020*(FY(1)+FY(2))/2.
      FTRAP=FTRAP+.030*(FY(2)+FY(3))/2.
      FTRAP=FTRAP+.030*(FY(3)+FY(4))/2.
      DO 410 I=5,ICNT
  410 FTRAP=FTRAP+.025*(FY(I-1)+FY(I))/2.
      XMY=-FY(ICNT)+FTRAP
      WRITE(6,415) FTRAP,XMY
  415 FORMAT(/*   FY INTEGRAL =*1PE13.5/*   MOMENT ABOUT NOSE =*1PE13.5)
      GO TO 201
  420 WRITE(6,421) (XX(I),FZ(I),FY(I),I=1,ICNT)
  421 FORMAT(1H1,T11*X*,T25*FZ*,T40*FY*/(1P3E15.5))
      WRITE(6,425) XMY
```

```
425 FORMAT(/*   MOMENT ABOUT NOSE =*1PE13.5)
400 STOP
      END
```